arXiv:1904.05363v1 [gr-qc] 10 Apr 2019

Testing the nature of dark compact objects: a status report

Vitor Cardoso

CENTRA, Departamento de Física, Instituto Superior Técnico, Universidade de Lisboa, Avenida Rovisco Pais 1, 1049 Lisboa, Portugal
CERN 1 Esplanade des Particules, Geneva 23, CH-1211, Switzerland
email: vitor.cardoso@ist.utl.pt
https://centra.tecnico.ulisboa.pt/network/grit/

Paolo Pani

Dipartimento di Fisica, "Sapienza" Università di Roma & Sezione INFN Roma1, Piazzale Aldo Moro 5, 00185, Roma, Italy
email: paolo.pani@uniroma1.it
https://www.roma1.infn.it/~pani

May 20, 2022

Abstract

Very compact objects probe extreme gravitational fields and may be the key to understand outstanding puzzles in fundamental physics. These include the nature of dark matter, the fate of spacetime singularities, or the loss of unitarity in Hawking evaporation. The standard astrophysical description of collapsing objects tells us that massive, dark and compact objects are black holes. Any observation suggesting otherwise would be an indication of beyond-the-standard-model physics. Null results strengthen and quantify the Kerr black hole paradigm. The advent of gravitational-wave astronomy and precise measurements with very long baseline interferometry allow one to finally probe into such foundational issues. We overview the physics of exotic dark compact objects and their observational status, including the observational evidence for black holes with current and future experiments.

Contents

1 Introduction **4**
- 1.1 Problems on the horizon . . . 5
- 1.2 Quantifying the evidence for black holes . . . 6
- 1.3 The dark matter connection . . . 7
- 1.4 Taxonomy of compact objects: a lesson from particle physics . . . 7
- 1.5 The small ϵ-limit . . . 8

2 Structure of stationary compact objects **9**
- 2.1 Anatomy of compact objects . . . 9
  - 2.1.1 Event horizons, trapped surfaces, apparent horizons . . . 10
  - 2.1.2 Quantifying the shades of dark objects: the closeness parameter ϵ . . . 11
  - 2.1.3 Quantifying the softness of dark objects: the curvature parameter . . . 12
  - 2.1.4 Geodesic motion and associated scales . . . 13
  - 2.1.5 Photon spheres . . . 15
- 2.2 Escape trajectories and shadows . . . 16
- 2.3 The role of the spin . . . 17
  - 2.3.1 Ergoregion . . . 17
  - 2.3.2 Multipolar structure . . . 18

3 ECO taxonomy: from DM to quantum gravity **20**
- 3.1 A compass to navigate the ECO atlas: Buchdahl's theorem . . . 21
- 3.2 Self-gravitating fundamental fields . . . 21
- 3.3 Perfect fluids . . . 23
- 3.4 Anisotropic stars . . . 24
- 3.5 Wormholes . . . 25
- 3.6 Dark stars . . . 26
- 3.7 Gravastars . . . 27
- 3.8 Fuzzballs and collapsed polymers . . . 27
- 3.9 "Naked singularities" and superspinars . . . 28
- 3.10 $2-2$ holes and other geons . . . 29
- 3.11 Firewalls, compact quantum objects and dirty BHs . . . 29

4 Dynamics of compact objects **31**
- 4.1 Quasinormal modes . . . 31
- 4.2 Gravitational-wave echoes . . . 35
  - 4.2.1 Quasinormal modes, photon spheres, and echoes . . . 35
  - 4.2.2 A black-hole representation and the transfer function . . . 36
  - 4.2.3 A Dyson-series representation . . . 40
  - 4.2.4 Echo modeling . . . 42
  - 4.2.5 Echoes: a historical perspective . . . 44
- 4.3 The role of the spin . . . 45
  - 4.3.1 QNMs of spinning Kerr-like ECOs . . . 46
  - 4.3.2 Echoes from spinning ECOs . . . 48

4.4 The stability problem . . . 48
4.4.1 The ergoregion instability . . . 49
4.4.2 Nonlinear instabilities I: long-lived modes and their backreaction . . 50
4.4.3 Nonlinear instabilities II: causality, hoop conjecture, and BH formation 51
4.5 Binary systems . . . 52
4.5.1 Multipolar structure . . . 52
4.5.2 Tidal heating . . . 52
4.5.3 Tidal deformability and Love numbers . . . 54
4.5.4 Accretion and drag in inspirals around and inside DM objects . . . 56
4.5.5 GW emission from ECOs orbiting or within neutron stars . . . 57
4.6 Formation and evolution . . . 57

5 Observational evidence for horizons 59
5.1 Tidal disruption events and EM counterparts . . . 59
5.2 Equilibrium between ECOs and their environment: Sgr A* . . . 60
5.3 Bounds with shadows: Sgr A* and M87 . . . 61
5.4 Tests with accretion disks . . . 62
5.5 Signatures in the mass-spin distribution of dark compact objects . . . 63
5.6 Multipole moments and tests of the no-hair theorem . . . 64
5.6.1 Constraints with comparable-mass binaries . . . 64
5.6.2 Projected constraints with EMRIs . . . 66
5.7 Tidal heating . . . 66
5.8 Tidal deformability . . . 68
5.9 Resonance excitation . . . 69
5.10 QNM tests . . . 69
5.11 Inspiral-merger-ringdown consistency . . . 70
5.12 Tests with GW echoes . . . 70
5.13 Stochastic background . . . 72
5.14 Motion within ECOs . . . 73

6 Discussion and observational bounds 74

"The crushing of matter to infinite density by infinite tidal gravitation forces is a phenomenon with which one cannot live comfortably. From a purely philosophical standpoint it is difficult to believe that physical singularities are a fundamental and unavoidable feature of our universe [...] one is inclined to discard or modify that theory rather than accept the suggestion that the singularity actually occurs in nature."

Kip Thorne, Relativistic Stellar Structure and Dynamics (1966)

"No testimony is sufficient to establish a miracle, unless the testimony be of such a kind, that its falsehood would be more miraculous than the fact which it endeavors to establish."

David Hume, An Enquiry concerning Human Understanding (1748)

1 Introduction

The discovery of the electron and the known neutrality of matter led in 1904 to J. J. Thomson's "plum-pudding" atomic model. Data from new scattering experiments was soon found to be in tension with this model, which was eventually superseeded by Rutherford's, featuring an atomic nucleus. The point-like character of elementary particles opened up new questions. How to explain the apparent stability of the atom? How to handle the singular behavior of the electric field close to the source? What is the structure of elementary particles? Some of these questions were elucidated with quantum mechanics and quantum field theory. Invariably, the path to the answer led to the discovery of hitherto unknown phenomena and to a deeper understanding of the fundamental laws of Nature.

The history of elementary particles is a timeline of the understanding of the electromagnetic (EM) interaction, and is pegged to its characteristic $1/r^2$ behavior (which necessarily implies that other structure *has* to exist on small scales within any sound theory). Arguably, the elementary particle of the gravitational interaction are black holes (BHs). Within General Relativity (GR), BHs are indivisible and are in fact the simplest macroscopic objects that one can conceive. The uniqueness theorems – establishing that the two-parameter Kerr family of BHs describes any vacuum, stationary and asymptotically flat, regular solution to GR – have turned BHs into somewhat of a miracle elementary particle [1].

Can BHs, as envisioned in vacuum GR, hold the same surprises that the electron and the hydrogen atom did when they started to be experimentally probed? Are there any parallels that can be useful guides? The BH interior is causally disconnected from the exterior by an event horizon. Unlike the classical description of atoms, the GR description of the BH exterior is self-consistent and free of pathologies. The "inverse-square law problem" – the GR counterpart of which is the appearance of pathological curvature singularities – is swept to inside the horizon and therefore harmless for the external world. There are strong indications that classical BHs are perturbatively stable against small fluctuations, and attempts to produce naked singularities, starting from BH spacetimes,

have failed. BHs are not only curious mathematical solutions to Einstein's equations (as were they initially dismissed as), but also their *formation* process is sound and well understood. In fact, classically there is nothing spectacular with the presence or formation of an event horizon. The equivalence principle dictates that an infalling observer crossing this region (which, by definition, is a *global* concept) feels nothing extraordinary: in the case of macroscopic BHs all of the local physics at the horizon is rather unremarkable.

Why, then, should one question the existence of BHs? [1] There are a number of important reasons to do so, starting from the obvious one: we *can* do it. The landmark detection of gravitational waves (GWs) showed that we are now able to analyze and understand the details of the signal produced when two compact objects merge [4, 5]. An increase in sensitivity of current detectors and the advent of next-generation interferometers on ground and in space will open the frontier of *precision* GW astrophysics. GWs are produced by the coherent motion of the sources as a whole: they are ideal probes of strong gravity, and play the role that EM waves did to test the Rutherford model. In parallel, novel techniques such as radio and deep infrared interferometry [6, 7] will very soon provide direct *images* of the center of our galaxy, where a dark, massive and compact object is lurking [8–11]. Data from such missions has the potential to inform us on the following outstanding issues:

1.1 Problems on the horizon

Classically, spacetime singularities seem to be always cloaked by horizons and hence inaccessible to distant observers; this is in essence the content of the weak cosmic censorship conjecture [12, 13]. However, there is as yet no proof that the field equations always evolve regular initial data towards regular final states.

Classically, the BH exterior is pathology-free, but the interior is not. The Kerr family of BHs harbors singularities and closed timelike curves in its interior, and more generically it features a Cauchy horizon signaling the breakdown of predictability of the theory [14–17]. The geometry describing the interior of an astrophysical spinning BH is currently unknown. A resolution of this problem most likely requires accounting for quantum effects. It is conceivable that these quantum effects are of no consequence whatsoever on physics outside the horizon. Nevertheless, it is conceivable as well that the resolution of such inconsistency leads to new physics that resolves singularities and does away with horizons, at least in the way we understand them currently. Such possibility is not too dissimilar from what happened with the atomic model after the advent of quantum electrodynamics.

[1] This is a peculiar question, being asked more than a century after the first BH solution was derived. Even though Schwarzschild and Droste wrote down the first nontrivial regular, asymptotic flat, vacuum solution to the field equations already in 1916 [2, 3], several decades would elapse until such solutions became accepted. The dissension between Eddington and Chandrasekhar over gravitational collapse to BHs is famous – Eddington firmly believed that nature would find its way to prevent full collapse – and it took decades for the community to overcome individual prejudices. Progress in our understanding of gravitational collapse, along with breakthroughs in the understanding of singularities and horizons, contributed to change the status of BHs. Together with observations of phenomena so powerful that could only be explained via massive compact objects, the theoretical understanding of BHs turned them into undisputed kings of the cosmos. The irony lies in the fact that they quickly became the *only* acceptable solution. So much so, that currently an informal definition of a BH might well be "any dark, compact object with mass above roughly three solar masses."

Black holes have a tremendously large entropy, which is hard to explain from microscopic states of the progenitor star. Classical results regarding for example the area (and therefore entropy) increase [18] and the number of microstates can be tested using GW measurements [19,20], but assume classical matter. Indeed, semi-classical quantum effects around BHs are far from being under control. Quantum field theory on BH backgrounds leads to loss of unitarity, a self-consistency requirement that any predictive theory ought to fulfill. The resolution of such conundrum may involve non-local effects changing the near-horizon structure, or doing away with horizons completely [21–35].

As a matter of fact, there is no tested nor fully satisfactory theory of quantum gravity, in much the same way that one did not have a quantum theory of point charges at the beginning of the 20th century.

GR is a purely classical theory. One expects quantum physics to become important beyond some energy scale. It is tacitly assumed that such "quantum gravity effects" are relevant only near the Planck scale: at lengths $\ell_P \sim \sqrt{G\hbar/c^3} \sim 10^{-35}\,$meters, the Schwarzschild radius is of the order of the Compton wavelength of the BH and the notion of a classical system is lost. However, it has been argued that, in the orders of magnitude standing between the Planck scale and those accessible by current experiments, new physics can hide. To give but one example, if gravity is fundamentally a higher-dimensional interaction, then the fundamental Planck length can be substantially *larger* [36, 37]. In addition, some physics related to compact objects have a logarithmic dependence on the (reasonably-defined) Planck length [38] (as also discussed below). Curiously, some attempts to quantize the area of BHs predict sizable effects even at a classical level, resulting in precisely the same phenomenology as that discussed in the rest of this review [39–43]. Thus, quantum-gravity effects may be within reach.

1.2 Quantifying the evidence for black holes

Horizons are not only a rather generic prediction of GR, but their existence is in fact *necessary* for the consistency of the theory at the classical level. This is the root of Penrose's (weak) Cosmic Censorship Conjecture [12, 13], which remains one of the most urgent open problems in fundamental physics. In this sense, the statement that there is a horizon in any spacetime harboring a singularity in its interior is such a remarkable claim, that (in an informal description of Hume's statement above) it requires similar remarkable evidence.

It is in the nature of science that paradigms have to be constantly questioned and subjected to experimental and observational scrutiny. Most specially because if the answer turns out to be that BHs do not exist, the consequences are so extreme and profound, that it is worth all the possible burden of actually testing it. As we will argue, the question is not just whether the strong-field gravity region near compact objects is consistent with the BH geometry of GR, but rather to *quantify* the limits of observations in testing event horizons. This approach is common practice in other contexts. Decades of efforts in testing the pillars of GR resulted in formalisms (such as the parametrized post-Newtonian approach [44]) which quantify the constraints of putative deviations from GR. For example, we know that the weak equivalence principle is valid to at least within one part in 10^{15} [45]. On

the other hand, no such solid framework is currently available to quantify deviations from the standard BH paradigm. In fact, as we advocate in this work, the question to be asked is not whether there is a horizon in the spacetime, but how close to it do experiments or observations go. It is important to highlight that some of the most important tests of theories or paradigms – and GR and its BH solutions are no exception – arise from entertaining the existence of alternatives. It is by allowing a large space of solutions that one can begin to exclude – with observational and experimental data – some of the alternatives, thereby producing a stronger paradigm.

1.3 The dark matter connection

Known physics all but exclude BH alternatives as explanations for the dark, massive and compact objects out there. Nonetheless, the Standard Model of fundamental interactions is not sufficient to describe the cosmos – at least on the largest scales. The nature of dark matter (DM) is one of the longest-standing puzzles in physics [46, 47]. Given that the evidence for DM is – so far – purely gravitational, further clues may well be hidden in strong-gravity regions or GW signals generated by dynamical compact objects.

As an example, new fundamental fields (such as axions, axion-like particles, etc [48, 49]), either minimally or non-minimally coupled to gravity, are essential for cosmological models, and are able to explain all known observations concerning DM. Even the simplest possible theory of minimally coupled, massive scalar fields give rise to self-gravitating *compact* objects, which are dark if their interaction with Standard Model particles is weak. These are called boson stars or oscillatons, depending on whether the field if complex or real, respectively. Such dark objects have a maximum mass[2] which is regulated by the mass of the fundamental boson itself and by possible self-interaction terms; they form naturally through gravitational collapse and may cluster around an ultracompact configuration through "gravitational cooling" [50–53].

Furthermore, DM could be composed of entirely different fields or particles, and many of these are expect to lead to new classes of dark compact objects [54–56].

1.4 Taxonomy of compact objects: a lesson from particle physics

From a phenomenological standpoint, BHs and neutron stars could be just two "species" of a larger family of astrophysical compact objects, which might co-exist with BHs rather than replacing them. These objects are theoretically predicted in extended theories of gravity but also in other scenarios in the context of GR, such as beyond-the-Standard-Model fundamental fields minimally coupled to gravity, or of exotic states of matter.

In this context, it is tempting to draw another parallel with particle physics. After the Thomson discovery of the electron in 1897, the zoo of elementary particles remained almost unpopulated for decades: the proton was discovered only in the 1920s, the neutron and the positron only in 1932, few years before the muon (1936). Larger and more sensitive

[2] A crucial property of BHs in GR is that – owing to the scale-free nature of vacuum Einstein's equation – their mass is a free parameter. This is why the same Kerr metric can describe any type of BH in the universe, from stellar-mass (or even possibly primordial) to supermassive. It is extremely challenging to reproduce this property with a material body, since matter fields introduce a scale.

particle accelerators had been instrumental to discover dozens of new species of elementary particles during the second half of the XXth century, and nowadays the Standard Model of particle physics accounts for hundreds of particles, either elementary or composite. Compared to the timeline of particle physics, the discovery of BHs, neutron stars, and binary thereof is much more recent; it is therefore natural to expect that the latest advance in GW astronomy and very long baseline interferometry can unveil new species in the zoo of astrophysical compact objects. Of course, this requires an understanding of the properties of new families of hypothetical compact objects and of their signatures.

1.5 The small ϵ-limit

In addition to the above phenomenological motivations, dark compact objects are also interesting from a mathematical point of view. For instance, given the unique properties of a BH, it is interesting to study how a dark compact object approaches the "BH limit" (if the latter exists!) as its compactness increases. Continuity arguments would suggest that any deviation from a BH should vanish in this limit, but this might occur in a highly nontrivial way, as we shall discuss. The first issue in this context is how to parametrize "how close" a self-gravitating object is to a BH in a rigorous way, by introducing a "closeness" parameter ϵ, such that $\epsilon \to 0$ corresponds to the BH limit. As we shall discuss, there are several choices for ϵ, for example the tidal deformability, the inverse of the maximum redshift in the spacetime, or a quantity related to the compactness M/R such as $\epsilon = 1 - 2M/R$, where M is the object mass in the static case and R is its radius.

In the context of DM self-gravitating objects ϵ is expected to be of order unity. However, when quantifying the evidence for horizons or in the context of quantum corrected spacetimes, one is usually interested in the $\epsilon \ll 1$ limit. The physics of such hypothetical objects is interesting on its own: these objects are by construction regular everywhere and causality arguments imply that all known BH physics must be recovered in the $\epsilon \to 0$ limit. Thus, the small ϵ-limit may prove useful in the understanding of BH themselves, or to help cast a new light in old murky aspects of objects with a teleological nature. Moreover, as we will see, such limit is amenable to many analytical simplifications and describes reasonably well even finite ϵ spacetimes. In this regard, the $\epsilon \to 0$ limit can be compared to large spacetime-dimensionality limit in Einstein field equations [57], or even the large $\mathcal{N}$ limit in QCD [58].

2 Structure of stationary compact objects

"Mumbo Jumbo is a noun and is the name of a grotesque idol said to have been worshipped by some tribes. In its figurative sense, Mumbo Jumbo is an object of senseless veneration or a meaningless ritual."
Concise Oxford English Dictionary

The precise understanding of the nature of dark, massive and compact objects can follow different routes,

i. a pragmatic approach of testing the spacetime close to compact, dark objects, irrespective of their nature, by devising model-independent observations that yield unambiguous answers; this often requires consistency checks and null-hypothesis tests of the Kerr metric.

ii. a less ambitious and more theoretically-driven approach, which starts by constructing objects that are very compact, yet horizonless, within some framework. It proceeds to study their formation mechanisms and stability properties, and then discarding solutions which either do not form or are unstable on short timescales; finally, understand the observational imprints of the remaining objects, and how they differ from BHs.

In practice, when dealing with outstanding problems where our ignorance is extreme, pursuing both approaches simultaneously is preferable. Indeed, using concrete models can sometimes be a useful guide to learn about broad, model-independent signatures. As it will become clear, one can design exotic horizonless models which mimic all observational properties of a BH with arbitrary accuracy. While the statement "BHs exist in our Universe" is *fundamentally unfalsifiable*, alternatives can be ruled out with a single observation, just like Popper's black swans [59].

Henceforth we shall refer to horizonless compact objects other than a neutron star as *Exotic Compact Objects (ECOs)*. The aim of this section is to contrast the properties of BHs with those of ECOs and to find a classification for different models.

2.1 Anatomy of compact objects

For simplicity, let us start with the case of a spherically symmetric object and assume that, at least its exterior, is described by GR. Static, spherically symmetric spacetimes are described (in standard coordinates with r being the areal radius) by the line element

$$ds^2 = -f(r)dt^2 + g(r)^{-1}dr^2 + r^2 d\Omega^2 \,. \tag{1}$$

with $d\Omega^2 = d\theta^2 + \sin^2\theta d\phi^2$. Birkhoff's theorem guarantees that any vacuum, spherically-symmetric spacetime (in particular, the exterior an isolated compact, spherically-symmetric

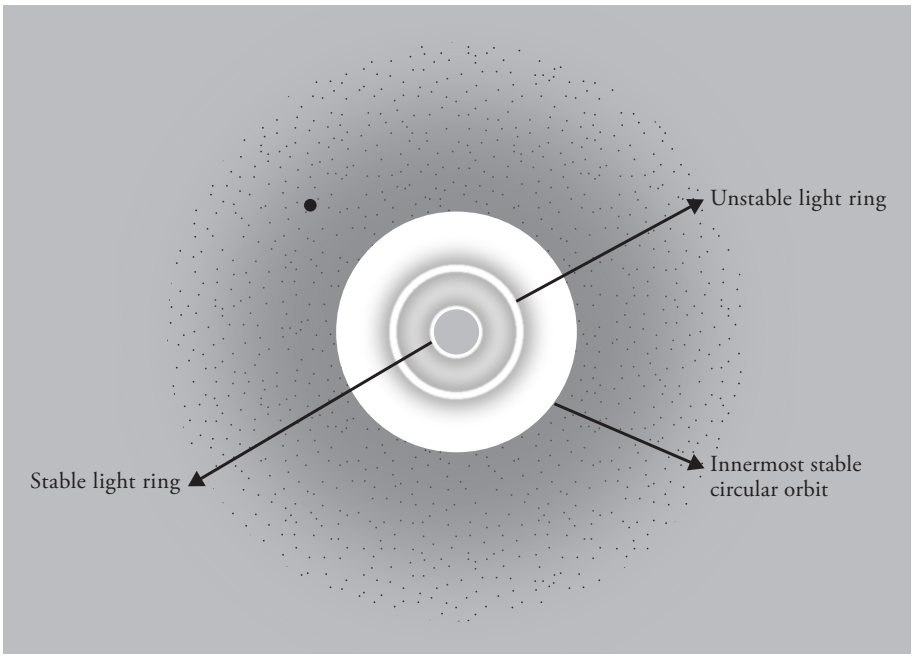


Figure 1: An equatorial slice of a very compact object, together with the most significant (from a geodesic perspective) locations. At large distances away from the central region, physics is nearly Newtonian: planets – such as the small dot on the figure – can orbit on stable orbits. The external gray area is the entire region where stable circular motion is possible. At the innermost stable circular orbit ($r = 6M$), timelike circular motion is marginally stable, and unstable as one moves further within. High-frequency EM waves or GWs can be on circular orbit in one very special location: the light ring ($r = 3M$). Such motion is unstable, and can also be associated with the "ringdown" excited during mergers. For horizonless objects, as one approaches the geometric center another significant region may appear: a second, *stable* light ring. Once rotation is turned on, regions of negative energy ("ergoregions") are possible. The astrophysical properties of a dark compact object depends on where in this diagram its surface is located.

object) is described by the Schwarzschild geometry, for which

$$f(r) = g(r)^{-1} = 1 - \frac{2M}{r}\,, \tag{2}$$

and M is the total mass of the spacetime (we use geometrical $G = c = 1$ units, except if otherwise stated).

2.1.1 Event horizons, trapped surfaces, apparent horizons

A BH owns its name [60] to the fact that nothing – not even light – can escape from the region enclosed by its *horizon*. Since the latter is the real defining quantity of a BH,

it is important to define it rigorously. In fact, there are several inequivalent concepts of horizon [61, 62]. In asymptotically-flat spacetime, a BH is the set of events from which no future-pointing null geodesic can reach future null infinity. The *event horizon* is the (null) boundary of this region. The event horizon is a *global* property of an entire spacetime: on a given spacelike slice, the event horizon cannot be computed without knowing the entire future of the slice. Strictly speaking, an event horizon does not "form" at a certain time, but it is a nonlocal property; as such, it is of limited practical use in dynamical situations.

On the other hand, in a $3+1$ splitting of spacetime, a *trapped surface* is defined as a smooth closed 2-surface on the slice whose future-pointing outgoing null geodesics have negative expansion [61, 63, 64]. Roughly speaking, on a trapped surface light rays are all directed inside the trapped surface *at that given time*. The *trapped region* is the union of all trapped surfaces, and the outer boundary of the trapped region is called the *apparent horizon*. At variance with the event horizon, the apparent horizon is defined locally in time, but it is a property that depends on the choice of the slice. Under certain hypothesis – including the assumption that matter fields satisfy the energy conditions – the existence of a trapped surface (and hence of an apparent horizon) implies that the corresponding slice contains a BH [61]. The converse is instead not true: an arbitrary (spacelike) slice of a BH spacetime might not contain any apparent horizon. If an apparent horizon exists, it is necessarily contained within an event horizon, or it coincides with it. In a stationary spacetime, the event and apparent horizons always coincide at a classical level (see Refs. [65–67] for possible quantum effects).

In practice, we will be dealing mostly with quasi-stationary solutions, when the distinction between event and apparent horizon is negligible. For the sake of brevity, we shall often refer simply to a "horizon", having in mind the apparent horizon of a quasi-stationary solution. Notwithstanding, there is no direct observable associated to the horizon [38, 68, 69]. There are signatures which can be directly associated to timelike surfaces, and whose presence would signal new physics. The absence of such signatures strengthens and quantifies the BH paradigm.

2.1.2 Quantifying the shades of dark objects: the closeness parameter ϵ

"Alas, I abhor informality."
That Mitchell and Webb Look, Episode 2

Since we will mostly be discussing objects which look like BHs on many scales, it is useful to introduce a "closeness" parameter ϵ that indicates how close one is to a BH spacetime. There is an infinity of possible choices for such parameter (and in fact, different choices have been made in the literature, e.g., Refs. [29,70]). At least in the case of spherical symmetric, Birkhoff's theorem provides a natural choice for the closeness parameter: if the object has a surface at r_0, then ϵ is defined as

$$r_0 = 2M(1+\epsilon)\,. \tag{3}$$

We are thus guaranteed that when $\epsilon \to 0$, a BH spacetime is recovered. For spherical objects the above definition is coordinate-independent ($2\pi r_0$ is the proper equatorial cir-

cumference of the object). Furthermore, one can also define the proper distance between the surface and r_0, $\int_{2M}^{r_0} dr f^{-1/2} \sim 4M\sqrt{\epsilon}$, which is directly related to ϵ. Some of the observables discussed below show a dependence on $\log\epsilon$, making the distinction between radial and proper distance irrelevant.

We should highlight that this choice of closeness parameter is made for convenience. None of the final results depend on such an arbitrary choice. In fact, there are objects – such as boson stars – without a well defined surface, since the matter fields are smooth everywhere. In such case r_0 can be taken to be an effective radius beyond which the density drops sharply to zero. In some cases it is possible that the effective radius depends on the type of perturbations or on its frequency. It sometimes proves more useful, and of direct significance, to use instead the coordinate time τ (measurable by our detectors) that a radial-directed light signal takes to travel from the light ring to the surface of the object. For spherically symmetric spacetimes, there is a one-to-one correspondence with the ϵ parameter, $\tau = M(1 - 2\epsilon - \log(4\epsilon^2)) \sim -2M\log\epsilon$, where the last step is valid when $\epsilon \to 0$. In the rest, when convenient, we shall refer to this time scale rather than to r_0.

Overall, we shall use the magnitude of ϵ to classify different models of dark objects. A neutron star has $\epsilon \sim \mathcal{O}(1)$ and models with such value of the closeness parameter (e.g., boson stars, stars made of DM, see below) are expected to have dynamical properties which resemble those of a stellar object rather than a BH. For example, they are characterized by observables that display $\mathcal{O}(1)$ corrections relative to the BH case and are therefore easier to distinguish. On the other hand, to test the BH paradigm in an agnostic way, or for testing the effects of quantum gravity, one often has in mind $\epsilon \ll 1$. For instance, in certain models $r_0 - 2M = 2M\epsilon$ or the proper distance $\sim M\sqrt{\epsilon}$ are of the order of the Planck length ℓ_P; in such case $\epsilon \sim 10^{-40}$ or even smaller. These models are more challenging to rule out.

Finally, in dynamical situations ϵ might be effectively time dependent. Even when $\epsilon \sim \ell_P/M$ at equilibrium, off-equilibrium configurations might have significantly large ϵ (see, e.g., Refs. [71–74]).

2.1.3 Quantifying the softness of dark objects: the curvature parameter

In addition the closeness parameter ϵ, another important property of a dark object is its curvature scale. The horizon introduces a cut-off which limits the curvature that can be probed by an external observer. For a BH the largest curvature (as measured by the Kretschmann scalar $\mathcal{K}$) occurs at the horizon and reads

$$\mathcal{K}^{1/2} \sim \frac{1}{M^2} \approx 4.6 \times 10^{-13} \left(\frac{10M_\odot}{M}\right)^2 \text{cm}^{-2}\,. \tag{4}$$

For astrophysical BHs the curvature at the horizon is always rather small, and it might be large only if sub-$M_\odot$ primordial BHs exist in the universe. As a reference, the curvature at the center of an ordinary neutron star is $\mathcal{K}^{1/2} \sim 10^{-14}\,\text{cm}^{-2}$.

By comparison with the BH case, one can introduce two classes of models [75]: (i) *"soft" ECOs*, for which the maximum curvature is comparable to that at the horizon of the corresponding BH; and (ii) *"hard" ECOs*, for which the curvature is much larger. In the

first class, the near-surface geometry smoothly approaches that at the horizon in the BH limit (hence their "softness"), whereas in the second class the ECO can support large curvatures on its surface without collapsing, presumably because the underlying theory involves a new length scale, $\mathcal{L}$, such that $\mathcal{L} \ll M$. In these models high-energy effects drastically modify the near-surface geometry (hence their "hardness"). An example are certain classes of wormholes (see Section 3).

An interesting question is whether the maximum curvature $\mathcal{K}_{\rm max}$ depends on ϵ. Indeed, an ECO with a surface just above the BH limit ($\epsilon \to 0$) may always require large *internal* stresses in order to prevent its collapse, so that the curvature in the interior is very large, even if the exterior is exactly the Schwarzschild geometry. In other words, an ECO can be soft in the exterior but hard in the interior. Examples of this case are thin-shell gravastars and strongly anisotropic stars (see Section 3). Thus, according to this classification all ECOs might be "hard" in the $\epsilon \to 0$ limit. Likewise, the exterior of hard ECOs might be described by soft ECO solutions far from the surface, where the curvature is perturbatively close to that of a BH.

2.1.4 Geodesic motion and associated scales

The most salient geodesic features of a compact object are depicted in Fig. 1, representing the equatorial slice of a spherically-symmetric spacetime.

The geodesic motion of timelike or null particles in the geometry (1) can be described with the help of two conserved quantities, the specific energy $E = f\,\dot{t}$ and angular momentum $L = r^2\dot{\varphi}$, where a dot stands for a derivative with respect to proper time [76]. The radial motion can be computed via a normalization condition,

$$\dot{r}^2 = g\left(\frac{E^2}{f} - \frac{L^2}{r^2} - \delta_1\right) \equiv E^2 - V_{\rm geo}\,, \tag{5}$$

where $\delta_1 = 1, 0$ for timelike or null geodesics, respectively. The null limit can be approached letting $E, L \to \infty$ and rescaling all quantities appropriately. Circular trajectories are stable only when $r \geq 6M$, and unstable for smaller radii. The $r = 6M$ surface defines the innermost stable circular orbit (ISCO), and has an important role in controlling the inner part of the accretion flow onto compact objects. It corresponds to the orbital distance at which a geometrically thin accretion disk is typically truncated [77] and it sets the highest characteristic frequency for compact emission region ("hotspots") orbiting around accreting compact objects [78, 79]. Another truly relativistic feature is the existence of circular null geodesics, i.e., of circular motion for high-frequency EM waves or GWs. In the Schwarzschild geometry, a circular null geodesic is possible only at $r = 3M$ [76]. This location defines a surface called the *photon sphere*, or, on an equatorial slice, a *light ring*. The photon sphere has a number of interesting properties, and is useful to understand certain features of compact spacetimes.

For example, assume that an experimenter far away throws (high-frequency) photons in all directions and somewhere a compact object is sitting, as in Fig. 2. Photons that have a very large impact parameter (or large angular momentum), never get close to the object. Photons with a smaller impact parameter start feeling the gravitational pull of

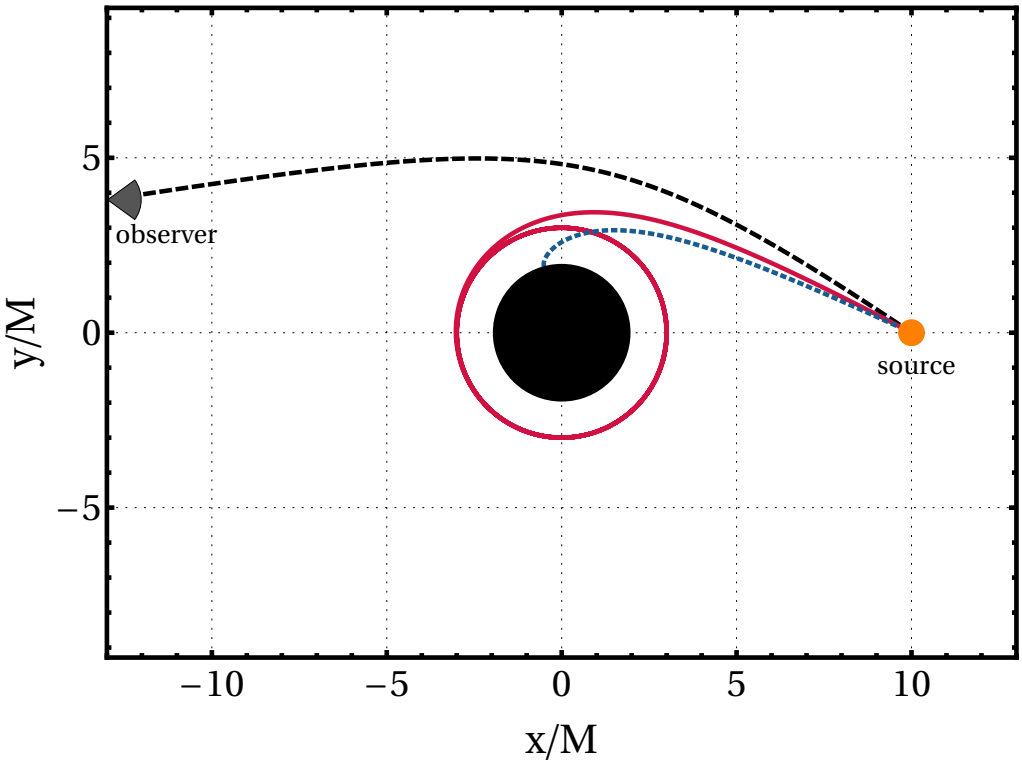


Figure 2: A source (for example, a star) emits photons in all directions in a region of spacetime where a compact object exists (black circle). Photons with high impact parameter are weakly bent (dashed, black curve), while those with small impact parameter (short-dashed blue) are absorbed and hit the object. The separatrix corresponds to photons that travel an infinite amount of time around the light ring (solid red curve) before being scattered or absorbed. Such critical photons have an impact parameter $b = 3\sqrt{3}M$ [76].

the object and may be slightly deflected, as the ray in the figure. Below a critical impact parameter all photons "hit" the compact object. It is a curious mathematical property that the critical impact parameter corresponds to photons that circle the light ring an infinite number of orbits, before being either absorbed or scattered. Thus, the light ring is fundamental for the description of how compact objects and BHs "look" like when illuminated by accretion disks or stars, thus defining their so-called *shadow*, see Sec. 2.2 below.

The photon sphere also has a bearing on the spacetime response to any type of high-frequency waves, and therefore describes how high-frequency GWs linger close to the horizon. At the photon sphere, $V''_{\rm geo} = -2E^2/(3M^2) < 0$. Thus, circular null geodesics are unstable: a displacement δ of null particles grows exponentially [80, 81]

$$\delta(t) \sim \delta_0 e^{\lambda t}\,, \qquad \lambda = \sqrt{\frac{-f^2 V''_r}{2E^2}} = \frac{1}{3\sqrt{3}M}\,. \tag{6}$$

A geodesic description anticipates that light or GWs may persist at or close to the photon sphere on timescales $3\sqrt{3}M \sim 5M$. Because the geodesic calculation is local, these conclusions hold irrespectively of the spacetime being vacuum all the way to the horizon or not.

For any regular body, the metric functions f, g are well behaved at the center, never change sign and asymptote to unity at large distances. Thus, the effective potential $V_{\rm geo}$ is negative at large distances, vanishes with zero derivative at the light ring, and is positive close to the center of the object. This implies that there must be a second light ring in the spacetime, and that it is stable [82–84]. Inside this region, there is stable timelike circular motion everywhere[3].

2.1.5 Photon spheres

An ultracompact object with surface at $r_0 = 2M(1+\epsilon)$, with $\epsilon \ll 1$, features exactly the same geodesics and properties close to its photon sphere as BHs. From Eq. (6), we immediately realize that after a three e-fold timescale, $t \sim 15M$, the amplitude of the original signal is only 5% of its original value. On these timescales one can say that the signal died away. If on such timescales the ingoing part of the signal did not have time to bounce off the surface of the object and return to the light ring, then for an external observer the relaxation is identical to that of a BH. This amounts to requiring that

$$\epsilon \lesssim \epsilon_{\rm crit} \sim 0.019\,. \tag{7}$$

Thus, the horizon plays no special role in the response of high frequency waves, nor could it: it takes an infinite (coordinate) time for a light ray to reach the horizon. The above threshold on ϵ is a natural sifter between two classes of compact, dark objects. For objects characterized by $\epsilon \gtrsim 0.019$, light or GWs can make the roundtrip from the photon sphere to the object's surface and back, before dissipation of the photon sphere modes occurs. For objects satisfying (7), the waves trapped at the photon sphere relax away by the time that the waves from the surface hit it back.

We can thus use the properties of the ISCO and photon sphere to distinguish between different classes of models:

- *Compact object*: if it features an ISCO, or in other words if its surface satisfies $r_0 < 6M$ ($\epsilon < 2$). Accretion disks around compact objects of the same mass should have similar characteristics;
- *Ultracompact object (UCO) [85]*: a compact object that features a photon sphere, $r_0 < 3M$ ($\epsilon < 1/2$). For these objects, the phenomenology related to the photon sphere might be very similar to that of a BH;
- *Clean-photon sphere object (ClePhO)*: an ultracompact object which satisfies condition (7) and therefore has a "clean" photon sphere, $r_0 < 2.038M$ ($\epsilon \lesssim 0.019$). The early-time dynamics of ClePhOs is expected to be the same as that of BHs. At late times, ClePhOs should display unique signatures of their surface.

[3]Incidentally, this also means that the circular timelike geodesic at $6M$ is not really the "innermost stable circular orbit". We use this description to keep up with the tradition in BH physics.

An ECO can belong to any of the above categories. There are indications that the photon sphere is a fragile concept and that it suffers radical changes in the presence of small environmental disturbances [86]. The impact of such result on the dynamics on compact objects is unknown.

2.2 Escape trajectories and shadows

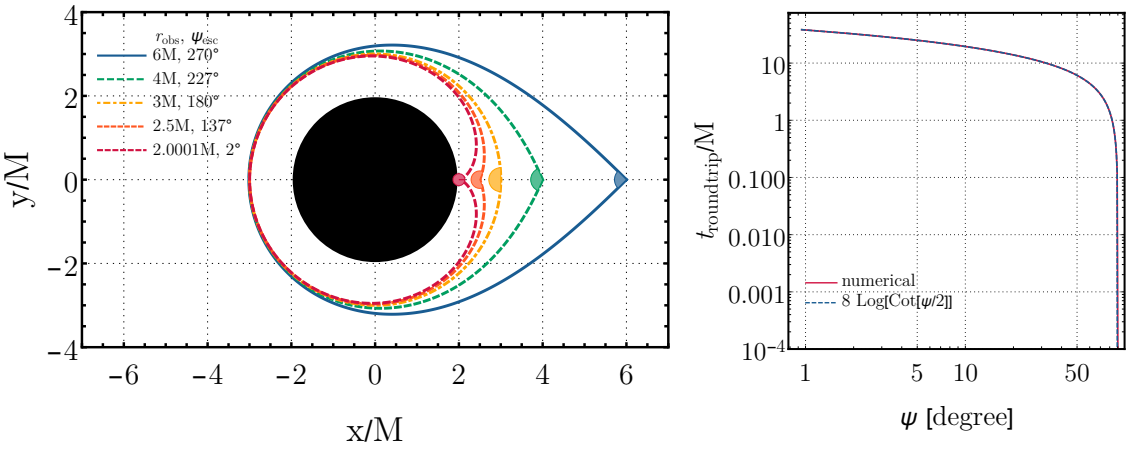


Figure 3: Left: Critical escape trajectories of radiation in the Schwarzschild geometry. A locally static observer (located at $r = r_{\rm obs}$) emits photons isotropically, but those emitted within the colored conical sectors will not reach infinity. Right: Coordinate roundtrip time of photons as a function of the emission angle $\psi > \psi_{\rm esc}$ and for $\epsilon \ll 1$.

An isolated BH would appear truly as a "hole" in the sky, since we observe objects by receiving the light they either emit or reflect. The boundary of this hole, i.e. the "silhouette" of a BH, is called the *shadow* and is actually larger than the BH horizon. More rigorously, the shadow of a BH is the region in the observer's sky comprising the directions of photons that asymptotically approach the event horizon when traced back in time. This property is intimately related with the existence of a photon sphere.

Indeed, according to Eq. (5), there exists a critical value of the angular momentum $L \equiv KME$ for a light ray to be able to escape to infinity. By requiring that a light ray emitted at a given point will not find turning points in its motion, Eq. (5) yields $K_{\rm esc} = 3\sqrt{3}$ [76]. Suppose that the light ray is emitted by a locally static observer at $r = r_0$. In the local rest frame, the velocity components of the photon are [87]

$$v_\varphi^{\rm local} = \frac{MK}{r_0}\sqrt{f_0}\,, \qquad v_r^{\rm local} = \sqrt{1 - K^2M^2\frac{f_0}{r_0^2}}\,, \tag{8}$$

where $f_0 \equiv f(r_0) = 1 - 2M/r_0$. With this, one can easily compute the escape angle, $\sin\psi_{\rm esc} = 3M\sqrt{3f_0}/r_0$. In other words, the solid angle for escape is

$$\Delta\Omega_{\rm esc} = 2\pi\left(1 - \sqrt{1 - \frac{27M^2(r_0 - 2M)}{r_0^3}}\right) \sim 27\pi\left(\frac{r_0 - 2M}{8M}\right)\,, \tag{9}$$

where the last step is valid for $\epsilon \ll 1$. For angles larger than these, the light ray falls back and either hits the surface of the object, if there is one, or will be absorbed by the horizon. The escape angle is depicted in Fig. 3 for different emission points r_0. The rays that are not able to escape reach a maximum coordinate distance,

$$r_{\rm max} \sim 2M \left(1 + \frac{4 f_0 M^2}{r_0^2 \sin^2 \psi}\right) . \tag{10}$$

This result is accurate away from $\psi_{\rm esc}$, whereas for $\psi \to \psi_{\rm esc}$ the photon approaches the photon sphere ($r = 3M$). The coordinate time that it takes for photons that travel initially outward, but eventually turn back and hit the surface of the object, is shown in Fig. 3 as a function of the locally measured angle ψ, and is of order $\sim M$ for most of the angles ψ, for $\epsilon \ll 1$. A closed form expression away from $\psi_{\rm crit}$, which describes well the full range (see Fig. 3) reads

$$t_{\rm roundtrip} \sim 8M \log(\cot(\psi/2)) . \tag{11}$$

When averaging over ψ, the coordinate roundtrip time is then $32M\,{\rm Cat}/\pi \approx 9.33M$, for any $\epsilon \ll 1$, where "Cat" is Catalan's constant. Remarkably, this result is independent of ϵ in the $\epsilon \to 0$ limit.

In other words, part of the light coming from *behind* a UCO is "trapped" by the photon sphere. If the central object is a good absorber, an observer staring at the object sees a "hole" in the sky with radius $r_0 = 3M$. On the other hand, radiation emitted near the surface of the object (as for example due to an accretion flow) can escape to infinity, with an escape angle that vanishes as $\Delta\Omega_{\rm esc} \sim \epsilon$ in the $\epsilon \to 0$ limit. This simple discussion anticipates that the shadow of a non-accreting UCO can be very similar to that of a BH, and that the accretion flow from ECOs with $\epsilon \to 0$ can also mimic that from an accreting BH [88].

2.3 The role of the spin

While the overall picture drawn in the previous sections is valid also for rotating objects, angular momentum introduces qualitatively new features. Spin breaks spherical symmetry, introduces frame dragging, and breaks the degeneracy between co- and counter-rotating orbits. We focus here on two properties related to the spin which are important for the phenomenology of ECOs, namely the existence of an ergoregion and the multipolar structure of compact spinning bodies.

2.3.1 Ergoregion

An infinite-redshift surface outside a horizon is called an *ergosurface* and is the boundary of the so-called *ergoregion*. In a stationary spacetime, this boundary is defined by the roots of $g_{tt} = 0$. Since the Killing vector $\xi^\mu = (1, 0, 0, 0)$ becomes spacelike in the ergoregion, $\xi^\mu \xi^\mu g_{\mu\nu} = g_{tt} > 0$, the ergosurface is also the static limit: an observer within the ergoregion cannot stay still with respect to distant stars; the observer is forced to co-rotate with the spacetime due to strong frame-dragging effects. Owing to this property, negative-energy (i.e., bound) states are possible within the ergoregion. This is the chief property that allows

for energy and angular momentum extraction from a BH through various mechanisms, e.g. the Penrose's process, superradiant scattering, the Blandford-Znajek mechanism, etc. [89]. An ergoregion necessarily exists in the spacetime of a stationary and axisymmetric BH and the ergosurface must lay outside the horizon or coincide with it [89]. On the other hand, a spacetime with an ergoregion but without an event horizon is linearly unstable (see Sec. 4.3).

2.3.2 Multipolar structure

As a by-product of the BH uniqueness and no-hair theorems [61,90] (see also [91–93]), the multipole moments of any stationary BH in isolation can be written as [94],

$$\mathcal{M}_\ell^{\rm BH} + i\mathcal{S}_\ell^{\rm BH} = M^{\ell+1}\left(i\chi\right)^\ell \,, \tag{12}$$

where $\mathcal{M}_\ell$ ($\mathcal{S}_\ell$) are the Geroch-Hansen mass (current) multipole moments [94, 95], the suffix "BH" refers to the Kerr metric, and

$$\chi \equiv \frac{\mathcal{S}_1}{\mathcal{M}_0^2} \tag{13}$$

is the dimensionless spin. Equation (12) implies that $\mathcal{M}_\ell^{\rm BH}$ ($\mathcal{S}_\ell^{\rm BH}$) vanish when ℓ is odd (even), and that all moments with $\ell \geq 2$ can be written only in terms of the mass $\mathcal{M}_0 \equiv M$ and angular momentum $\mathcal{S}_1 \equiv J$ (or, equivalently, χ) of the BH. Therefore, any independent measurement of three multipole moments (e.g. the mass, the spin and the mass quadrupole $\mathcal{M}_2$) provides a null-hypothesis test of the Kerr metric and, in turn, it might serve as a genuine strong-gravity confirmation of GR [47, 96–101].

The vacuum region outside a spinning object is not generically described by the Kerr geometry, due to the absence of an analog to Birkhoff's theorem in axisymmetry (for no-hair results around horizonless objects see Ref. [75, 102]). Thus, the multipole moments of an axisymmetric ECO will generically satisfy relations of the form

$$\mathcal{M}_\ell^{\rm ECO} = \mathcal{M}_\ell^{\rm BH} + \delta\mathcal{M}_\ell \,, \tag{14}$$

$$\mathcal{S}_\ell^{\rm ECO} = \mathcal{S}_\ell^{\rm BH} + \delta\mathcal{S}_\ell \,, \tag{15}$$

where $\delta\mathcal{M}_\ell$ and $\delta\mathcal{S}_\ell$ are model-dependent corrections, whose precise value can be obtained by matching the metric describing the interior of the object to that of the exterior.

For models of ECOs whose exterior is perturbatively close to Kerr, it has been conjectured that in the $\epsilon \to 0$ limit, the deviations from the Kerr multipole moments (with $\ell \geq 2$) vanish as [75]

$$\frac{\delta\mathcal{M}_\ell}{M^{\ell+1}} \to a_\ell \frac{\chi^\ell}{\log\epsilon} + b_\ell\,\epsilon + \dots \,, \tag{16}$$

$$\frac{\delta\mathcal{S}_\ell}{M^{\ell+1}} \to c_\ell \frac{\chi^\ell}{\log\epsilon} + d_\ell\,\epsilon + \dots \,, \tag{17}$$

or *faster*, where a_ℓ, b_ℓ, c_ℓ, and d_ℓ are model-dependent numbers which satisfy certain selection and $\mathbb{Z}_2$ rules [75]. The coefficients a_ℓ and c_ℓ are related to the spin-induced contributions to the multipole moments and are typically of order unity or smaller, whereas

the coefficients b_ℓ and d_ℓ are related to the nonspin-induced contributions. It is worth mentioning that, in all ECO models known so far, $b_\ell = d_\ell = 0$. For example, for ultracompact gravastars $b_\ell = d_\ell = 0$ for any ℓ, $a_\ell = 0$ ($c_\ell = 0$) for odd (even) values of ℓ, and the first nonvanishing terms are $a_2 = -8/45$ [103] and $c_3 = -92/315$ [104].

In other words, the deviations of the multipole moments from their corresponding Kerr value must die sufficiently fast as the compactness of the object approaches that of a BH, or otherwise the curvature at the surface will grow and the perturbative regime breaks down [75]. The precise way in which the multipoles die depends on whether they are induced by spin or by other moments.

Note that the scaling rules (16) and (17) imply that in this case a quadrupole moment measurement will always be dominated by the spin-induced contribution, unless

$$\chi \ll \sqrt{\epsilon \left| \frac{b_2}{a_2} \log \epsilon \right|}\,. \tag{18}$$

For all models known so far, $b_\ell = 0$ so obviously only the spin-induced contribution is important. Even more in general, assuming $b_2/a_2 \sim \mathcal{O}(1)$, the above upper bound is unrealistically small when $\epsilon \to 0$, e.g. $\chi \ll 10^{-19}$ when $\epsilon \approx 10^{-40}$. This will always be the case, unless some fine-tuning of the model-dependent coefficients occurs.

3 ECO taxonomy: from DM to quantum gravity

A nonexhaustive summary of possible self-gravitating compact objects is shown in Table 1. Different objects arise in different contexts. We refer the reader to specific works (e.g., Ref. [105]) for a more comprehensive review of the models.

Model	Formation	Stability	EM signatures	GWs
Fluid stars	✓ [87]	✓ [82, 85, 106–110]	✓	✓ [82, 106, 109, 111]
Anisotropic stars	✗	✓ [112–114]	✓ [115–117]	✓ [112, 116, 117]
Boson stars & oscillatons	✓ [50, 51, 118–120]	✓ [83, 121–125]	✓ [88, 126, 127]	✓ [128–135]
Gravastars	✗	✓ [124, 136]	✓ [137–139]	∼ [109, 110, 132, 133, 135, 139–145]
AdS bubbles	✗	✓ [146]	∼ [146]	✗
Wormholes	✗	✓ [147, 148]	✓ [149–152]	∼ [133, 135, 145]
Fuzzballs	✗	✗ (but see [153–156])	✗	∼ (but see [132, 145, 157])
Superspinars	✗	✓ [158, 159]	✗ (but see [160])	∼ [132, 145]
$2-2$ holes	✗	✗ (but see [161])	✗ (but see [161])	∼ [132, 145]
Collapsed polymers	✗ (but see [162, 163])	✓ [164]	✗ [163]	∼
Quantum bounces / Dark stars	✗ (but see [165, 166])	✗	✗	∼ [167]
Compact quantum objects*	✗ [70, 168, 169]	✗	✗	✓ [35]
Firewalls*	✗	✗	✗	∼ [132, 170]

Table 1: Catalogue of some proposed horizonless compact objects. A ✓ tick means that the topic was addressed. With the exception of boson stars, however, most of the properties are not fully understood yet. The symbol ∼ stands for incomplete treatment. An asterisk * stands for the fact that these objects *are* BHs, but could have phenomenology similar to the other compact objects in the list.

3.1 A compass to navigate the ECO atlas: Buchdahl's theorem

Within GR, Buchdahl's theorem states that, under certain assumptions, the maximum compactness of a self-gravitating object is $M/r_0 = 4/9$ (i.e., $\epsilon \geq 1/8$) [171]. This result prevents the existence of ECOs with compactness arbitrarily close to that of a BH. A theorem is only as good as its assumptions; one might "turn it around" and look at the assumptions of Buchdahl's theorem to find possible ways to evade it[4]. More precisely, Buchdahl's theorem assumes that [172]:

1. GR is the correct theory of gravity;
2. The solution is spherically symmetric;
3. Matter is described by a single, perfect fluid;
4. The fluid is either isotropic or mildly anisotropic, in the sense that the tangential pressure is smaller than the radial one, $P_r \gtrsim P_t$;
5. The radial pressure and energy density are non-negative, $P_r \geq 0$, $\rho \geq 0$.
6. The energy density decreases as one moves outwards, $\rho'(r) < 0$.

Giving up each of these assumptions (or combinations thereof) provides a way to circumvent the theorem and suggests a route to classify ECOs based on which of the underlying assumptions of Buchdahl's theorem they violate (see Fig. 4).

3.2 Self-gravitating fundamental fields

One of the earliest and simplest known examples of a self-gravitating compact configuration is that of a (possibly complex) minimally-coupled massive scalar field Φ, described by the action

$$S = \int d^4x\sqrt{-g}\left(\frac{R}{16\pi} - g^{\mu\nu}\bar{\Phi}_{,\mu}\Phi_{,\nu} - \frac{\mu_S^2\bar{\Phi}\Phi}{2}\right) . \tag{19}$$

The mass m_S of the scalar is related to the mass parameter as $m_S = \hbar\mu_S$, and the theory is controlled by the dimensionless coupling

$$\frac{G}{c\hbar}M\mu_S = 7.5\cdot 10^9\left(\frac{M}{M_\odot}\right)\left(\frac{m_B c^2}{\text{eV}}\right) , \tag{20}$$

where M is the total mass of the bosonic configuration.

Self-gravitating solutions for the theory above are broadly referred to as boson stars, and can be generalized through the inclusion of nonlinear self-interactions [118, 125, 173–177] (see Refs. [51, 83, 178, 179] for reviews). If the scalar is *complex*, there are *static*, spherically-symmetric geometries, while the field itself oscillates [173, 174] (for reviews, see Refs. [51, 83, 178, 179]). Analogous solutions for complex massive vector fields were also

[4] A similar approach is pursued to classify possible extensions of GR [99].

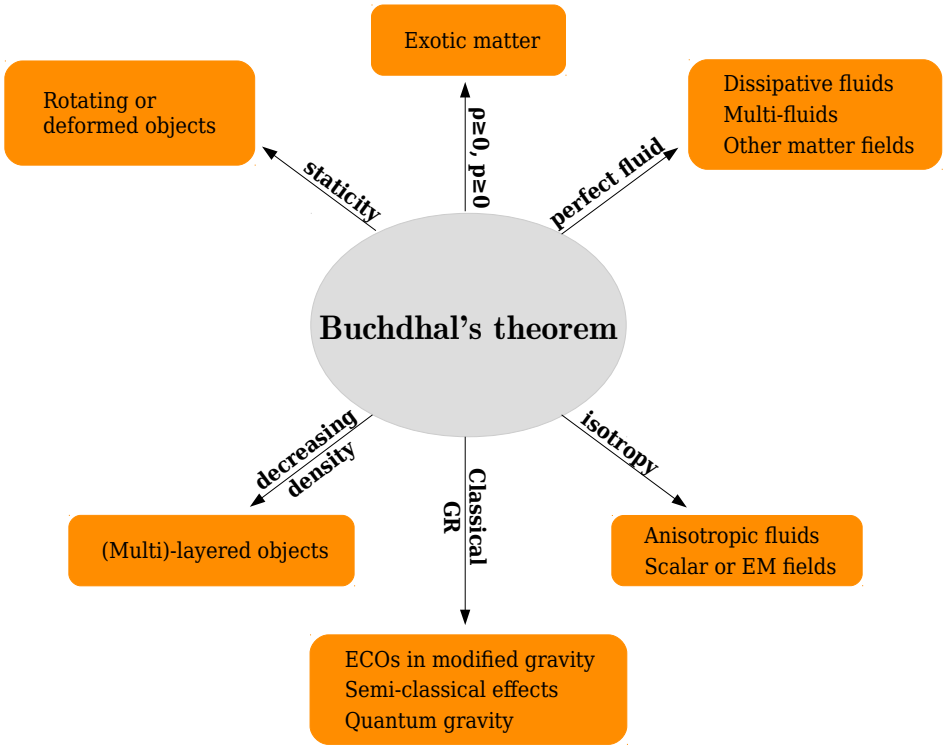


Figure 4: Buchdahl's theorem deconstructed.

shown to exist [125]. Recently, multi-oscillating boson stars which are not exactly static spacetimes were constructed, and these could represent intermediate states between static boson stars which underwent violent dynamical processes [180]. On the other hand, *real* scalars give rise to long-term stable oscillating geometries, but with a non-trivial time-dependent stress-energy tensor, called oscillatons [118]. Both solutions arise naturally as the end-state of gravitational collapse [118, 119, 181], and both structures share similar features.

Static boson stars form a one-parameter family of solutions governed by the value of the bosonic field at the center of the star. The mass M displays a maximum above which the configuration is unstable against radial perturbations, just like ordinary stars. The maximum mass and compactness of a boson star depend strongly on the boson self-interactions. As a rule of thumb, the stronger the self-interaction the higher the maximum compactness and mass of a stable boson stars [51, 179] (see Table 2).

The simplest boson stars are moderately compact in the nonspinning case [83,125,184]. Their mass-radius relation is shown in Fig. 5. Once spin [184] or nonlinear interactions [83, 182,183] are added, boson star spacetimes can have light rings and ergoregions. The stress-energy tensor of a self-interacting bosonic field contains anisotropies, which in principle allow to evade naturally Buchdahl's theorem. However, there are no boson-star solutions which evade the Buchdahl's bound: in the static case, the most compact configuration has

Model	Potential $V(\lvert\Phi\rvert^2)$	Maximum mass $M_{\rm max}/M_\odot$
Minimal [173, 174]	$\mu^2\lvert\Phi\rvert^2$	$8\left(\frac{10^{-11}\text{eV}}{m_S}\right)$
Massive [182]	$\mu^2\lvert\Phi\rvert^2+\frac{\alpha}{4}\lvert\Phi\rvert^4$	$5\sqrt{\alpha\hbar}\left(\frac{0.1\,\text{GeV}}{m_S}\right)^2$
Solitonic [183]	$\mu^2\lvert\Phi\rvert^2\left[1-\frac{2\lvert\Phi\rvert^2}{\sigma_0^2}\right]^2$	$5\left[\frac{10^{-12}}{\sigma_0}\right]^2\left(\frac{500\,\text{GeV}}{m_S}\right)$

Table 2: Scalar potential and maximum mass for some scalar boson-star models. In our units, the scalar field Φ is dimensionless and the potential V has dimensions of an inverse length squared. The bare mass of the scalar field is $m_S := \mu\hbar$. For minimal boson stars, the scaling of the maximum mass is exact. For massive boson stars and solitonic boson stars, the scaling of the maximum mass is approximate and holds only when $\alpha \gg \mu^2$ and when $\sigma_0 \ll 1$, respectively. Adapted from Ref. [133].

$r_0 \approx 2.869M$ ($\epsilon \approx 0.44$) [129].

There seem to be no studies on the classification of such configurations (there are solutions known to display photon spheres, but it is unknown whether they can be as compact as ClePhOs) [129, 184].

Because of their simplicity and fundamental character, boson stars are interesting on their own. A considerable interest in their properties arose with the understanding that light scalars are predicted to occur in different scenarios, and ultralight scalars can explain the DM puzzle [185]. Indeed, dilute bosonic configurations provide an alternative model for DM halos.

3.3 Perfect fluids

The construction of boson stars is largely facilitated by their statistics, which allow for a large number of bosons to occupy the same level. Due to Pauli's exclusion principle, a similar construction for fermions is therefore more challenging, and approximate strategies have been devised [87, 174]. In most applications, such fundamental description is substituted by an effective equation of state, usually of polytropic type, which renders the corresponding Einstein equations much easier to solve [87].

When the stresses are assumed to be isotropic, static spheres in GR made of ordinary fluid satisfy the Buchdahl limit on their compactness, $2M/r_0 < 8/9$ [171]; strictly speaking, they would not qualify as a ClePhO. However, GWs couple very weakly to ordinary matter and can travel unimpeded right down to the center of stars. Close to the Buchdahl limit, the travel time is extremely large, $\tau \sim \epsilon^{-1/2}M$, and in practice such objects would behave as ClePhOs [189]. In addition, polytrope stars with a light ring (sometimes referred to as ultra-compact stars) *always* have superluminal sound speed [107]. Neutron stars – the only object in our list for which there is overwhelming evidence – are not expected to have light rings nor behave as ClePhOs for currently accepted equations of state [85]. The mass-radius relation for a standard neutron star is shown in Fig. 5.

Some fermion stars, such as neutron stars, live in DM-rich environments. Thus, DM can be captured by the star due to gravitational deflection and a non-vanishing cross-

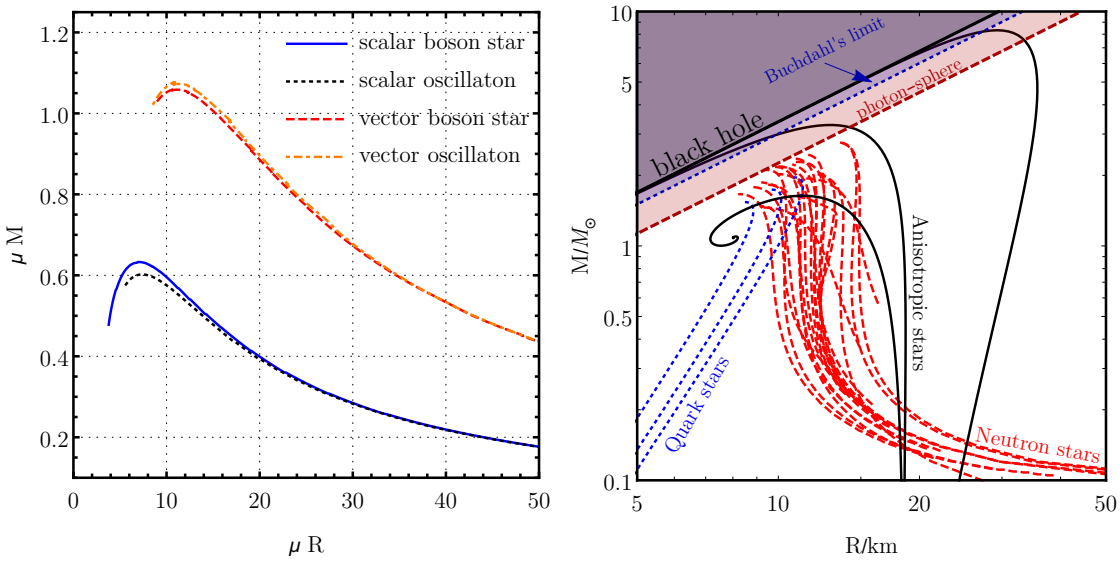


Figure 5: **Left:** Comparison between the total mass of a boson star (*complex* scalar or vector fields) and an oscillaton (*real* scalar or vector fields), as a function of their radius R. R is defined as the radius containing 98% of the total mass. The procedure to find the diagram is outlined in the main text. From Ref. [120]. **Right:** Mass-radius diagram for nonspinning fluid stars in GR. The red dashed (blue dotted) lines are ordinary NSs (quark stars) for several representative equations of state [186, 187] (data taken from [188]); the black continuous lines are strongly-anisotropic stars [112]. Note that only the latter have photon spheres in their exterior and violate Buchdahl's bound.

section for collision with the star material [190–192,192,193]. The DM material eventually thermalizes with the star, producing a composite compact object. Compact solutions made of both a perfect fluid and a massive complex [194–199] or real scalar or vector field [52,120] were built, and model the effect of bosonic DM accretion by compact stars. Complementary to these studies, accretion of fermionic DM has also been considered, by modeling the DM core with a perfect fluid and constructing a physically motivated equation of state [200–202]. The compactness of such stars is similar to that of the host neutron stars, and does not seem to exceed the Buchdahl limit.

3.4 Anisotropic stars

The Buchdahl limit can be circumvented when the object is subjected to large anisotropic stresses [203]. These might arise in a variety of contexts: at high densities [204–206], when EM or fermionic fields play a role, or in pion condensed phase configurations in neutron stars [207], superfluidity [208], solid cores [204], etc. In fact, anisotropy is common and even a simple soap bubble support anisotropic stresses [209]. Anisotropic stars were studied in GR, mostly at the level of static spherically symmetric solutions [113–116, 203, 210–218]. These studies are not covariant, which precludes a full stability analysis or nonlinear

evolution of such spacetimes. Progress on this front has been achieved recently [112, 219, 220].

The compactness of very anisotropic stars may be arbitrarily close to that of a BH; compact configurations can exceed the Buchdahl limit, and some can be classified as ClePhOs. In some of these models, compact stars exist *across a wide range of masses*, evading one of the outstanding issues with BH mimickers, i.e. that most approach the BH compactness in a very limited range of masses, thus being unable to describe both stellar-mass and supermassive BH candidates across several orders of magnitude in mass [112]. Such property of BHs in GR, visible in Fig. 5, is a consequence of the scale-free character of the vacuum field equations. It is extremely challenging to reproduce once a scale is present, as expected for material bodies. Fig. 5 summarizes the mass-radius relation for fluid stars.

3.5 Wormholes

Boson and fermion stars discussed above arise from a simple theory, with relatively simple equations of motion, and have clear dynamics. Their formation mechanism is embodied in the field equations and requires no special initial data. On the other hand, the objects listed below are, for the most part, generic constructions with a well-defined theoretical motivation, but for which the formation mechanisms are not well understood.

Wormholes were originally introduced as a useful tool to teach GR, its mathematical formalism and underlying geometric description of the universe [221–223]. Wormholes connect different regions of spacetime. They are not vacuum spacetimes and require matter. The realization that wormholes can be stabilized and constructed with possibly reasonable matter has attracted a considerable attention on these objects [222–224].

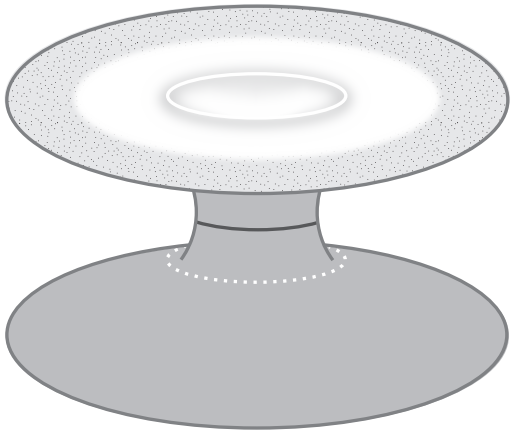


Figure 6: Embedding-like diagram of a wormhole connecting two different asymptotically-flat universes. The black solid line denotes the wormhole's throat. There are two light rings in the spacetime, one for which universe.

Different wormhole spacetimes can have very different properties. Since we are interested in understanding spacetimes that mimic BHs, consider the following two simple examples of a non-spinning geometries [145,222,225]. In the first example, we simply take the Schwarzschild geometry describing a mass M down to a "throat" radius $r_0 > 2M$. At r_0, we "glue" such spacetime to another copy of Schwarzschild. In Schwarzschild coordinates, the two metrics are identical and described by

$$ds^2 = -\left(1-\frac{2M}{r}\right)dt^2 + \left(1-\frac{2M}{r}\right)^{-1}dr^2 + r^2 d\Omega^2\,. \tag{21}$$

Because Schwarzschild's coordinates do not extend to $r < 2M$, we use the tortoise coordinate $dr/dr_* = \pm\,(1-2M/r)$, to describe the full spacetime, where the upper and lower sign refer to the two different universes connected at the throat. Without loss of generality we assume $r_*(r_0) = 0$, so that one domain is $r_* > 0$ whereas the other domain is $r_* < 0$. The surgery at the throat requires a thin shell of matter with surface density and surface pressure [226]

$$\sigma = -\frac{1}{2\pi r_0}\sqrt{1-2M/r_0}\,, \qquad p = \frac{1}{4\pi r_0}\frac{(1-M/r_0)}{\sqrt{1-2M/r_0}}\,, \tag{22}$$

Although the spacetime is everywhere vacuum (except at the throat) the junction conditions force the pressure to be large when the throat is close to the Schwarzschild radius.

A similar example, this time of a non-vacuum spacetime, is the following geometry [225]

$$ds^2 = -\left(1-\frac{2M}{r}+\lambda^2\right)dt^2 + \left(1-\frac{2M}{r}\right)^{-1}dr^2 + r^2 d\Omega^2\,. \tag{23}$$

The constant λ is assumed to be extremely small, for example $\lambda \sim e^{-M^2/\ell_P^2}$ where ℓ_P is the Planck length. There is no event horizon at $r = 2M$, such location is now the spacetime throat. Note that, even though such spacetime was constructed to be arbitrarily close to the Schwarzschild spacetime, the throat at $r = 2M$ is a region of large (negative) curvature, for which the Ricci and Kretschmann invariant are, respectively,

$$R = -\frac{1}{8\lambda^2 M^2}\,, \quad R_{abcd}R^{abcd} = \frac{1+24\lambda^4}{64\lambda^4 M^4}\,. \tag{24}$$

Thus, such invariants diverge at the throat in the small λ-limit.

The above constructions show that wormholes can be constructed to have any arbitrary mass and compactness. The procedure is oblivious to the formation mechanism, it is unclear if these objects can form without carefully tuned initial conditions, nor if they are stable. Wormholes in more generic gravity theories have been constructed, some of which can potentially be traversable [227–231]. In such theories, energy conditions might be satisfied [232].

3.6 Dark stars

Quantum field theory around BHs or around dynamic horizonless objects gives rise to phenomena such as particle creation. Hawking evaporation of astrophysical BHs, and

corresponding back-reaction on the geometry is negligible [233]. Quantum effects on collapsing *horizonless* geometries (and the possibility of halting collapse to BHs altogether) are less clear [234–240]. There are arguments that semiclassical effects might suffice to halt collapse and to produce *dark stars*, even for macroscopic configurations [28, 241–246], but see Ref. [236] for counter-arguments. For certain conformal fields, it was shown that a possible end-state are precisely wormholes of the form (23). Alternative proposals, made to solve the information paradox, argue that dark stars could indeed arise, but as a "massive remnant" end state of BH evaporation [21, 32].

3.7 Gravastars

Similar ideas that led to the proposal of "dark stars" were also in the genesis of a slightly different object, "gravitational-vacuum stars" or *gravastars* [22, 247]. These are configurations supported by a negative pressure, which might arise as an hydrodynamical description of one-loop QFT effects in curved spacetime, so they do not necessarily require exotic new physics [248]. In these models, the Buchdahl limit is evaded both because the internal effective fluid is anisotropic [249] and because the pressure is negative (and thus violates some of the energy conditions [250]). Gravastars have been recently generalized to include anti-de Sitter cores, in what was termed *AdS bubbles*, and which may allow for holographic descriptions [146, 251]. Gravastars are a very broad class of objects, and can have arbitrary compactness, depending on how one models the supporting pressure. The original gravastar model was a five-layer construction, with an interior de Sitter core, a thin shell connecting it to a perfect-fluid region, and another thin-shell connecting it to the external Schwarzschild patch. A simpler construction that features all the main ingredients of the original gravastar proposal is the thin-shell gravastar [136], in which a de Sitter core is connected to a Schwarzschild exterior through a thin shell of perfect-fluid matter. Gravastars can also be obtained as the BH-limit of constant-density stars, past the Buchdahl limit [250, 252]. It is interesting that such stars were found to be dynamically stable in this regime [252]. It has been conjectured that gravastars are a natural outcome of the inflationary universe [253], or arising naturally within the gauge-gravity duality [146, 251].

3.8 Fuzzballs and collapsed polymers

So far, quantum effects were dealt with at a semi-classical level only. A proper theory of quantum gravity needs to be able to solve some of the inherent problems in BH physics, such as the lack of unitarity in BH evaporation or the origin and nature of the huge Bekenstein-Hawking entropy $S = k_{\rm B}c^3A/(4\hbar G)$ ($k_{\rm B}$ is Boltzmann's constant and A is the BH area). In other words, what is the statistical-mechanical account of BH entropy in terms of some microscopic degrees of freedom? String theory is able to provide a partial answer to some of these questions. In particular, for certain (nearly) supersymmetric BHs, the Bekenstein-Hawking entropy, as computed in the strongly-coupled supergravity description, can be reproduced in a weakly-coupled D-brane description as the degeneracy of the relevant microstates [254–258].

Somewhat surprisingly, the geometric description of *individual microstates* seems to be regular and horizonless [23,258–261]. This led to the "fuzzball" description of classical BH geometries, where a BH is dual to an ensemble of such microstates. In this picture, the BH geometry emerges in a coarse-grained description which "averages" over the large number of coherent superposition of microstates, producing an effective horizon at a radius where the individual microstates start to "differ appreciably" from one another [262,263]. In this description, quantum gravity effects are not confined close to the BH singularity, rather the entire interior of the BH is "filled" by fluctuating geometries – hence this picture is often referred to as the "fuzzball" description of BHs.

Unfortunately, the construction of microstates corresponding to a fixed set of global charges has only been achieved in very special circumstances, either in higher-dimensional or in non asymptotically-flat spacetimes. Explicit regular, horizonless microstate geometries for asymptotically flat, four-dimensional spacetimes that could describe astrophysical bodies have not been constructed. Partly because of this, the properties of the geometries are generically unknown. These include the "softness" of the underlying microstates when interacting with GWs or light; the curvature radius or redshift of these geometries in their interior; the relevant lengthscale that indicates how far away from the Schwarzschild radius is the fuzziness relevant, etc.

A similar motivation led to the proposal of a very different BH interior in Refs. [72,162]; the interior is described by an effective equation of state corresponding to a gas of highly excited strings close to the Hagedorn temperature. The behavior of such gas is similar to some polymers, and this was termed the collapse-polymer model for BH interiors. In both proposals, large macroscopic BHs are described by objects with a regular interior, and the classical horizon is absent. In these models, our parameter ϵ is naturally of the order $\sim \mathcal{O}(\ell_P/M) \in (10^{-39}, 10^{-46})$ for masses in the range $M \in (10, 10^8) M_\odot$.

3.9 "Naked singularities" and superspinars

Classical GR seems to be protected by Cosmic Censorship, in that evolutions leading to spacetime singularities also produce horizons cloaking them. Nevertheless, there is no generic proof that cosmic censorship is valid, and it is conceivable that it is a fragile, once extensions of GR are allowed. A particular impact of such violations was discussed in the context of the Kerr geometry describing spinning BHs. In GR, the angular momentum J of BHs is bounded from above by $J \leq GM^2/c$. In string theory however, such "Kerr bound" does not seem to play any fundamental role and could conceivably receive large corrections. It is thus possible that there are astrophysical objects where it is violated. Such objects were termed *superspinars* [264], but it is part of a larger class of objects which would arise if singularities (in the classical theory of GR) would be visible. The full spacetime description of superspinars and other such similar objects is lacking: to avoid singularities and closed-timelike curves unknown quantum effects need to be invoked to create an effective surface somewhere in the spacetime. There are indications that strong GW bursts are an imprint of such objects [265], but a complete theory is necessary to understand any possible signature.

3.10 $2-2$ holes and other geons

As we remarked already, the questioning of the BH paradigm in GR comes hand in hand with the search for an improved theory of the gravitational interaction, and of possible quantum effects. A natural correction to GR would take the form of higher-curvature terms in the Lagrangian $\mathcal{L} = R + c_1 R^2 + c_2 R_{abcd} R^{abcd} + ...$ with couplings c_j suppressed by some scale [266–268]. The study of (shell-like) matter configurations in such theories revealed the existence novel horizonless configurations, termed "2-2-holes", which closely matches the exterior Schwarzschild solution down to about a Planck proper length of the Schwarzschild radius of the object [161]. In terms of the parameter ϵ introduced above, the theory predicts objects where $\epsilon \sim (\ell_P/M)^2 \in (10^{-78}, 10^{-92})$ [161]. The existence and stability of proper star-like configurations was not studied. More generic theories result in a richer range of solutions, many of which are solitonic in nature and can be ultracompact (see e.g. Refs. [269–273]. Recently, a quantum mechanical framework to describe astrophysical, horizonless objects devoid of curvature singularities was put forward in the context of nonlocal gravity (arising from infinite derivative gravity) [238,274,275]. The corresponding stars can be ultracompact, although never reaching the ClePhO category.

3.11 Firewalls, compact quantum objects and dirty BHs

Many of the existing proposals to solve or circumvent the breakdown of unitarity in BH evaporation involve changes in the BH structure, without doing away with the horizon. Some of the changes could involve "soft" modifications of the near-horizon region, such that the object still looks like a regular GR BH [30,35,276]. However, the changes could also be drastic and involve "hard" structures localized close to the horizon such as firewalls and other compact quantum objects [31, 35, 277]. Alternatively, a classical BH with modified dispersion relations for the graviton could effectively appear as having a hard surface [278, 279]. A BH surrounded by some hard structure – of quantum origin such as firewalls, or classical matter piled up close to the horizon – behaves for many purposes as a compact horizonless object.

The zoo of compact objects is summarized in Fig. 7. In all these cases, both quantum-gravity or microscopic corrections at the horizon scale select ClePhOs as well-motivated alternatives to BHs. Despite a number of supporting arguments – some of which urgent and well founded – it is important to highlight that there is no horizonless ClePhO for which we know sufficiently well the physics at the moment.

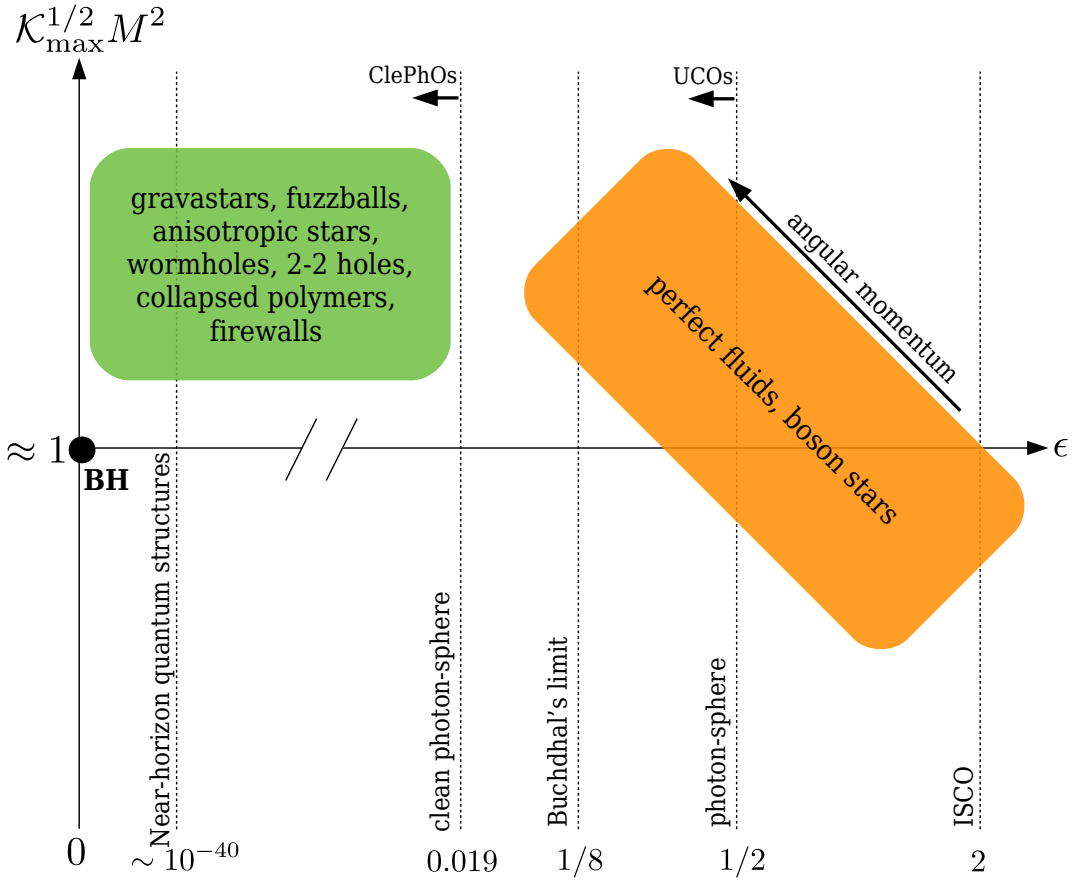


Figure 7: Schematic representation of ECO models in a compactness-curvature diagram. The horizontal axis shows the compactness parameter ϵ associated to the object, which can be also mapped (in a model-dependent way) to a characteristic light-crossing timescale. The vertical axis shows the maximum curvature (as measured by the Kretschmann scalar $\mathcal{K}$) of the object normalized by the corresponding quantity for a BH with the same mass M. All known ECO models with $\epsilon \to 0$ have large curvature in their interior, i.e. the leftmost bottom part of the diagram is conjectured to be empty. Angular momentum tends to decrease ϵ and to increase $\mathcal{K}_{\rm max}$.

4 Dynamics of compact objects

"There is a crack in everything. That's how the light gets in."
Leonard Cohen, Anthem (1992)

EM observations of compact bodies are typically performed in a context where spacetime fluctuations are irrelevant, either due to the long timescales involved or because the environment has a negligible backreaction on the body itself. For example, EM observations of accretion disks around a compact object can be interpreted using a stationary background geometry. Such geometry is a solution to the field equations describing the compact body while neglecting the accretion disk, the dynamics of which is governed by the gravitational pull of the central object and by internal forces. This approximation is adequate since the total amount of energy density around compact objects is but a small fraction of the object itself, and the induced changes in the geometry can be neglected [170]. In addition, the wavelength of EM waves of interest for Earth-based detectors is always much smaller that any lengthscale related to coherent motion of compact objects: light can be treated as a null particle following geodesics on a stationary background. Thus, the results of the previous sections suffice to discuss EM observations of compact objects, as done in Sec. 5 below.

For GW astronomy, however, it is the spacetime fluctuations themselves that are relevant. A stationary geometry approximation would miss GW emission entirely. In addition, GWs generated by the coherent motion of sources have a wavelength of the order of the size of the system. Therefore, the geodesic approximation becomes inadequate (although it can still be used as a guide). Compact binaries are the preferred sources for GW detectors. Their GW signal is naturally divided in three stages, corresponding to the different cycles in the evolution driven by GW emission [280–282]: the inspiral stage, corresponding to large separations and well approximated by post-Newtonian theory; the merger phase when the two objects coalesce and which can only be described accurately through numerical simulations; and finally, the ringdown phase when the merger end-product relaxes to a stationary, equilibrium solution of the field equations [282–284]. All three stages provide independent, unique tests of gravity and of compact GW sources. Overall, GWs are almost by definition attached to highly dynamical spacetimes, such as the coalescence and merger of compact objects. We turn now to that problem.

4.1 Quasinormal modes

Consider first an isolated compact object described by a stationary spacetime. Again, we start with the spherically-symmetric case and for simplicity. Birkhoff's theorem then implies that the exterior geometry is Schwarzschild. Focus on a small disturbance to such static spacetime, which could describe a small moving mass (a planet, a star, etc), or the late-stage in the life of a coalescing binary (in which case the disturbed "isolated compact object" is to be understood as the final state of the coalescence).

In the linearized regime, the geometry can be written as $g_{\mu\nu} = g^{(0)}_{\mu\nu} + h_{\mu\nu}$, where $g^{(0)}_{\mu\nu}$ is the geometry corresponding to the stationary object, and $h_{\mu\nu}$ are the small deviations induced on it by whatever is causing the dynamics. The metric fluctuations can be combined in a single master function Ψ which in vacuum is governed by a master partial differential equation of the form [283, 285]

$$\frac{\partial^2\Psi(t,z)}{\partial z^2} - \frac{\partial^2\Psi(t,z)}{\partial t^2} - V(r)\Psi(t,z) = S(t,z)\,. \tag{25}$$

where z is a suitable coordinate. The source term $S(t,z)$ contains information about the cause of the disturbance $\Psi(t,z)$. The information about the angular dependence of the wave is encoded in the way the separation was achieved, and involves an expansion in tensor harmonics. One can generalize this procedure and consider also scalar or vector (i.e., EM) waves. These can also be reduced to a master function of the type (25), and separation is achieved with spin-s harmonics for different spins s of field. These angular functions are labeled by an integer $l \geq |s|$. For a Schwarzschild spacetime, the effective potential is

$$V = f\left(\frac{l(l+1)}{r^2} + (1-s^2)\frac{2M}{r^3}\right)\,, \tag{26}$$

with $s = 0, \pm 1, \pm 2$ for scalar, vector or (axial) tensor modes. The $s = \pm 2$ equation does not describe completely all of the gravitational degrees of freedom. There is an another (polar) gravitational mode (in GR, there are two polarizations for GWs), also described by Eq. (25) with a slightly more complicated potential [106, 283, 286]. Note that such results apply only when there are no further degrees of freedom that couple to the GR modes [287–291].

The solutions to Eq. (25) depend on the source term and initial conditions, just like for any other physical system. We can gain some insight on the general properties of the system by studying the source-free equation in Fourier space. This corresponds to studying the "free" compact object when the driving force died off. As such, it gives us information on the late-time behavior of any compact object. By defining the Fourier transform through $\Psi(t,r) = \frac{1}{\sqrt{2\pi}}\int e^{-i\omega t}\psi(\omega,r)d\omega$, one gets the following ODE

$$\frac{d^2\psi}{dz^2} + \left(\omega^2 - V\right)\psi = 0\,. \tag{27}$$

For a Schwarzschild spacetime, the "tortoise" coordinate z is related to the original r by $dr/dz = f$, i.e.

$$z = r + 2M\log\left(\frac{r}{2M} - 1\right)\,, \tag{28}$$

such that $z(r)$ diverges logarithmically near the horizon. In terms of z, Eq. (27) is equivalent to the time-independent Schrödinger equation in one dimension and it reduces to the wave equation governing a string when $M = l = 0$. For a string of length L with fixed ends, one imposes Dirichlet boundary conditions and gets an eigenvalue problem for ω. The boundary conditions can only be satisfied for a discrete set of *normal* frequencies, $\omega = n\pi/L$ ($n = 1, 2, ...$). The corresponding wavefunctions are called normal modes and

form a basis onto which one can expand any configuration of the system. The frequency is purely real because the associated problem is conservative.

If one is dealing with a BH spacetime, the appropriate conditions (required by causality) correspond to having waves traveling outward to spatial infinity ($\Psi \sim e^{i\omega(z-t)}$ as $z \to \infty$) and inwards to the horizon ($\Psi \sim e^{-i\omega(z+t)}$ as $z \to -\infty$) [see Fig. 8]. The effective potential displays a maximum approximately at the photon sphere, $r \approx 3M$, the exact value depending on the type of perturbation and on the value of l ($r \to 3M$ in the $l \to \infty$ limit). Due to backscattering off the effective potential (26), the eigenvalues ω are not known in closed form, but they can be computed numerically [106, 283, 286]. The fundamental $l = 2$ mode (the lowest dynamical multipole in GR) of gravitational perturbations reads [292]

$$M\omega_{\rm BH} \equiv M(\omega_R + i\omega_I) \approx 0.373672 - i0.0889623\,. \tag{29}$$

Remarkably, the entire spectrum is the same for both the axial or the polar gravitational sector [286]. The frequencies are complex and are therefore called *quasinormal mode* (QNM) frequencies. Their imaginary component describes the decay in time of fluctuations on a timescale $\tau \equiv 1/|\omega_I|$, and hints at the stability of the geometry. Unlike the case of a string with fixed end, we are now dealing with an open system: waves can travel to infinity or down the horizon and therefore it is physically sensible that any fluctuation damps down. The corresponding modes are QNMs, which in general do *not* form a complete set [106].

Boundary conditions play a crucial role in the structure of the QNM spectrum. If a reflective surface is placed at $r_0 = 2M(1+\epsilon) \gtrsim 2M$, where (say) Dirichlet or Neumann boundary conditions have to be imposed, the spectrum changes considerably. The QNMs in the $\epsilon \to 0$, low-frequency limit read [293–295]

$$M\omega_R \simeq -\frac{M\pi}{2|z_0|}\left(q + \frac{s(s+1)}{2}\right) \sim |\log\epsilon|^{-1}\,, \tag{30}$$

$$M\omega_I \simeq -\beta_{ls}\frac{M}{|z_0|}(2M\omega_R)^{2l+2} \sim -|\log\epsilon|^{-(2l+3)}\,, \tag{31}$$

where $z_0 \equiv z(r_0) \sim 2M\log\epsilon$, q is a positive odd (even) integer for polar (axial) modes (or equivalently for Dirichlet (Neumann) boundary conditions), and $\beta_{ls} = \left[\frac{(l-s)!(l+s)!}{(2l)!(2l+1)!!}\right]^2$ [89, 295, 296]. Note that the two gravitational sectors are no longer isospectral. More importantly, the perturbations have smaller frequency and are much longer lived, since a decay channel (the horizon) has disappeared. For example, for $\epsilon = 10^{-6}$ we find numerically the fundamental scalar modes

$$M\omega_{\rm polar} \approx 0.13377 - i\,2.8385\times 10^{-7}\,, \tag{32}$$

$$M\omega_{\rm axial} \approx 0.13109 - i\,2.3758\times 10^{-7}\,. \tag{33}$$

These QNMs were computed by solving the exact linearized equations numerically but agree well with Eqs. (30) and (31).

The above scaling with ϵ can be understood in terms of modes trapped between the peak of the potential (26) at $r \sim 3M$ and the "hard surface" at $r = r_0$ [109, 132, 145, 295,

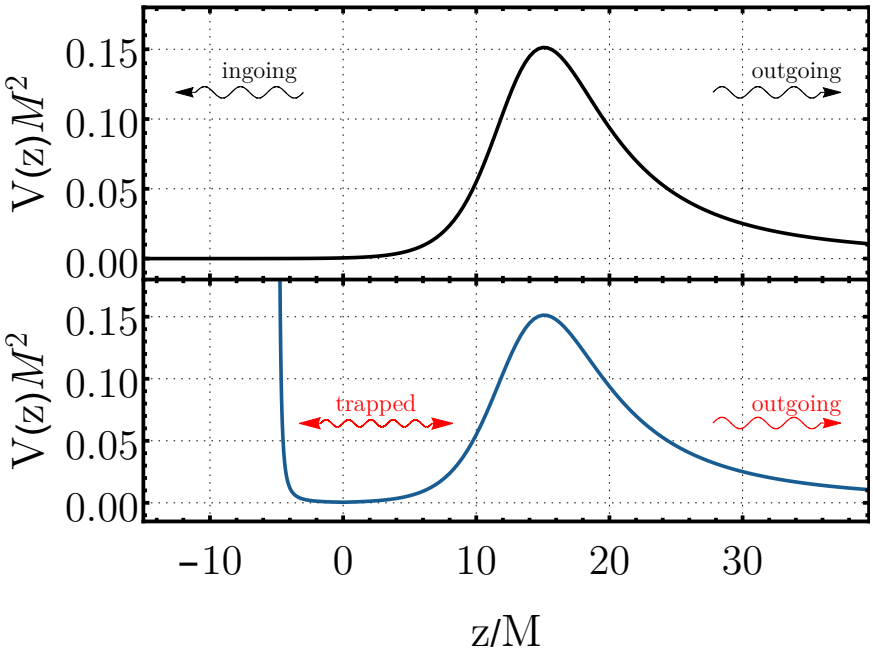


Figure 8: Typical effective potential for perturbations of a Schwarzschild BH (top panel) and of an horizonless compact object (bottom panel). The effective potential is peaked at approximately the photon sphere, $r \approx 3M$. For BHs, QNMs are waves which are outgoing at infinity ($z \to +\infty$) and ingoing at the horizon ($z \to -\infty$), whereas the presence of a potential well (provided either by a partly reflective surface, a centrifugal barrier at the center, or by the geometry) supports quasi-trapped, long-lived modes.

297] [see Fig. 8]. Low-frequency waves are almost trapped by the potential, so their wavelength scales as the size of the cavity (in tortoise coordinates), $\omega_R \sim 1/z_0$, just like the normal modes of a string. The (small) imaginary part is given by waves which tunnel through the potential and reach infinity. The tunneling probability can be computed analytically in the small-frequency regime and scales as $|\mathcal{A}|^2 \sim (M\omega_R)^{2l+2} \ll 1$ [296]. After a time t, a wave trapped inside a box of size z_0 is reflected $N = t/z_0$ times, and its amplitude reduces to $A(t) = A_0\left(1-|\mathcal{A}|^2\right)^N \sim A_0\left(1-t|\mathcal{A}|^2/z_0\right)$. Since, $A(t) \sim A_0 e^{-|\omega_I|t} \sim A_0(1-|\omega_I|t)$ in this limit, we immediately obtain

$$\omega_R \sim 1/z_0\,, \qquad \omega_I \sim |\mathcal{A}|^2/z_0 \sim \omega_R^{2l+3}\,. \tag{34}$$

This scaling agrees with exact numerical results and is valid for any l and any type of perturbation.

The reverse-engineering of the process, i.e., a reconstruction of the scattering potential V from a mode measurement was proposed in Ref. [110, 298, 299]. The impact of

measurement error on such reconstruction is yet to be assessed.

Clearly, a perfectly reflecting surface is an idealization. In certain models, only low-frequency waves are reflected, whereas higher-frequency waves probe the internal structure of the specific object [40, 300]. In general, the location of the effective surface and its properties (e.g., its reflectivity) can depend on the energy scale of the process under consideration. Partial absorption is particularly important in the case of spinning objects, as discussed in Sec. 4.3.

4.2 Gravitational-wave echoes

4.2.1 Quasinormal modes, photon spheres, and echoes

The effective potential V for wave propagation reduces to that for geodesic motion ($V_{\rm geo}$) in the high-frequency, high-angular momentum (i.e., eikonal) regime. Thus, some properties of geodesic motion have a wave counterpart [80, 81]. The instability of light rays along the null circular geodesic translates into some properties of waves around objects compact enough to feature a photon sphere. A wave description needs to satisfy "quantization conditions", which can be worked out in a WKB approximation. Since GWs are quadrupolar in nature, the lowest mode of vibration should satisfy

$$M\omega_R^{\rm geo} = 2\frac{\dot\varphi}{\dot t} = \frac{2}{3\sqrt{3}} \sim 0.3849\,. \tag{35}$$

In addition the mode is damped, as we showed, on timescales $3\sqrt{3}M$. Overall then, the geodesic analysis predicts

$$M\omega^{\rm geo} \sim 0.3849 - i\,0.19245\,. \tag{36}$$

This crude estimate, valid in principle only for high-frequency waves, matches well even the fundamental mode of a Schwarzschild BH, Eq. (29).

Nevertheless, QNM frequencies can be defined for any dissipative system, not only for compact objects or BHs. Thus, the association with photon spheres has limits, for instance it neglects possible coupling terms [287], nonminimal kinetic terms [301], etc. Such an analogy is nonetheless enlightening in the context of objects so compact that they have photon spheres and resemble Schwarzschild deep into the geometry, in a way that condition (7) is satisfied [132, 145, 302, 303].

For a BH, the excitation of the spacetime modes happens at the photon sphere [80]. Such waves travel outwards to possible observers or down the event horizon. The structure of GW signals at late times is therefore expected to be relatively simple. This is shown in Fig. 9, for the scattering of a Gaussian pulse of axial quadrupolar modes off a BH. The pulse crosses the photon sphere, and excites its modes. The ringdown signal, a fraction of which travels to outside observers, is to a very good level described by the lowest QNMs. The other fraction of the signal generated at the photon sphere travels downwards and into the horizon. It dies off and has no effect on observables at large distances.

Contrast the previous description with the dynamical response of ultracompact objects for which condition (7) is satisfied (i.e., a ClePhO) [cf. Fig. 9]. The initial description of

the photon sphere modes still holds, by causality. Thus, up to timescales of the order $|z_0| \sim -M \log \epsilon$ (the roundtrip time of radiation between the photon sphere and the surface) the signal is *identical* to that of BHs [132,145]. At later times, however, the pulse traveling inwards is bound to see the object and be reflected either at its surface or at its center. In fact, this pulse is semi-trapped between the object and the light ring. Upon each interaction with the light ring, a fraction exits to outside observers, giving rise to a series of *echoes* of ever-decreasing amplitude. From Eqs. (30)–(31), repeated reflections occur in a characteristic echo delay time [132, 145, 303] [see Fig. 10]

$$\tau_{\rm echo} \sim 4M |\log \epsilon| \,. \tag{37}$$

However, the main burst is typically generated at the photon sphere and has therefore a *frequency content* of the same order as the BH QNMs (29). The initial signal is of high frequency and a substantial component is able to cross the potential barrier. Thus, asymptotic observers see a series of echoes whose amplitude is getting smaller and whose frequency content is also going down. It is crucial to understand that echoes occur in a *transient* regime; at *very late times*, the signal is dominated by the lowest-damped QNMs, described by Eqs. (30)–(31).

We end this discussion by highlighting that GW echoes are a feature of very compact ECOs, but also arise in many other contexts: classical BHs surrounded by a "hard-structure" close to the horizon [170,277,305], or far from it [170,306,307], or embedded in a theory that effectively makes the graviton see a hard wall there [278,279] will respond to incoming GWs producing echoes. Finally, as we described earlier, even classical but very compact neutron or strange quark stars may be prone to exciting echoes [111,112,189,308].

4.2.2 A black-hole representation and the transfer function

The QNMs of a spacetime were defined as the eigenvalues of the homogeneous ordinary differential equation (27). Their role in the full solution to the homogeneous problem becomes clear once we re-write Eq. (25) in Fourier space,

$$\frac{d^2\psi}{dz^2} + \left(\omega^2 - V\right)\psi = \mathcal{S}\,, \tag{38}$$

where $\mathcal{S}$ is the Fourier transformed source term S. Since the potential is zero at the boundaries, two independent homogeneous solutions are

$$\psi_- = \begin{cases} e^{-i\omega z} & z \to -\infty \\ A_{\rm in} e^{-i\omega z} + A_{\rm out} e^{i\omega z} & z \to +\infty \end{cases}\,, \tag{39}$$

and

$$\psi_+ = \begin{cases} B_{\rm in} e^{-i\omega z} + B_{\rm out} e^{i\omega z} & z \to -\infty \\ e^{i\omega z} & z \to +\infty \end{cases}\,, \tag{40}$$

Note that ψ_+ was chosen to satisfy outgoing conditions at large distances; this is the behavior we want to impose on a system which is assumed to be isolated. On the other

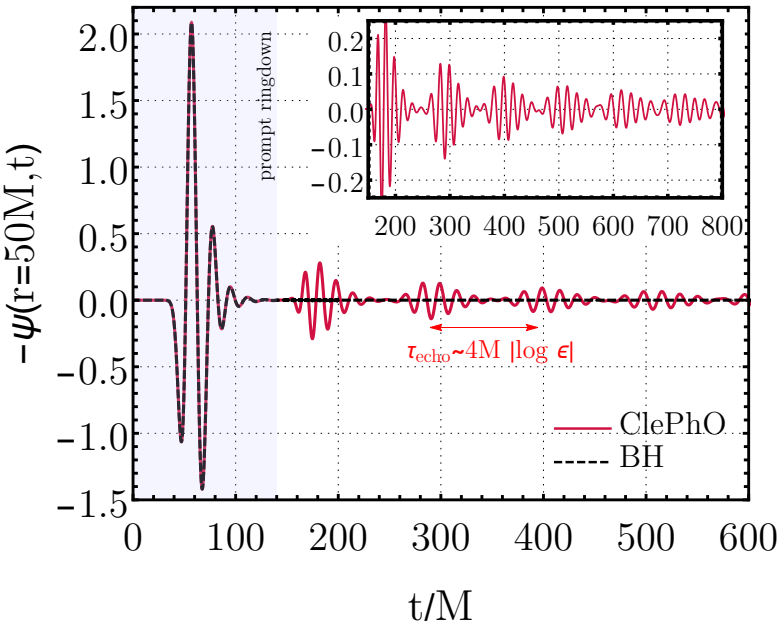


Figure 9: Ringdown waveform for a BH (dashed black curve) compared to a ClePhO (solid red curve) with a reflective surface at $r_0 = 2M(1+\epsilon)$ with $\epsilon = 10^{-11}$. We considered $l = 2$ axial gravitational perturbations and a Gaussian wavepacket $\psi(r,0) = 0$, $\dot{\psi}(r,0) = e^{-(z-z_m)^2/\sigma^2}$ (with $z_m = 9M$ and $\sigma = 6M$) as initial condition. Note that each subsequent echo has a smaller frequency content and that the damping of subsequent echoes is much larger than the late-time QNM prediction ($e^{-\omega_I t}$ with $\omega_I M \sim 4\times 10^{-10}$ for these parameters). Data available online [292].

hand, ψ_- satisfies the correct near-horizon boundary condition *in the case of a BH*. Define reflection and transmission coefficients,

$$\mathcal{R}_{\rm BH} = \frac{B_{\rm in}}{B_{\rm out}}\,, \qquad \mathcal{T}_{\rm BH} = \frac{1}{B_{\rm out}}\,. \tag{41}$$

Given the form of the ODE, the Wronskian $W \equiv \psi_-\psi_+' - \psi_-'\psi_+$ is a constant (here $' \equiv d/dz$), which can be evaluated at infinity to yield $W = 2i\omega A_{\rm in}$. The general solution to our problem can be written as [309]

$$\psi = \psi_+ \int^z \frac{\mathcal{S}\psi_-}{W} dz + \psi_- \int^z \frac{\mathcal{S}\psi_+}{W} dz + A_1\psi_- + A_2\psi_+\,, \tag{42}$$

where A_1, A_2 constants. If we impose the boundary conditions appropriate for BHs, we find

$$\psi_{\rm BH} = \psi_+ \int_{-\infty}^z \frac{\mathcal{S}\psi_-}{W} dz + \psi_- \int_z^\infty \frac{\mathcal{S}\psi_+}{W} dz\,. \tag{43}$$

This is thus the response of a BH spacetime to some source. Notice that close to the horizon the first term drops and $\psi_{\rm BH}(r\sim r_+) \sim e^{-i\omega z}\int_z^\infty \frac{\mathcal{S}\psi_+}{W} dz$. For detectors located

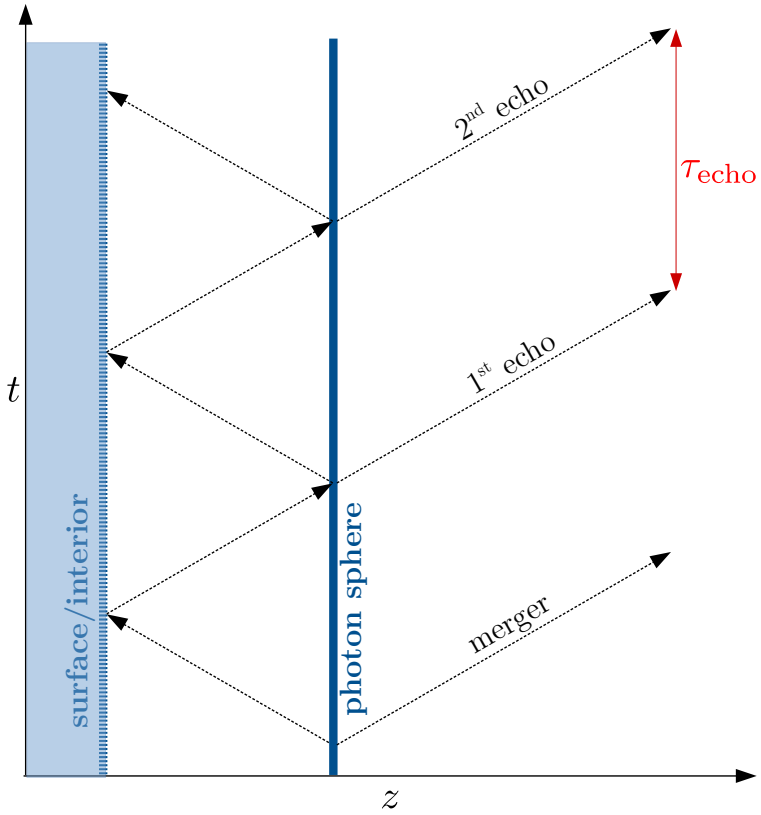


Figure 10: Schematic Penrose diagram of GW echoes from an ECO. Adapted from Ref. [304] (similar versions of this plot appeared in other contexts in Refs. [293, 297]).

far away from the source, on the other hand $\psi_{\rm BH}(r\to\infty)\sim e^{i\omega z}\int_{-\infty}^{\infty}\frac{\mathcal{S}\psi_-}{W}dz$. It is easy to see now that QNMs correspond to poles of the propagator [283], and hence they do indeed have a significant contribution to the signal, both at infinity and near the horizon.

Consider now that instead of a BH, there is an ultracompact object. Such object has a surface at r_0, corresponding to large negative tortoise z_0. Then, the boundary condition (39) on the left needs to be changed to

$$\psi_{\rm ECO}\sim e^{-i\omega z}+\mathcal{R}e^{i\omega z}\,,\quad z\to z_0\,, \tag{44}$$

where we assume the compact object surface to have a (possible frequency-dependent) reflectivity $\mathcal{R}$. We will now show that the spacetime response to an ultracompact object can be expressed in terms of the BH response and a transfer function [297] (for a previous attempt along these lines see Ref. [310]). First, notice that the ODE to be solved is exactly the same, with different conditions on one of the boundaries. We can thus still pick the two independent homogeneous solutions (39) and (40), but choose different integration

constants in (42) so that the boundary condition is satisfied. Adding a homogeneous solution $\mathcal{K}\psi_+ \int_{-\infty}^{\infty} \frac{\mathcal{S}\psi_+}{W} dz$ to (43) is allowed since it still satisfies outgoing conditions at large spatial distances. We then find at small negative z

$$\psi_{\rm ECO} = \left(e^{-i\omega z} + \mathcal{K}(B_{\rm in}e^{-i\omega z} + B_{\rm out}e^{i\omega z})\right) \int_{z_0}^{\infty} \frac{\mathcal{S}\psi_+}{W} dz \,. \tag{45}$$

where $\mathcal{K}$ is a constant. On the other hand, to obey the boundary condition (44), one must impose $\psi_{\rm ECO} = k_0 \left(e^{-i\omega z} + \mathcal{R}e^{i\omega z}\right)$ with an unknown constant k_0. Matching outgoing and ingoing coefficients, we find

$$\mathcal{K} = \frac{\mathcal{T}_{\rm BH}\mathcal{R}}{1 - \mathcal{R}_{\rm BH}\mathcal{R}} \,. \tag{46}$$

Thus, a detector at large distances sees now a signal

$$\psi_{\rm ECO}(r \to \infty) = \psi_{\rm BH}(r \to \infty) + \mathcal{K}e^{2i\omega z}\psi_{\rm BH}(r \sim r_+) \,. \tag{47}$$

In other words, the signal seen by detectors is the same as the one from a BH, modified by a piece that is controlled by the reflectivity of the compact object.

Following Ref. [297], the extra term can be expanded as a geometric series

$$\mathcal{K} = \mathcal{T}_{\rm BH}\mathcal{R} \sum_{n=1}^{\infty} (\mathcal{R}_{\rm BH}\mathcal{R})^{n-1} \,. \tag{48}$$

A natural interpretation emerges: a main burst of radiation is generated for example when an object crosses the light ring (where the peak of the effective potential is located). A fraction of this main burst is outward traveling and gives rise to the "prompt" response $\psi_{\rm BH}(r \to \infty)$, which is equivalent to the response of a BH. However, another fraction is traveling inwards. The first term is the result of the primary reflection of $\psi_{\rm BH}$ at z_0. Note the time delay factor $2(z - z_0)$ between the first pulse and the main burst due the pulse's extra round trip journey between the boundary the peak of the scattering potential, close to the light ring at $z \sim 0$. When the pulse reaches the potential barrier, it is partially transmitted and emerges as a contribution to the signal. The successive terms are "echoes" of this first reflection which bounces an integer number of times between the potential barrier and the compact object surface. Thus, a mathematically elegant formulation gives formal support to what was a physically intuitive picture.

The derivation above assumes a static ECO spacetime, and a potential which vanishes at its surface. An extension of the procedure above to include both a more general potential and spin is worked out in Ref. [311]. Recently, such a "transfer-function" representation of echoes was embedded into an effective-field-theory scheme [312], showing that linear "Robin" boundary conditions at $r = r_0$ dominate at low energies. In this method the (frequency dependent) reflection coefficient and the surface location can be obtained in terms of a single low-energy effective coupling.

The previous description of echoes and of the full signal is reasonable and describes all the known numerical results. At the technical level, more sophisticated tools are required

to understand the signal: the intermediate-time response is dominated by the BH QNMs, which are *not* part of the QNM spectrum of an ECO [145, 170, 313]. While this fact is easy to understand in the time domain due to causality (in terms of time needed for the perturbation to probe the boundaries [145]), it is not at all obvious in the frequency domain. Indeed, the poles of the ECO Green's functions in the complex frequency plane are different from the BH QNMs. The late-time signal is dominated by the dominant ECO poles, whereas the prompt ringdown is governed by the by the dominant QNMs of the corresponding BH spacetime.

4.2.3 A Dyson-series representation

The previous analysis showed two important aspects of the late-time behavior of very compact objects: (i) that it can be expressed in terms of the corresponding BH response if one uses a transfer function $\mathcal{K}$; (ii) that the signal after the main burst and precursor are a sequence of echoes, trapped between the object and the (exterior) peak of the potential.

The response of any system with a non-trivial scattering potential and nontrivial boundary conditions includes echo-like components. To see that, let's use a very different approach to solve (38), namely the Lippman-Schwinger integral solution used in quantum mechanics [314]. In this approach, the setup is that of flat spacetime, and the scattering potential is treated as a *perturbation*. In particular, the field is written as

$$\psi = \psi_0 + \int_{z_0}^{\infty} g(z,z')\, V(z')\psi(z')\, dz' \,, \tag{49}$$

where

$$g(z,z') = \frac{e^{i\omega|z-z'|} + \mathcal{R}\, e^{i\omega(z+z')}}{2i\omega} \,, \tag{50}$$

is the Green's function of the free wave operator $d^2/dx^2 + \omega^2$ with boundary condition (44), and $\psi_0 = \int_{z_0}^{\infty} g(z,z')\mathcal{S}(z')dz'$ is the free-wave amplitude. The formal solution of Eq. (49) is the Dyson series

$$\psi = \sum_{k=1}^{\infty} \int_{z_0}^{\infty} g(z,z_1)\cdots g(z_{k-1},z_k) V(z_1)\cdots V(z_{k-1})\mathcal{S}(z_k) dz_1 \cdots dz_k \,, \tag{51}$$

which effectively works as an expansion in powers of V/ω^2, so we expect it to converge rapidly for high frequencies and to be a reasonable approximation also for fundamental modes. It is possible to reorganize (51) and express it as a series in powers of $\mathcal{R}$. We start by separating the Green's function (50) into $g = g_o + \mathcal{R} g_r$, with

$$g_o(z,z') = \frac{e^{i\omega|z-z'|}}{2i\omega} \,, \tag{52}$$

the open system Green's function, and

$$g_r(z,z') = \frac{e^{i\omega(z+z')}}{2i\omega} \,, \tag{53}$$

the "reflection" Green's function. We can then write (49) as

$$\psi = \int_{z_0}^{\infty} g_o(z,z')\mathcal{S}(z')dz' + \mathcal{R}\int_{z_0}^{\infty} g_r(z,z')\mathcal{S}(z')dz' + \int_{z_0}^{\infty} g(z,z')V(z')\psi(z')dz' \,. \quad (54)$$

Now, in the same way as a Dyson series is obtained, we replace the $\psi(\omega,x')$ in the third integral with the entirety of the rhs of Eq. (54) evaluated at x'. Collecting powers of $\mathcal{R}$ yields

$$\begin{aligned}\psi &= \int g_o\mathcal{S} + \iint g_o V g_o \mathcal{S} + \mathcal{R}\left[\int g_r\mathcal{S} + \iint (g_r V g_o + g_o V g_r)\mathcal{S}\right] \\ &+ \mathcal{R}^2 \iint g_r V g_r \mathcal{S} + \iint g\, V g\, V\psi \,. \end{aligned} \quad (55)$$

If we continue this process we end up with a geometric-like series in powers of R,

$$\psi = \psi_o + \sum_{n=1}^{\infty}\psi_n \,, \quad (56)$$

with each term a Dyson series itself:

$$\psi_o = \sum_{k=1}^{\infty}\int_{z_0}^{\infty} g_o(z,z_1)\cdots g_o(z_{k-1},z_k)V(z_1)\ \cdots V(z_{k-1})\mathcal{S}(z_k)dz_1\cdots dz_k \,. \quad (57)$$

The reflectivity terms can be re-arranged as:

$$\begin{aligned}\psi_n &= \sum_{k=n}^{\infty}\frac{\mathcal{R}^n}{n!(k-n)!}\sum_{\sigma\in P_k}\int_{z_0}^{+\infty} g_r(z_{\sigma(1)-1},z_{\sigma(1)})\cdots g_r(z_{\sigma(n)-1},z_{\sigma(n)})g_o(z_{\sigma(n+1)-1},z_{\sigma(n+1)}) \\ &\cdots g_o(z_{\sigma(k)-1},z_{\sigma(k)}) \times V(x_1)\cdots V(z_{k-1})\,\mathcal{S}(z_k)\,dz_1\cdots dz_k \,, \end{aligned} \quad (58)$$

where $x_0 := x$, P_k is the permutation group of degree k and $\frac{1}{n!(k-n)!}\sum_{\sigma\in P_k}$ represents the sum on all possible distinct ways of ordering n g_r's and $k-n$ g_o's, resulting in a total of $\frac{|P_k|}{n!(k-n)!} = \binom{k}{n}$ terms [314].

Although complex-looking, Eq. (58) has a special significance, giving the amplitude of the (Fourier-transformed) n-th *echo* of the initial burst [314]. When $\mathcal{R}=0$ then $\psi=\psi_o$, the open system waveform. There are no echoes as expected. When $\mathcal{R}\neq 0$ there are additional (infinite) Dyson-series terms. The series is expected to converge, (i.e., the contribution of ψ_n becomes smaller for large n), because of two features of Eq. (58): first, if $|\mathcal{R}|<1$, $\mathcal{R}^n$ contributes to damp the contribution of large-n terms. Moreover, the Dyson series starts at $k=n$. Since g_o and g_r are of the same order of magnitude, it is natural to expect that the series starting ahead (with less terms) has a smaller magnitude and contributes less to ψ than the ones preceding them. This can be verified numerically.

Finally, an important outcome of this analysis is that echoes that arise later have a smaller frequency component than the first ones: the Dyson series is basically an expansion on powers of V/ω^2; thus by starting at $k=n$, ψ_n skips the high frequency contribution to the series until that term. This is easily explained on physical grounds: high frequency components "leak" easily from the cavity (the cavity being formed by the ultracompact object and the potential barrier). Lower frequency components are harder to tunnel out. Thus, at late times only low frequencies are present.

4.2.4 Echo modeling

The GW signal composed of echoes is a *transient* signal, which captures the transition between the photosphere ringdown. GW echoes are not well described by the QNMs of the ECO, which dominate the response only at very late times. Thus, a proper understanding of the signal in the "echoing stage" requires the full understanding of the theory and ensuing dynamics of the object. Unfortunately, as we discussed, there is a plethora of proposed candidate theories and objects, with unknown properties. Thus, the GW signal is known accurately for only a handful of special setups, and under very specific assumptions on the matter content [132,302]. For this reason the echo signal is very rich, and different approaches have been recently developed to model it.

Templates for matched-filters. The first phenomenological time-domain echo template was proposed in Ref. [304]. It is based on a standard GR inspiral-merger-ringdown template $\mathcal{M}(t)$ and five extra free parameters,

$$h(t) \equiv A \sum_{n=0}^{\infty} (-1)^{n+1} \eta^n \mathcal{M}(t + t_{\rm merger} - t_{\rm echo} - n\Delta t_{\rm echo}, t_0)\,, \tag{59}$$

with $\mathcal{M}(t, t_0) \equiv \Theta(t, t_0)\mathcal{M}(t)$ and where

$$\Theta(t, t_0) \equiv \frac{1}{2}\left\{1 + \tanh\left[\frac{1}{2}\omega(t)(t - t_{\rm merger} - t_0)\right]\right\}\,, \tag{60}$$

is a smooth cut-off function. The parameters are the following: $\Delta t_{\rm echo} = 2\tau_{\rm echo}$ is the time-interval in between successive echoes, see Eq. (37) for nonspinning objects and Eq. (73) below when rotation is included; $t_{\rm echo}$ is the time of arrival of the first echo, which can be affected by nonlinear dynamics near merger and does not necessarily coincide with $\Delta t_{\rm echo}$; t_0 is a cutoff time which dictates the part of the GR merger template used to produce the subsequent echoes; $\eta \in [0, 1]$ is the (frequency-dependent) damping factor of successive echoes; A is the overall amplitude of the echo template with respect to the main burst at the merger (at $t = t_{\rm merger}$). Finally, $\omega(t)$ is a phenomenological time-dependent mode frequency that is used in standard inspiral-merger-ringdown phenomenological models [5]. For a given model, the above parameters are not necessarily independent, as discussed below. The $(-1)^{n+1}$ term in Eq. (59) is due to the phase inversion of the truncated model in each reflection. This implies that Dirichlet boundary conditions are assumed on the surface (or, more generally, that the reflection coefficient is real and negative, see discussion in Ref. [315]). The phase inversion does not hold for Neumann-like boundary conditions or for wormholes [315]. This template was used in actual searches for echoes in the post-merger phases of LIGO/Virgo BH events, with conflicting claims discussed in Sec. 5.12. Extensions of the original template [304] have been developed and analyzed in Ref. [316].

A more phenomenological time-domain template, less anchored to the physics of echoes was proposed in Ref. [317], using a superposition of sine-Gaussians with several free parameters. This template is very generic, but on the other hand suffers from a proliferation of parameters, which should not be in fact independent.

Note that the above two templates were directly modelled for spinning ECOs, since their underlying ingredients are very similar to the nonspinning case.

A frequency-domain template for nonspinning ECOs was built in Ref. [315] by approximating the BH potential with a Pöschl-Teller potential [80,318], thus finding an analytical approximation to the transfer function defined in Eq. (48). The template construction assumes that the source is localized in space, which allows to solve for the Green's function analytically. The final form of the ECO response in the frequency domain reads

$$h(\omega) = h_{\rm BH}^{\rm ringdown}(\omega)\left[1+\mathcal{R}\frac{\pi - e^{2i\omega d}\Upsilon\cosh\left(\frac{\pi\omega_R}{\alpha}\right)}{\pi + e^{2i\omega d}\mathcal{R}\Upsilon\cosh\left(\frac{\pi\omega_R}{\alpha}\right)}\right], \tag{61}$$

where $h_{\rm BH}^{\rm ringdown}$ is the standard BH ringdown template, ω_R is the real part of the QNMs of the corresponding BH, α is a parameter of the Pöschl-Teller potential, defined by $\omega_R = \sqrt{V_0 - \alpha^2/4}$, $V_{\rm max}$ being the value of the exact potential at the maximum, d is the width of the cavity of the potential (i.e. the distance between the surface and the potential barrier) and $\Upsilon = \Gamma\left(\frac{1}{2} - i\frac{\omega+\omega_R}{\alpha}\right)\Gamma\left(\frac{1}{2} - i\frac{\omega-\omega_R}{\alpha}\right)\frac{\Gamma\left(1+\frac{i\omega}{\alpha}\right)}{\Gamma\left(1-\frac{i\omega}{\alpha}\right)}$. The above expression assumes that the source is localized near the surface, a more general expression is provided in Ref. [315]. Therefore, this template depends only on two physical inputs: the reflection coefficient $\mathcal{R}$ – which can be in general a complex function of the frequency – and the width of the cavity d, which is directly related to the compactness of the object. For a given model of given compactness, $\mathcal{R}(\omega)$ and d are fixed and the model does not contain other free parameters. For example, the damping factor introduced in the previous template can be written in terms of $\mathcal{R}$ and the reflection coefficient of the BH potential, $\mathcal{R}_{\rm BH}$ (see Eq. (41)) as $\eta = |\mathcal{R}\mathcal{R}_{\rm BH}|$ [315]. Since $\mathcal{R}_{\rm BH}$ is frequency dependent so must be η, even in the case of perfect reflectivity ($\mathcal{R} = 1$). The time-domain waveform contains all the features previously discussed for the echo signal, in particular amplitude and frequency modulation and phase inversion of each echo relative to the previous one for certain boundary conditions [315].

Note that practically all generic modeling of echoes which do not start from a first-principles calculation of the GW signal assume equal-spacing for the echoes. This seems certainly a good approximation for stationary geometries, but will fail for collapsing objects for example [73, 74].

Wavelets for burst searches. Heuristic expressions for the echoing signal are useful, but the performance of template-based search techniques is highly dependent on the (unknown, in general) "faithfulness" of such templates. Based on the excellent performance of wavelet analysis for glitch signals, Ref. [319] proposed a "morphology-independent" echo-search. The analysis is based on generalized wavelets which are "combs" of sine-Gaussians, characterized by a time separation between the individual sine-Gaussians as well as a fixed phase shift between them, an amplitude damping factor, and a widening factor. Even though actual echo signals are unlikely to resemble any single generalized wavelet and may not even have well-defined values for any of the aforementioned quantities, superpositions of generalized wavelets are expected to capture a wide variety of

physical echo waveforms. The comb is composed of a number N_G of sine-Gaussians,

$$h = \sum_{n=0}^{N_G} A\eta^n \exp\left(-(t-t_n)^2/(w^{2n}\tau^2)\right) \cos\left(2\pi f_0(t-t_n) + \phi_0 + n\Delta\phi\right), \tag{62}$$

with f_0 a central frequency, τ is a damping time, Δt the time between successive sine-Gaussians, $\Delta\phi$ is a phase difference between them, η is a damping factor between one sine-Gaussian and the next, and w is a widening factor. Here, A is an overall amplitude, t_0 the central time of the first echo and ϕ_0 a reference phase.

Searches with Fourier windows. A similar but independent search technique was devised in Ref. [311], and uses the fact that echoes should pile up power at very specific frequencies (those implied by the cavity delay time) which are nearly equally spaced (cf. Eq. (30)) (but see [73,74]). Thus, the technique consists on producing a "combing" window in Fourier space, able to match (maximizing over extrinsic parameters) the frequencies of the cavity. The specific shape of the tooth-comb was found not to be determinant, as long as it is able to capture the power in the resonant mode.

4.2.5 Echoes: a historical perspective

There exist in the literature examples of works where the main gist of the idea behind echoes is present, albeit only for specific examples and without the full appreciation of the role of the light ring. Already in 1978, the study of the instability of spinning horizonless compact objects (see Sec. 4.4.1) led to the understanding that the driving mechanism were the recurrent reflections of quasi-bound states within the ergoregion [293]. *Mutatis mutandis*, these modes produce the echoes discussed above. Indeed, a Penrose diagram similar to that Fig. 10 was already shown in Ref. [293] (without a discussion of the GW emission slowly leaking from the potential barrier).

Probably the first example of echoes dates back to 2000, with the study of axial GWs emitted during the scatter of point particles around constant-density compact stars [111]. The GW signal shows a series of clear echoes after the main burst of radiation, which are associated to the quasi-trapped s-modes of ultracompact stars [320]. The original reference did not attempt to explain the pattern in the signal, but all the results of that work fit perfectly in the description of echoes we just provided: axial modes do not couple to the fluid and travel free to the geometrical center of the star, which is therefore the effective surface in this particular case. The time delay of the echoes in Fig. 1 of Ref. [111] is very well described by the GW's roundtrip time to the center, $\tau_{\rm echo} \sim \frac{27\pi}{8}\epsilon^{-1/2}M$, where $r_0 = \frac{9}{4}M(1+\epsilon)$ is the radius of the star [189] and $r_0 = \frac{9}{4}M$ is the Buchdahl's limit [171].

Shortly after, but in a very different context, the overall picture of echoes would emerge in the fuzzball program. In Refs. [263,321], the authors express the reflection coefficient of low-energy scalars as a sum over the number of bounces at the "throat" of these geometries. The idea behind is similar to the expansion (48), and results in a series of "echoes" [321]. A quantitative calculation of the response, as well as the role of the light ring, were left undone.

In the context of wormhole physics (particularly the geometry (23)), the main features of the response of ClePhOs were identified in Ref. [225]. The postmerger train of echoes of the main burst was not addressed quantitatively.

Finally, in yet a different context, Ref. [170] discussed the late-time response of "dirty" BHs, modeling environmental effects (such as stars, gas etc) and showed that there are "secondary pulses" of radiation in the late-time response. These secondary pulses are just the echoes of a "mirrored" version of our original problem, where now it is the far region responsible for extra features in the effective potential, and hence the cavity is composed of the photosphere and the far region where matter is located.

4.3 The role of the spin

The previous sections dealt with static background spacetimes. Rotation introduces qualitatively new effects. For a Kerr BH, spinning with horizon angular velocity Ω along the azimuthal angle ϕ, perturbations are well understood using the Newman-Penrose formalism and a decomposition in so-called spin-weighted spheroidal harmonics [76, 322, 323]. It is still possible to reduce the problem to a PDE similar to Eq. (25), but the effective potential is frequency-dependent; breaks explicitly the azimuthal symmetry, i.e. it depends also on the azimuthal number m (fluctuations depend on the azimuthal angle as $\sim e^{im\phi}$); is generically complex, although there exist transformations of the perturbation variables that make it real [295, 324]; In particular, the explicit dependence on m gives rise to a Zeeman splitting of the QNMs as functions of the spin, whereas the frequency dependence gives rise to the interesting phenomenon of *superradiance* whereby modes with frequency ω are amplified when $\omega(\omega - m\Omega) < 0$. In particular, the potential is such that $V(r \to \infty) = \omega^2$, whereas $V(r \to r_+) = k^2$, with $k = \omega - m\Omega$. The relation between null geodesics and BH QNMs in the eikonal limit is more involved but conceptually similar to the static case [325].

Further features arise if the object under consideration is not a Kerr BH. In general, the vacuum region outside a spinning object is not described by the Kerr geometry. However, when $\epsilon \to 0$ any deviation from the multipolar structure of a Kerr BH must die off sufficiently fast [75, 104] (see Sec. 2.3.2). Explicit examples are given in Refs. [103, 116, 138, 139, 217, 326]. Therefore, if one is interested in the very small ϵ limit, one can study a *Kerr-like ECO* [158, 294, 304, 310], i.e. a geometry described by the Kerr metric when $r > r_0 = r_+(1 + \epsilon)$ and with some membrane with model-dependent reflective properties at $r = r_0$. Beyond the $\epsilon \to 0$ limit, ECOs may have arbitrary multipole moments and even break equatorial symmetry [75,327]. In such cases, it may not be possible to separate variables [104, 328, 329] and the results below may not hold.

4.3.1 QNMs of spinning Kerr-like ECOs

Scalar, EM and gravitational perturbations in the exterior Kerr geometry are described in terms of Teukolsky's master equations [322, 323, 330]

$$\Delta^{-s}\frac{d}{dr}\left(\Delta^{s+1}\frac{d_s R_{lm}}{dr}\right)+\left[\frac{K^2-2is(r-M)K}{\Delta}+4is\omega r-\lambda\right]\ {}_sR_{lm} = 0\,, \quad (63)$$

$$\left[\left(1-x^2\right)\ {}_sS_{lm,x}\right]_{,x}+\left[(a\omega x)^2-2a\omega sx+s+\ {}_sA_{lm}-\frac{(m+sx)^2}{1-x^2}\right]\ {}_sS_{lm} = 0\,, \quad (64)$$

where $a=\chi M$, ${}_sS_{lm}(\theta)e^{im\phi}$ are spin-weighted spheroidal harmonics, $x\equiv\cos\theta$, $K=(r^2+a^2)\omega-am$, and the separation constants λ and ${}_sA_{lm}$ are related by $\lambda\equiv\ {}_sA_{lm}+a^2\omega^2-2am\omega$. When $\chi=0$, the angular eigenvalues are $\lambda=(l-s)(l+s+1)$, whereas for $\chi\neq 0$ they can be computed numerically or with approximated analytical expansions [331].

It is convenient to make a change of variables by introducing the function [324]

$${}_sX_{lm}=\Delta^{s/2}\left(r^2+a^2\right)^{1/2}\left[\alpha\ {}_sR_{lm}+\beta\Delta^{s+1}\frac{d_sR_{lm}}{dr}\right]\,, \quad (65)$$

where α and β are certain radial functions. Introducing the tortoise coordinate r_*, defined such that $dr_*/dr=(r^2+a^2)/\Delta$, the master equation (63) becomes

$$\frac{d_s^2X_{lm}}{dr_*^2}-V(r,\omega)\ {}_sX_{lm}=0\,, \quad (66)$$

where the effective potential is

$$V(r,\omega)=\frac{U\Delta}{(r^2+a^2)^2}+G^2+\frac{dG}{dr_*}\,, \quad (67)$$

and

$$G = \frac{s(r-M)}{r^2+a^2}+\frac{r\Delta}{(r^2+a^2)^2}\,, \quad (68)$$

$$U = \frac{2\alpha'+(\beta'\Delta^{s+1})'}{\beta\Delta^s}-\frac{1}{\Delta}\left[K^2-is\Delta'K+\Delta(2isK'-\lambda)\right]\,. \quad (69)$$

The prime denotes a derivative with respect to r and the functions α and β can be chosen such that the resulting potential is *purely real* (definitions of α and β can be found in Ref. [324] and [295] for EM and gravitational perturbations respectively). It is natural to define the generalization of Eq. (44) as [295]

$$X_{\rm ECO}\sim e^{-ikz}+\mathcal{R}e^{ikz}\,,\quad z\to z_0\,, \quad (70)$$

where now $\mathcal{R}$ generically depends on the frequency and on the spin and z is the Kerr tortoise coordinate defined by $dz/dr=(r^2+a^2)/\Delta$.

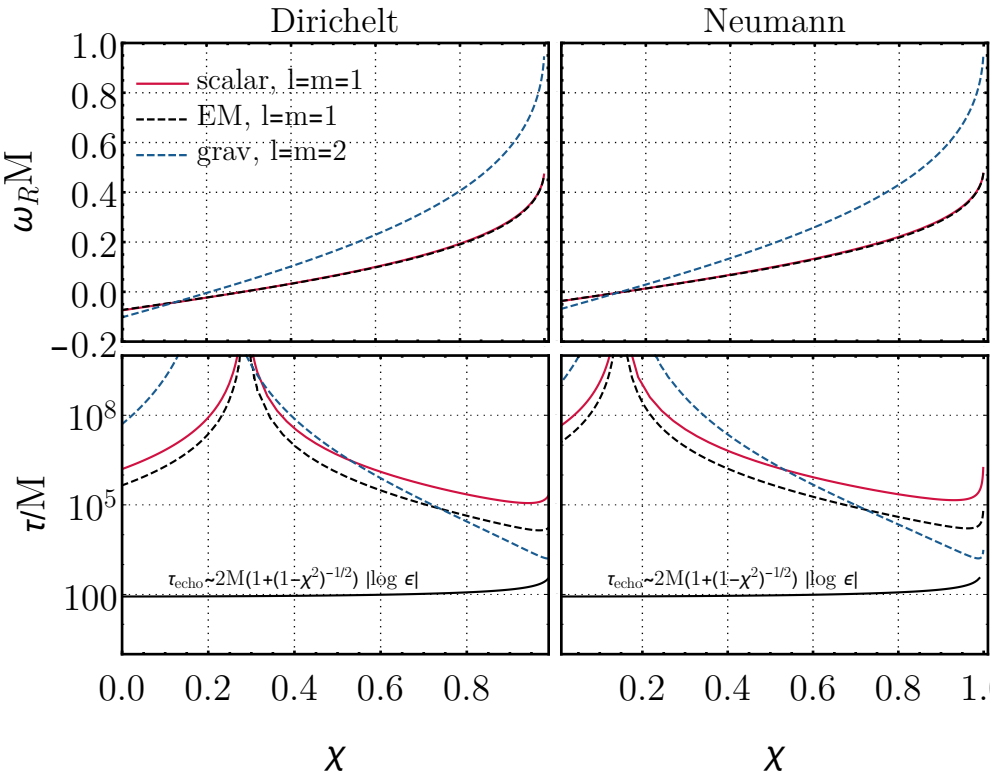


Figure 11: Frequency (top panels) and damping/growing time (bottom panels) of scalar, EM, and gravitational QNMs of a Kerr-like ECO with a perfectly reflective surface for either Dirichlet (left panels) or Neumann (right panels) boundary conditions. We choose $\epsilon = 10^{-10}$ [data adapted from Ref. [295]]. Modes are stable (i.e., they decay in time) for $\omega_R < 0$, whereas they turn unstable (i.e., they grow in time) when $\omega_R > 0$. The damping/growing time diverges for marginally stable modes, when $\omega_R = 0$. In the bottom panels, the continuous black curve represents the characteristic echo delay time, much shorter than the instability time scale.).

To search for the characteristic or QNMs of the system, Eq. (66) is to be solved with boundary condition (70) at $z \sim z_0$ and (outgoing) $X \sim e^{i\omega z}$ at infinity [295]. A small frequency approximation yields [294–296]

$$M\omega_R \simeq m\Omega - \frac{M\pi}{2|z_0|}\left(q + \frac{s(s+1)}{2}\right), \tag{71}$$

$$M\omega_I \simeq -\frac{\beta_{ls}}{|z_0|}\left(\frac{2M^2 r_+}{r_+ - r_-}\right)\left[\omega_R(r_+ - r_-)\right]^{2l+1}(\omega_R - m\Omega), \tag{72}$$

where now $z_0 \sim M[1 + (1-\chi^2)^{-1/2}]\log\epsilon$. This result shows how angular momentum can bring about substantial qualitative changes. The spacetime is unstable for $\omega_R(\omega_R - m\Omega) < 0$ (i.e., in the superradiant regime [89,332]), on a timescale $\tau_{\rm inst} \equiv 1/\omega_I$. This phenomenon

is called *ergoregion instability* [89, 332–334] (see Sec. 4.4.1 below). In the $\epsilon \to 0$ limit and for sufficiently large spin, $\omega_R \sim m\Omega$ and $\omega_I \sim |\log\epsilon|^{-2}$. Note that, owing to the $\omega_R - m\Omega$ term in Eq. (72), polar and axial modes are not isospectral in the spinning case, even when $\epsilon \to 0$: indeed, they have the same frequency but a slightly different time scale. Numerical results, shown in Fig. 11, are in excellent agreement with the above analytical approximations whenever $\omega M \ll 1$, which also implies small rotation rates [295]. For very large spins there exists a more complex analytical approximation [335]. Note that in the superradiant regime the "damping" factor, $\omega_I/\omega_R > 0$, so that, at very late times (when the pulse frequency content is indeed described by these formulas), the amplitude of the QNMs *increases* due to the instability. This effect is small – for example, $\omega_I/\omega_R \approx 4\times10^{-6}$ when $\epsilon = 0.001$, $l = 2$ and $\chi = 0.7$ – and, more importantly, it does not affect the first several echoes, since the latter appear on a timescale much shorter than the instability time scale (see Fig. 11).

4.3.2 Echoes from spinning ECOs

GW echoes from spinning ECOs have been investigated actively [304, 310, 311, 332, 336]. The overall picture is similar to the static case, with two notable differences. The echo delay time (37) now reads [304]

$$\tau_{\rm echo} \sim 2M[1 + (1-\chi^2)^{-1/2}]|\log\epsilon|\,, \tag{73}$$

in the $\epsilon \to 0$ limit. This time scale corresponds to the period of the *corotating* mode, $\tau_{\rm echo} \sim (\omega_R - m\Omega)^{-1}$. In addition, as we discussed above the spacetime is unstable over a time scale $\tau = 1/|\omega_I|$. Such timescale is parametrically longer than $\tau_{\rm echo}$ (see Fig. 11) and does not affect the first $N \approx \tau/\tau_{\rm echo} \sim |\log\epsilon|$ echoes. As we explained earlier, the signal can only be considered as a series of well-defined pulses at early stages, when the pulse still contains a substantial amount of high-frequency components. Thus, amplification occurs only at late times; the early-time evolution of the pulse generated at the photon sphere is more complex.

The transfer function of Eq. (46) can be generalized to spinning "Kerr-like" ECO subjected to boundary condition (70) near the surface. The final result reads formally the same, although $\mathcal{T}_{\rm BH}$ and $\mathcal{R}_{\rm BH}$ are defined in terms of the amplitudes of the waves scattered off the Kerr effective potential [311, 337]. Echoes from Kerr-like wormholes (i.e., a spinning extension of the Damour-Solodukhin solution [225]) have been studied in Ref. [336]. Phenomenological templates for echoes from Kerr-like objects were constructed in Refs. [304, 310, 316, 317] and are discussed in Sec. 4.2.4.

4.4 The stability problem

"There is nothing stable in the world; uproar's your only music."
John Keats, Letter to George and Thomas Keats, Jan 13 (1818)

Appealing solutions are only realistic if they form and remain as long-term stable

solutions of the theory. In other words, solutions have to be stable when slightly perturbed or they would not be observed (or they would not even form in the first place). There are strong indications that the exterior Kerr spacetime is stable, although a rigorous proof is still missing [338]. On the other hand, some – and possibly most of – horizonless compact solutions are linearly or nonlinearly unstable.

Some studies of linearized fluctuations of ultracompact objects are given in Table 1. We will not discuss specific models, but we would like to highlight some general results.

4.4.1 The ergoregion instability

Several models of UCOs and ClePhOs are stable under *radial* perturbations [85, 136] (see Table 1). However, UCOs (and especially ClePhOs) can develop negative-energy regions once spinning. In such a case, they develop a *linear* instability under *non-radial* perturbations, which is dubbed as ergoregion instability. Such instability affects any horizonless geometry with an ergoregion [124, 294, 332–334, 339] and is deeply connected to superradiance [89]. The underlying mechanism is simple: a negative-energy fluctuation in the ergoregion is forced to travel outwards; at large distances only positive-energy states exist, and energy conservation implies that the initial disturbance gives rise to a positive fluctuation at infinity plus a larger (negative-energy) fluctuation in the ergoregion. Repetition of the process leads to a cascading instability. The only way to prevent such cascade from occurring is by absorbing the negative energy states, which BHs do efficiently (and hence Kerr BHs are stable against massless fields), but perfectly-reflecting horizonless objects must then be unstable.

This instability was discovered by Friedman for ultracompact slowly-rotating stars with an ergoregion [340], and later extended in Refs. [341, 342]. Application to Kerr-like horizonless objects started in Ref. [293], whereas an analysis for gravastars, boson stars, and other objects was done in Refs. [124, 153, 158, 343]. More recently, Refs. [294, 295] gave a detailed analysis of scalar, electromagnetic, and gravitational perturbations of a partially-reflective Kerr-like ECO in the $\epsilon \to 0$ limit.

The overall summary of these studies is that the instability time scale depends strongly on the spin and on the compactness of the objects. The ergoregion-instability timescale can very long [124,294,333]. For concreteness, for gravastars with $\epsilon \sim 0.1-1$ the ergoregion is absent even for moderately high spin [343]. However, at least for perfectly-reflecting Kerr-like ECOs in the $\epsilon \to 0$ limit, the critical spin above which the object is unstable is very low [295] [see Eq. (72)]

$$\chi_{\rm crit} \sim \frac{\pi}{m|\log\epsilon|}\left(q+\frac{s(s+1)}{2}\right) . \tag{74}$$

For example, a totally reflecting surface a Planck length outside the horizon of a $10M_\odot$ ECO ($\epsilon = l_P/r_+ \approx 5\times 10^{-40}$) will generate an ergoregion instability if $\chi \gtrsim 0.07$ for $q=1$, $m=1$, and $s=-2$. Note that the instability time scale can be very large near the instability threshold. From Eq. (72), we can estimate the timescale of the instability of a spinning ClePhO,

$$\tau_{\rm inst} \equiv \frac{1}{\omega_I} \sim -|\log\epsilon| \frac{1+(1-\chi^2)^{-1/2}}{2\beta_{ls}} \left(\frac{r_+-r_-}{r_+}\right) \frac{[\omega_R(r_+-r_-)]^{-(2l+1)}}{\omega_R - m\Omega} . \tag{75}$$

As previously discussed, a spinning ClePhO is (superradiantly) unstable only above a critical value of the spin. For example, for $l = m = s = 2$ and $\chi = 0.7$, the above formula yields

$$\tau \in (5, 1) \left(\frac{M}{10^6 M_\odot} \right) \text{ yr} \quad \text{when} \quad \epsilon \in (10^{-45}, 10^{-22}) \,. \tag{76}$$

Generically, the ergoregion instability acts on timescales which are parametrically longer than the dynamical timescale, $\sim M$, of the object, but still short enough to be relevant in astrophysical scenarios. Although the evolution of this instability remains an open problem, it is likely that it will remove angular momentum from the object, spinning it down until the threshold condition, $\chi = \chi_{\rm crit}$, is reached [344]. The phenomenological consequences of this phenomenon will be discussed in Sec. 5.

A possible way to quench the instability is by absorbing the negative-energy modes trapped within the ergoregion. Kerr BHs can absorb such modes efficiently and are indeed expected to be stable even if they have an ergoregion. Given its long timescales, it is possible that the instability can be efficiently quenched by some dissipation mechanism of nongravitational nature, although this effect would be model-dependent [294, 295]. Unfortunately, the effect of viscosity in ECOs is practically unknown [82,345], and so are the timescales involved in putative dissipation mechanisms that might quench this instability. It is also possible that, when spinning, a partially-absorbing object can support quasi-trapped superradiant modes with $\omega_R < m\Omega$, which might lead to an instability similar to that of massive bosonic fields around Kerr BHs [89].

Finally, there are indications that instabilities of UCOs are merely the equivalent of Hawking radiation for these geometries, and that therefore there might be a smooth transition in the emission properties when approaching the BH limit [154, 225].

4.4.2 Nonlinear instabilities I: long-lived modes and their backreaction

Linearized gravitational fluctuations of any nonspinning UCO are extremely long-lived and decay no faster than logarithmically [82, 155, 156, 346]. Indeed, such perturbations can be again understood in terms of modes quasi-trapped within the potential barrier shown in Fig. 8: they require a photon sphere but are absent in the BH case (hence the photon sphere is sometimes referred to as "loosely trapped" or "transversely trapping" surface [347,348]). For a ClePhO, these modes are very well approximated by Eqs. (30)–(31) in the static case and by their aforementioned extension in the spinning case. The long damping time of these modes has led to the conjecture that any UCO is *nonlinearly* unstable and may evolve through a Dyson-Chandrasekhar-Fermi type of mechanism [82,346]. The endstate is unknown, and most likely depends on the equation of the state of the particular UCO: some objects may fragment and evolve past the UCO region into less compact configurations, via mass ejection, whereas other UCOs may be forced into gravitational collapse to BHs.

The above mechanism is supposed to be active for any spherically symmetric UCO, and also on spinning solutions. However, it is nonlinear in nature and not well understood so far. For example, there are indications that a putative nonlinear instability would occur on very long timescales only; a model problem predicts an exponential dependence on the size of the initial perturbation [349].

4.4.3 Nonlinear instabilities II: causality, hoop conjecture, and BH formation

The teleological nature of horizons leads to possible spacelike behavior in the way they evolve. In turn, this has led to constraints on the possible compactness of horizonless objects. Ref. [350] finds the conceptual bound

$$\epsilon \leq 4\dot{M}\,, \tag{77}$$

based on a special accreting geometry (so-called Vaidya spacetime) and on the requirement that the surface of the accreting ECO grows in a timelike or null way. The assumptions behind such result are relatively strong: the accreting matter is a very particular null dust, eternally accreting at a constant rate and without pressure. In addition, superluminal motion for the ECO *surface* is not forbidden, and may well be a rule for such compact geometries.

A different, but related, argument makes use of the hoop conjecture [351] (which, in broad terms, states that if a body is within its Schwarzschild radius, then it must be a BH [130, 352]). Take two ECOs of mass $m_2 \ll m_1$, inspiralling to produce a single ECO. The burst of energy emitted in ringdown modes is of order [281]

$$\frac{E_{\rm ringdown}}{m_1+m_2} \sim 0.44 \left(\frac{m_1 m_2}{(m_1+m_2)^2}\right)^2\,, \tag{78}$$

This estimate holds for BHs, and it seems plausible that it would approximately holds also for ECOs. A similar amount of energy goes *inwards*. Then, when the small body crosses the photon sphere of the large ECO, an amount of mass (78) is emitted inwards and is swallowed by the large ECO increasing its mass to $m_1 + E_{\rm ringdown}$. The hoop conjecture implies that $2(m_1 + E_{\rm ringdown}) \leq 2m_1(1+\epsilon)$, or

$$\epsilon \gtrsim 0.44 \frac{m_2^2}{m_1^2}\,, \tag{79}$$

to avoid BH formation. Thus, ϵ of Planckian order are not allowed. There are issues with this type of arguments: The GWs are not spherical and not localized (their wavelength is of the order or larger than the ECO itself), thus localizing it on a sphere of radius $2m_1(1+\epsilon)$ is impossible. Furthermore, the argument assume that all energy reaching the surface is accreted, whereas it might be efficiently absorbed by other channels.

The above argument can be made more powerful, making full use of the hoop conjecture: take two ECOs and boost them to large enough energies. Since all energy gravitates and is part of the hoop, the final object must be inside its Schwarzschild radius, hence it must be a BH (indeed, at large enough center of mass energies, the structure of the colliding objects is irrelevant [130, 353, 354]). It is very challenging to bypass this argument at a classical level. Nevertheless: (i) the argument does not forbid the existence of ECOs, it merely forces their interaction at high energy to result in BH formation; (ii) Most of the lines of reasoning for ECO formation (and existence) rely directly or indirectly on unknown quantum effects *associated with horizon or singularity formation* [167]. Thus, it is expected that horizons may form classically but that such picture is blurred by quantum effects (on presently unknown timescales and due to presently unknown dynamics).

4.5 Binary systems

Consider a compact binary of masses m_i ($i = 1, 2$), total mass $m = m_1 + m_2$, mass ratio $q = m_1/m_2 \geq 1$, and dimensionless spins χ_i. In a post-Newtonian (PN) approximation (i.e. a weak-field/slow-velocity expansion of Einstein's equations), dynamics is driven by energy and angular momentum loss, and particles are endowed with a series of multipole moments and with finite-size tidal corrections [355]. Up to 1.5PN order, the GW phase depends only on m_i and χ_i and is oblivious to the compactness of the binary components. Starting from 2PN order, the nature of the inspiralling objects is encoded in:

(i) the way they respond to their own gravitational field – i.e., on their own multipolar structure [356–358];

(ii) the way they respond when acted upon by the external gravitational field of their companion – through their tidal Love numbers (TLNs) [359];

(iii) on the amount of radiation that they possibly absorb, i.e. on tidal heating [360,361].

These effects are all included in the waveform produced during the inspiral, and can be incorporated in the Fourier-transformed GW signal as

$$\tilde{h}(f) = \mathcal{A}(f) e^{i(\psi_{\rm PP}+\psi_{\rm TH}+\psi_{\rm TD})} \,, \tag{80}$$

where f and $\mathcal{A}(f)$ are the GW frequency and amplitude, $\psi_{\rm PP}(f)$ is the "pointlike" phase [355], whereas $\psi_{\rm TH}(f)$, $\psi_{\rm TD}(f)$ are the contributions of the tidal heating and the tidal deformability, respectively.

4.5.1 Multipolar structure

Spin-orbit and spin-spin interactions are included in $\psi_{\rm PP}$, the latter also depending on all higher-order multipole moments. The dominant effect is that of the spin-induced quadrupole moment, M_2, which yields a 2PN contribution to the phase [356]

$$\psi_{\rm quadrupole} = \frac{75}{64} \frac{\left(m_2 M_2^{(1)} + m_1 M_2^{(2)}\right)}{(m_1 m_2)^2} \frac{1}{v} \,, \tag{81}$$

where the expansion parameter $v = (\pi m f)^{1/3}$ is the orbital velocity. By introducing the dimensionless spin-induced, quadrupole moment, $\bar{M}_2^{(i)} = M_2^{(1)}/(\chi_i^2 m_i^3)$, it is clear that the above correction is quadratic in the spin. For a Kerr BH, $\bar{M}_2^{(i)} = -1$, whereas for an ECO there will be generic corrections that anyway are bound to vanish as $\epsilon \to 0$ [75] (Sec. 2.3.2).

4.5.2 Tidal heating

A spinning BH absorbs radiation of frequency $\omega > m\Omega$, but amplifies radiation of smaller frequency [89]. In this respect, BHs are dissipative systems which behave just like a Newtonian viscous fluid [362,363]. Dissipation gives rise to various interesting effects in a

binary system – such as tidal heating [360,361], tidal acceleration, and tidal locking, as in the Earth-Moon system, where dissipation is provided by the friction of the oceans with the crust.

For low-frequency circular binaries, the energy flux associated to tidal heating at the horizon, $\dot{E}_H$, corresponds to the rate of change of the BH mass [364,365],

$$\dot{M} = \dot{E}_H \propto \frac{\Omega_K^5}{M^2}(\Omega_K - \Omega)\,, \tag{82}$$

where $\Omega_K \ll 1/M$ is the orbital angular velocity and the (positive) prefactor depends on the masses and spins of the two bodies. Thus, tidal heating is stronger for highly spinning bodies relative to the nonspinning by a factor $\sim \Omega/\Omega_K \gg 1$.

The energy flux (82) leads to a potentially observable phase shift of GWs emitted during the inspiral. The GW phase ψ is governed by $d^2\psi/df^2 = 2\pi(dE/df)/\dot{E}$, where $E \sim v^2$ is the binding energy of the binary. To the leading order, this yields (for circular orbits and spins aligned with the orbital angular momentum) [135]

$$\psi_{\rm TH}^{\rm BH} = \psi_{\rm N}\left(F(\chi_i,q)v^5\log v + G(q)v^8[1-3\log v]\right)\,, \tag{83}$$

where $\psi_{\rm N} \sim v^{-5}$ is the leading-order contribution to the point-particle phase (corresponding to the flux $\dot{E}_{\rm GW}$), and

$$F(\chi_i,q) = -\frac{10\left(q^3\left(3\chi_1^3+\chi_1\right)+3\chi_2^3+\chi_2\right)}{3(q+1)^3}\,, \tag{84}$$

$$G(\chi_i,q) = \frac{10}{27(q+1)^5}\left[q^5A_1 + A_2 + q^4B_1 + qB_2 + q^3C_1 + q^2C_2\right]\,, \tag{85}$$

with

$$A_i = 2\left(3\chi_i^2+1\right)\left(3-10\chi_i^2+3\Delta_i\right)\,, \tag{86}$$

$$B_i = 3\left(3\chi_i^2+1\right)\left(2-5\chi_i^2+2\Delta_j-5\chi_i\chi_j\right)\,, \tag{87}$$

$$C_i = -20\left(3\chi_i^2+1\right)\chi_i\chi_j\,, \tag{88}$$

$\Delta_i \equiv \sqrt{1-\chi_i^2}$ and $j \neq i$. Therefore, absorption at the horizon introduces a 2.5PN (4PN)$\times\log v$ correction to the GW phase of spinning (nonspinning) binaries, relative to the leading term.

Thus, it might be argued that an ECO binary can be distinguished from a BH binary, because $\dot{E}_H = 0$ for the former. However, the trapping of radiation in ClePhOs can efficiently mimic the effect of a horizon [135]. In order for absorption to affect the orbital motion, it is necessary that the time radiation takes to reach the companion, $T_{\rm rad}$, be much longer than the radiation-reaction time scale due to heating, $T_{\rm RR} \simeq E/\dot{E}_H$, where $E \simeq -\frac{1}{2}M(M\Omega_K)^{2/3}$ is the binding energy of the binary (assuming equal masses). For BHs, $T_{\rm rad} \to \infty$ because of time dilation, so that the condition $T_{\rm rad} \gg T_{\rm RR}$ is always satisfied. For ClePhOs, $T_{\rm rad}$ is of the order of the GW echo delay time, Eq. (73), and therefore increases logarithmically as $\epsilon \to 0$. Thus, an effective tidal heating might occur

even in the absence of a horizon if the object is sufficient compact. The critical value of ϵ increases strongly as a function of the spin. For orbital radii larger than the ISCO, the condition $T_{\rm rad} \gg T_{\rm RR}$ requires $\epsilon \ll 10^{-88}$ for $\chi \lesssim 0.8$, and therefore even Planck corrections at the horizon scale are not sufficient to mimic tidal heating. This is not necessarily true for highly spinning objects, for example $T_{\rm rad} \gg T_{\rm RR}$ at the ISCO requires $\epsilon \ll 10^{-16}$ for $\chi \approx 0.9$.

4.5.3 Tidal deformability and Love numbers

Finally, the nature of the inspiralling objects is also encoded in the way they respond when acted upon by the external gravitational field of their companion – through their tidal Love numbers (TLNs) [359]. An intriguing result in classical GR is that the TLNs of BHs are zero. This result holds: (i) in the nonspinning case for weak tidal fields [366, 367] and also for tidal fields of arbitrary amplitude [368]; (ii) in the spinning case [369–371] for weak tidal fields, at least in the axisymmetric case to second order in the spin [370] and generically to first order in the spin [371]. On the other hand, the TLNs of ECOs are small but finite [35, 103, 133, 139, 372, 373].

In spherical symmetry, the TLNs can be defined as the proportionality factor between the induced mass quadrupole moment, M_2, and the (quadrupolar) external tidal field, E_2. Let us consider the mutual tides induced on the two bodies of a binary system at orbital distance r due to the presence of a companion. In this case

$$M_2^{(1)} = \lambda_1 E_2^{(2)} \qquad M_2^{(2)} = \lambda_2 E_2^{(1)} \,, \tag{89}$$

where λ_i is the tidal deformability parameter of the i-th body. At Newtonian order, the external tidal field produced by the i-th object on its companion is simply

$$E_2^{(i)} \sim \frac{m_i}{r^3} \propto v^6 \,. \tag{90}$$

The above results can be used to compute the contributions of the tidal deformability to the binding energy of the binary, $E(f)$, and to the energy flux dissipated in GWs, $\dot{E}$. The leading-order corrections read [374]

$$E(f) = -\frac{mq}{2(1+q)^2} v^2 \left(1 - \frac{6q(k_1 q^3 + k_2)}{(1+q)^5} v^{10}\right) , \tag{91}$$

$$\dot{E}(f) = -\frac{32}{5} \frac{q^2}{(1+q)^4} v^{10} \left(1 + \frac{4\left(q^4(3+q)k_1 + (1+3q)k_2\right)}{(1+q)^5} v^{10}\right) , \tag{92}$$

where k_i is the (dimensionless) TLN of the $i-$th object, defined as $\lambda_i = \frac{2}{3} k_i m_i^5$. By plugging the above equations in $\frac{d^2\psi(f)}{df^2} = \frac{2\pi}{\dot{E}} \frac{dE}{df}$, we can solve for the tidal phase to leading order,

$$\psi_{\rm TD}(f) = -\psi_{\rm N} \frac{624\Lambda}{m^5} v^{10} \,, \tag{93}$$

where $39\Lambda = (1 + 12/q)\, m_1^5 k_1 + (1 + 12q) m_2^5 k_2$ is the weighted tidal deformability. Thus, the tidal deformability of the binary components introduces a 5PN correction (absent

in the BH case) to the GW phase relative to the leading-order GW term. This can be understood by noticing that the v^6 term in Eqs. (89) and (90) multiplies the $1/v$ term in Eq. (81), giving an overall factor v^5 which is a 5PN correction relative to $\psi_{\rm N} \sim v^{-5}$. This derivation is valid for nonspinning objects, the effect of spin is suppressed by a further 1.5PN order and introduces new classes of *rotational TLNs* [369, 371, 375–377].

The TLNs of a nonspinning ultracompact object of mass M and radius $r_0 = 2M(1+\epsilon)$ (with $\epsilon \ll 1$) in Schwarzschild coordinates vanish logarithmically in the BH limit [133], $k \sim 1/|\log\epsilon|$, opening the way to probe horizon scales. This scaling holds for any ECO whose exterior is governed (approximately) by vacuum-GR equations, and with generic Robin-type boundary conditions on the Zerilli function Ψ at the surface, $a\Psi + b\frac{d\Psi}{dz} = c$ [378]. In this case, in the $\epsilon \to 0$ limit one gets

$$k \sim \frac{2(4a-3c)}{15a\log\epsilon}\,. \tag{94}$$

Particular cases of the above scaling are given in Table I of Ref. [133]. Thus, the only exception to the logarithmic behavior concerns the zero-measure case $a = \frac{3}{4}c$, for which $k \sim \epsilon/\log\epsilon$. No ECO models described by these boundary conditions are known.

Such generic logarithmic behavior acts as a *magnifying glass* to probe near-horizon quantum structures [133, 135]. Since $k \sim \mathcal{O}(10^{-3} - 10^{-2})$ when $\epsilon \sim \ell_P/M$. As a comparison, for a typical neutron star $k_{\rm NS} \approx 200$, and probing quantum structures near the horizon will require a precision about 4 orders of magnitude better than current LIGO constraints [379]. Prospects to detect this effect are discussed in Sec. 5.8. The logarithmic mapping between k and ϵ makes it challenging constraint ϵ from measurements of the TLNs, because measurements errors propagate exponentially [135,380]. Nevertheless, this does not prevent to distinguish ECOs from BHs using TLNs, nor to perform model selection between different ECO models all with new microphysics at the Planck scale [378].

This is shown in Fig. 12 – inspired by standard analysis to discriminate among neutron-star equations of state [381,382]. The figure shows the tidal deformability $\lambda = \frac{2}{3}M^5|k|$ as a function of the object mass for three different toy models (gravastars, wormholes, and perfectly-reflecting Schwarzschild-like ECOs) characterized by the same Planckian scale of the correction, $\delta \equiv r_0 - 2M = \ell_P \approx 1.6 \times 10^{-33}\,{\rm cm}$.

To summarize, finite-size effects in the inspiral waveform provide three different null-hypothesis tests of BHs. BHs have vanishing TLNs but introduce a nonzero tidal heating ($\psi_{\rm TD} = 0$, $\psi_{\rm TH} \neq 0$), while ECOs have (logarithmically small) TLNs but zero tidal heating ($\psi_{\rm TD} \neq 0$, $\psi_{\rm TH} = 0$). In addition BHs have a very well defined set of multipole moments which depend on only two parameters (mass and angular momentum), whereas ECOs have in principle limitless possibilities. In addition, it is possible that the inspiral excites the characteristic modes of each of the objects, i.e., their QNMs. The extent to which this happens, and its impact on the inspiral stage are still to be understood [383].

The TLNs were computed for boson stars [133, 134, 384], very compact anisotropic fluid stars [112], and gravastars [133, 139]. The TLNs of simple-minded ultracompact Schwarzschild-exterior spacetimes with a stiff equation of state at the surface were computed in Ref. [133]. The TLNs of spacetimes mimicking "compact quantum objects" were recently investigated [35].

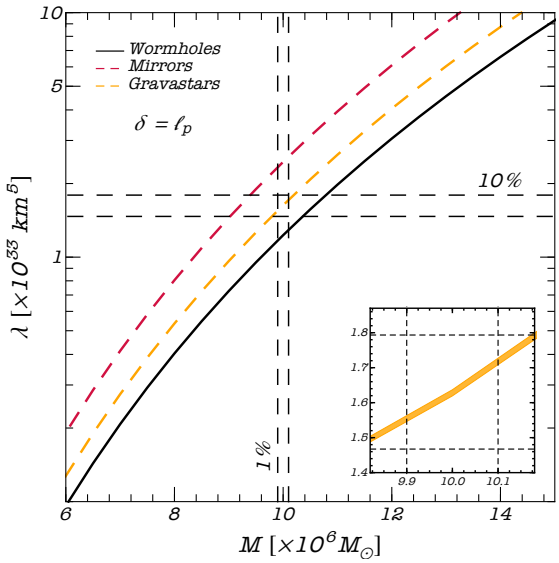


Figure 12: Tidal deformability λ as a function of the mass for three toy models of ECOs. For all models the surface is at Planckian distance from the Schwarzschild radius, $r_0 - 2M = \ell_P$. The dashed lines refer to a putative measurement of the TLN at the level of 10% for an object with $M = 10^7 M_\odot$, which would allow to distinguish among different models at more than 90% confidence level. The zoomed inset resolves the thickness of each curve, with a width given by the intrinsic error due to the quantum uncertainty principle [380]. Adapted from Ref. [378].

4.5.4 Accretion and drag in inspirals around and inside DM objects

When an object moves through any medium, it will be subject to (at least) two types of drag. One is direct and caused by accretion: the accreting object grows in mass and slows down. In addition, the moving body exerts a gravitational pull on all the medium, the backreaction of which produces dynamical friction (known also as "gravitational drag"), slowing the object down. To quantify these effects, it is important to know how the medium behaves. Collisionless media cause, generically, a gravitational drag different from that of normal fluids [83, 131]. The gravitational drag caused by media which is coherent on large scales may be suppressed [185], but further work is necessary to understand this quantitatively.

Consider now a binary of two compact objects, in which one is made of DM. At large separations inspiral will be driven mostly by GW emission. However, at small distances, the dynamics will generically be dominated by accretion and gravitational drag. The phase evolution of a binary, taking gravitational radiation, accretion and drag was studied when a small BH or neutron star inspirals around *and inside* a massive boson star [83,131]. These results can also be directly translated to inspirals within a DM environment [83, 131, 170, 385–387]. Full nonlinear simulations of the inspiral and merger of boson stars, oscillatons and axion stars include GW emission, drag and accretion and tidal deformations. Although considerably more difficult to systematize and perform, such studies have been undertaken

recently [388–393].

4.5.5 GW emission from ECOs orbiting or within neutron stars

It is conceivable that ECOs play also a role in GW (as well as EM) emission when orbiting close to neutron stars or white dwarfs. This might arise via two different possible ways. ECOs can form via gravitational collapse of DM or unknown quantum effects, and cluster around compact stars through tidal dissipation mechanisms. Alternatively, compact stars evolving in DM-rich environments may accrete a significant amount of DM in their interior: DM is captured by the star due to gravitational deflection and a non-vanishing cross-section for collision with the star material [52, 190–193]. The DM material eventually thermalizes with the star, and accumulates inside a finite-size core [52, 120, 191, 192].

Interaction of the core with the surrounding star may lead to characteristic EM signatures [52, 120]. Alternatively, a more generic imprint of such ECOs is GW emission, either via standard inspiralling processes [394, 395] or by small oscillations of such ECOs *inside* neutron stars or white dwarfs [395, 396].

4.6 Formation and evolution

In the context of DM physics, the formation and existence of ECOs is very reasonable [397]. We know that DM exists, that it interacts gravitationally and that its coupling to Standard Model fields is very weak. Therefore, gravitationally bound structures made of DM particles are dark (by definition) and can potentially be compact. Examples which are well understood include boson stars, made of scalars or vectors, which constitute one notable exception to our ignorance on the formation of ECOs. These configurations can arise out of the gravitational collapse of massive scalars (or vectors). Their interaction and mergers can be studied by evolving the Einstein-Klein-Gordon (-Maxwell) system, and there is evidence that accretion of less massive boson stars makes them grow and cluster around the configuration of maximum mass. In fact, boson stars have efficient *gravitational cooling* mechanisms that allow them to avoid collapse to BHs and remain very compact after interactions [50, 53, 118, 120]. Similar studies and similar conclusions hold for axion stars, where the coupling to the Maxwell field is taken into account [398]. If DM is built out of dark fermions, then formation should parallel that of standard neutron stars, and is also a well understood process.

However, although supported by sound arguments, the vast majority of the alternatives to BHs are, at best, incompletely described. Precise calculations (and often even a rigorous framework) incorporating the necessary physics are missing. Most models listed in Table 1 were built in a phenomenological way or they arise as solutions of Einstein equations coupled to exotic matter fields. For example, models of quantum-corrected objects do not include all the (supposedly large) local or nonlocal quantum effects that could prevent collapse from occurring. In the absence of a complete knowledge of the missing physics, it is unlikely that a ClePhO forms out of the merger of two ClePhOs. These objects are so compact that at merger they will be probably engulfed by a common apparent horizon. The end product is, most likely a BH as argued in Section 4.4.3. On the other hand, if large quantum effects do occur, they would probably act on short timescales to

prevent apparent horizon formation possibly in all situations. Thus, for example quantum backreaction has been argued to lead to wormhole solutions rather than BHs [237]. In some models, Planck-scale dynamics naturally leads to abrupt changes close to the would-be horizon, without fine tuning [161]. Likewise, in the presence of (exotic) matter or if GR is classically modified at the horizon scale, Birkhoff's theorem no longer holds, and a star-like object might be a more natural outcome than a BH. However, some studies suggest that compact horizonless bodies may form naturally as the result of gravitational collapse [399]. The generality of such result is unknown.

An important property of the vacuum field equations is their scale-invariance, inherited by BH solutions. Thus, the scaling properties of BHs are simple: their size scales with their mass, and if a non-spinning BH of mass M_1 is stable, then a BH of mass M_2 is stable as well, the timescales being proportional to the mass. Such characteristic is summarized in Fig. 5. Once matter is added, this unique property is lost. Thus, it is challenging to find theories able to explain, with horizonless objects, all the observations of dark compact objects with masses ranging over more than seven orders of magnitude, although some ECO models can account for that [112]. Such "short blanket" problem is only an issue if one tries to explain away *all* the dark compact objects with horizonless alternatives. If particle physics is a guidance, it is well possible that nature offers us a much more diverse universe content.

5 Observational evidence for horizons

"It is well known that the Kerr solution provides the unique solution for stationary BHs in the universe. But a confirmation of the metric of the Kerr spacetime (or some aspect of it) cannot even be contemplated in the foreseeable future."

S. Chandrasekhar, The Karl Schwarzschild Lecture,
Astronomische Gesellschaft, Hamburg (September 18, 1986)

Horizons act as perfect sinks for matter and radiation. The existence of a hard or smooth surface will lead in general to clear imprints. Classically, EM waves are the traditional tool to investigate astrophysical objects. There are a handful of interesting constraints on the location of the surface of ECOs using light [400–405]. However, testing the nature of dark, compact objects with EM observations is challenging. Some of these challenges, as we will discuss now, are tied to the incoherent nature of the EM radiation in astrophysics, and the amount of modeling and uncertainties associated to such emission. Other problems are connected to the absorption by the interstellar medium. As discussed in the previous section, testing quantum or microscopic corrections at the horizon scale with EM probes is nearly impossible. Even at the semiclassical level, Hawking radiation is extremely weak to detect and not exclusive of BH spacetimes [406–408].

The historical detection of GWs [4] opens up the exciting possibility of testing gravity in extreme regimes with unprecedented accuracy [5, 29, 98, 99, 135, 170, 409]. GWs are generated by coherent motion of massive sources, and are therefore subjected to less modeling uncertainties (they depend on far fewer parameters) relative to EM probes. The most luminous GWs come from very dense sources, but they also interact very feebly with matter, thus providing the cleanest picture of the cosmos, complementary to that given by telescopes and particle detectors.

Henceforth we will continue using the parameter ϵ defined by Eq. (3) to quantify the constraints that can be put on the presence/absence of a horizon. The current and projected bounds discussed below are summarized in Table 3 at the end of this section.

5.1 Tidal disruption events and EM counterparts

Main-sequence stars can be driven towards ECOs through different mechanisms, including two-body or resonant relaxation or other processes [410, 411]. At sufficiently short orbital distances, stars are either tidally disrupted (if they are within the Roche limit of the central ECO), or swallowed whole. In both cases, strong EM emission is expected for ECOs with a hard surface relative to the case of a BH [412–415]. If the ECO mass is above $\sim 10^{7.5} M_\odot$, such emission should be seen in broad surveys and produce bright optical and UV transients. Such an emission has been ruled out by Pan-STARRS 3π survey [416] at 99.7% confidence level, if the central massive objects have a hard surface at radius larger than $2M(1+\epsilon)$ with [405]

$$\epsilon \approx 10^{-4.4} \,. \tag{95}$$

The limit above was derived under the assumption of spherical symmetry, isotropic equation of state, and dropping some terms in the relevant equation. It assumes in addition that the infalling matter clusters at the surface (thereby excluding from the analysis those ECO models made of weakly interacting matter (e.g., boson stars) for which ordinary matter does not interact with the surface and accumulates in the interior).

5.2 Equilibrium between ECOs and their environment: Sgr A*

The previous results used a large number of objects and – in addition to the caveats just pointed – assume that all are horizonless. The compact radio source Sgr A* at the center of galaxy is – due to its proximity – a good candidate to improve on the above. Sgr A* has an estimated mass $M \sim 4 \times 10^6 M_\odot$, and is currently accreting at an extremely low level, with (accretion disk) luminosity $L_{\rm disk} \sim 10^{36} {\rm erg\,s^{-1}}$ (peaking at wavelength $\sim 0.1\,{\rm mm}$), about 10^{-9} times the Eddington luminosity for the central mass [417, 418]. The efficiency of the accretion disk at converting gravitational energy to radiation is less than 100%, which suggests a lower bound on the accretion rate $\dot{M} \geq L_{\rm disk} \sim 10^{15}\,{\rm g\,s^{-1}}$ (10^{-24} in geometric units).

Assume now that the system is in steady state, and that there is a hard surface at $r_0 = 2M(1+\epsilon)$. In such a case, the emission from the surface has a blackbody spectrum with temperature $T^4 = \dot{M}/(4\pi\sigma r_0^2) \sim 3.5 \times 10^3\,{\rm K}$ and bright in the infrared (wavelength $\sim 1\mu$m) [350]. However, measured infrared fluxes at $1 - 10\mu$m from Sgr A* are one to two orders of magnitude below this prediction. Initial studies used this to place an extreme constraint, $\epsilon \lesssim 10^{-35}$. However, the argument has several flaws [38, 419]:

i. It assumes that a thermodynamic and dynamic equilibrium must be established between the accretion disk and the central object, on relatively short timescales. However, strong lensing prevents this from happening; consider accretion disk matter, releasing isotropically (for simplicity) scattered radiation on the surface of the object. As discussed in Section 2.2, only a fraction $\sim \epsilon$ is able to escape during the first interaction with the star, cf. Eq. (9). The majority of the radiation will fall back onto the surface after a time $t_{\rm roundtrip} \sim 9.3M$ given by the average of Eq. (11) [5]. Suppose one injects, instantaneously, an energy δM onto the object. Then, after a time T_a, the energy emitted to infinity during $N = T_a/t_{\rm roundtrip}$ interactions reads

$$\Delta E \sim \left[1 - (1-\epsilon)^N\right] \delta M \approx \epsilon \left(\frac{T_a}{t_{\rm roundtrip}}\right) \delta M\,. \tag{96}$$

where the last step is valid for $\epsilon N \ll 1$.

We can assume $T_a = \tau_{\rm Salpeter} \approx 4.5 \times 10^7\,{\rm yr}$ and $\dot{M} = f_{\rm Edd}\dot{M}_{\rm Edd}$, where $\dot{M}_{\rm Edd} \approx 1.3 \times 10^{39}(M/M_\odot)\,{\rm erg/s}$ is the Eddington mass accretion rate onto a BH. Then, from Eq. (96) we get

$$\dot{E} \sim 10^{-25} \left(\frac{\epsilon}{10^{-15}}\right) \left(\frac{f_{\rm Edd}}{10^{-9}}\right)\,. \tag{97}$$

[5] One might wonder if the trapped radiation bouncing back and forth the surface of the object might not interact with the accretion disk. As we showed in Section 2.2, this does not happen, as the motion of trapped photons is confined to within the photosphere.

where we have normalized the fraction of the Eddington mass accretion rate, $f_{\rm Edd}$, to its typical value for Sgr A*. Requiring this flux to be compatible with the lack of observed flux from the central spot ($\dot{E} \lesssim 10^{-25}$), one finds $\epsilon \lesssim 10^{-15}$.

Assuming $L \sim \dot{E}$ and using the Stefan-Boltzmann law, Eq. (97) yields an estimate for the effective surface temperature of Sgr A* if the latter had a hard surface,

$$T \sim 7.8 \times 10^3 \left(\frac{4 \times 10^6 M_\odot}{M}\right)^{1/2} \left(\frac{\epsilon}{10^{-15}}\right)^{1/4} \left(\frac{\delta M}{10^{-7} M}\right)^{1/4} \text{K}\,. \tag{98}$$

ii. It assumes that the central object is returning in EM radiation most of the energy that it is taking in from the disk. However, even if the object were returning all of the incoming radiation on a sufficiently short timescale, a sizable fraction of this energy could be in channels other than EM. For freely-falling matter on a radial trajectory, its four-velocity $v^\mu_{(1)} = (E/f, -\sqrt{E^2 - f}, 0, 0)$. Particles at the surface of the object have $v^\mu_{(2)} = (\sqrt{f}, 0, 0, 0)$. When these two collide, their CM energy reads [420],

$$E_{\rm CM} = m_0 \sqrt{2} \sqrt{1 - g_{\mu\nu} v^\mu_{(1)} v^\mu_{(2)}} \sim \frac{m_0 \sqrt{2E}}{\epsilon^{1/4}}\,, \tag{99}$$

Thus, even for only moderately small ϵ, the particles are already relativistic. At these CM energies, all known particles (photons, neutrinos, gravitons, etc) should be emitted "democratically," and in the context of DM physics, new degrees freedom can also be excited. Even without advocating new physics beyond the 10 TeV scale, extrapolation of known hadronic interactions to large energies suggests that about 20% of the collision energy goes into neutrinos, whose total energy is a sizable fraction of that of the photons emitted in the process [421]. To account for these effects, we take

$$\epsilon \lesssim 10^{-14}\,, \tag{100}$$

as a reasonable conservative bound coming from this equilibrium argument.

If only a fraction of the falling material interacts with the object (for example, if it is made of DM with a small interaction cross-section), then the above constraint would deteriorate even further.

iii. The estimate (100) was reached without a proper handling of the interaction between the putative outgoing radiation and the disk itself, and assumes spherical symmetry. Thus, there might be large systematic uncertainties associated (and which occur for any astrophysical process where incoherent motion of the radiating charges play a key role).

5.3 Bounds with shadows: Sgr A* and M87

Recent progress in very long baseline interferometry allows for direct imaging of the region close to the horizon, with the potential to provide also constraints on putative surfaces. These images are also referred to as "shadows" since they map sky luminosity to the source

(typically an accretion disk), see Sec. 2.2. Two supermassive BHs have been studied, namely the Sgr A* source and the BH at the center of M87, whose imaging requires the lowest angular resolution [6, 10, 11, 422–426] .

The Event Horizon Telescope images of Sgr A* and M87* in the millimeter wavelength so far are consistent with a point source of radius $r_0 = (2-4)\,M$ [6, 10, 422, 426], or

$$\epsilon \sim 1\,. \tag{101}$$

This corresponds to the size of the photon sphere, which as we described in Section 2 will be the dominant relevant strong-field region for these observations. The absence of an horizon will influence the observed shadows, since some photons are now able to directly cross the object, or be reflected by it. There are substantial differences between the shadows of BHs and some horizonless objects (most notably boson stars [427–429]). Nevertheless, because of large astrophysical uncertainties and the focusing effect for photons when $\epsilon \to 0$ [Eq. (9)], all studies done so far indicate that it is extremely challenging to use such an effect to place a constraint much stronger than Eq. (101) [88, 430, 431].

In a similar spirit, tests based on strong-lensing events [432, 433] (in fact, a variant of shadows) or quantum versions of it [434] have been proposed. Adding to the list of possible discriminators, Ref. [435] studied the impact of supersonic winds blowing through BHs and boson stars. The conclusion is that, while qualitatively the stationary regime of downstream wind distribution is similar, the density may defer by almost an order of magnitude depending on the boson star configuration. At an observational level, these differences would show up presumably as friction on the compact object. However, quantitative tests based on observations are challenging to devise.

Finally, "hotspots" orbiting around supermassive objects can also provide information about near-horizon signatures [78, 79]. Recently, the first detection of these orbiting features at the ISCO of Sgr A* was reported [436], implying a bound of the same order as Eq. (101).

5.4 Tests with accretion disks

Tests on the spacetime geometry can also be performed by monitoring how *matter* moves and radiates as it approaches the compact object. Matter close to compact objects can form an accretion disk [77, 437], in which each element approximately moves in circular, Keplerian orbits. The disk is typically "truncated" at the ISCO (cf. Fig. 1), which represents a transition point in the physics of the accretion disk. It is in principle possible to extract the ISCO location and angular velocity – and hence infer properties of the central object such as the mass, spin, and quadrupole moment – from the EM signal emitted (mostly in the X-ray band) by the accreting matter, either for a stellar-mass BH or for a supermassive BH [438]. In practice, the physics of accretion disks is very complex and extracting such properties with a good accuracy is challenging.

A promising approach is the analysis of the *iron $K\alpha$ line* [439], one of the brightest components of the X-ray emission from accreting BH candidates. This line is broadened and skewed due to Doppler and (special and general) relativistic effects, which determine its characteristic shape. An analysis of this shape (assuming that the spacetime is described by the Kerr metric) provides a measurement of the BH spin and the inclination

of the accretion disk [440]. Although limited by systematic effects [438], this technique has been used also to test the spacetime metric [441–447] and to distinguish boson stars from BHs [126,127]. Another approach is the study of the thermal component of the spectrum from stellar-mass BHs using the so-called *continuum-fitting method* [440, 448, 449], which can provide information about the ISCO location and hence the BH spin [449]. The method can be also used to test the spacetime geometry [441, 445–447, 450–453] but is limited by the fact that deviations from the Kerr geometry are typically degenerate with the ISCO properties, e.g. with the spin of the object [438, 454]. Finally, an independent approach is the study of the *quasi-periodic oscillations* observed in the X-ray flux emitted by accreting compact objects [455–457]. The underlying mechanism is not well understood yet, but these frequencies are believed to originate in the innermost region of the accretion flow [458], and they might carry information about the spacetime near compact objects. Some of the proposed models try to explain such phenomena with combinations of the orbital and epicyclic frequencies of geodesics around the object. Based on these models, constraints on boson stars have been discussed in Ref. [459].

These approaches are helpful in providing indirect tests for the nature of the accreting central object, but are by construction unable to probe directly the existence of a surface. A possible alternative is the study of the time lag ("*reverberation*") between variability in the light curves in energy bands, corresponding to directly observed continuum emission from the corona around the BH and to X-rays reflected from the accretion disc [460]. Such technique was explored assuming the central object to be a BH; the impact of a different central object or of a putative hard surface is unknown.

5.5 Signatures in the mass-spin distribution of dark compact objects

The previous tests were based exclusively on EM measurements. There are tests which can be done either via EM or GW signals. An exciting example concerns the measurement of the spin of compact objects, which can be performed either via the aforementioned EM tests or from GW detections of binary inspirals and mergers [461]. This requires a large population of massive objects to have been detected and their spins estimated to some accuracy. EM or GW observations indicating statistical prevalence of slowly-spinning compact objects, across the entire mass range, indicate either a special formation channel for BHs, or could signal that such objects are in fact horizonless: the development of the ergoregion instability is expected to deplete angular momentum from spinning ClePhOs, independently of their mass, as we discussed in Section 4.4.1. Thus, the spin-mass distribution of horizonless compact objects skews towards low spin. Although the effectiveness of such process is not fully understood, it would lead to slowly-spinning objects as a final state, see Fig. 13. On the other hand, observations of highly-spinning BH candidates can be used to constrain ECO models.

Spin measurements in X-ray binaries suggest that some BH candidates are highly spinning [462]. However, such measurements are likely affected by unknown systematics; in several cases different techniques yield different results, c.f. Table 1 in [462]. Furthermore, the very existence of the ergoregion instability in ECOs surrounded by gas has never been investigated in detail, and the backreaction of the disk mass and angular momentum on

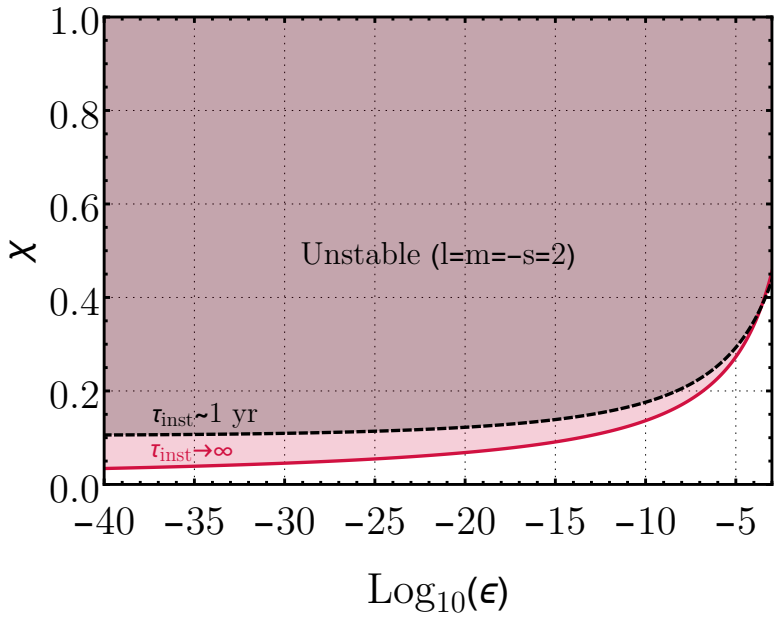


Figure 13: Exclusion plot in the $\chi - \epsilon$ plane due to the ergoregion instability of ECOs, assumed to be described by the Kerr geometry in their exterior. Shaded areas represent regions where a perfectly-reflecting ECO is unstable against gravitational perturbations with $l = m = 2$, as described by Eqs. (75) and (74).

the geometry, as well as the viscosity of the gas, may change the character and timescale of the instability. Finally, as discussed at the end of Sec. 4.4.1, dissipation within the object might also quench the instability completely [294, 295].

5.6 Multipole moments and tests of the no-hair theorem

5.6.1 Constraints with comparable-mass binaries

An estimate of the bounds on the spin-induced quadrupole moment from GW detection of compact-binary inspirals was performed in Refs. [356, 357] (see Fig. 14). As we discussed, this correction enters at 2PN order in the GW inspiral phase and is quadratic in the spin. Therefore, it requires relatively low-mass binaries (which perform many cycles in band before merger) and high spins. The quadrupole moment of the binary was parametrized as $\mathcal{M}_2^{(i)} = -\kappa_i \chi_i^2 m_i^3$ $(i = 1, 2)$, where $\kappa_i = 1$ for a Kerr BH.

For moderately large values of the spin ($\chi_i \approx 0.5$) and a binary at 500 Mpc, the projected bounds with Advanced LIGO are roughly $\kappa_s \equiv (\kappa_1 + \kappa_2)/2 \approx 50$. This constraint will become approximately 50 times more stringent with third-generation (3G) GW detectors (such as the Einstein Telescope [463] and Cosmic Explorer [464]). Similar constraints could be placed by the space detector LISA [465] for spinning supermassive binaries at luminosity distance of 3 Gpc [356]. Assuming an ECO model, a bound on κ_i can be mapped into a constraint on ϵ. The correction to the spin-induced quadrupole relative to the Kerr

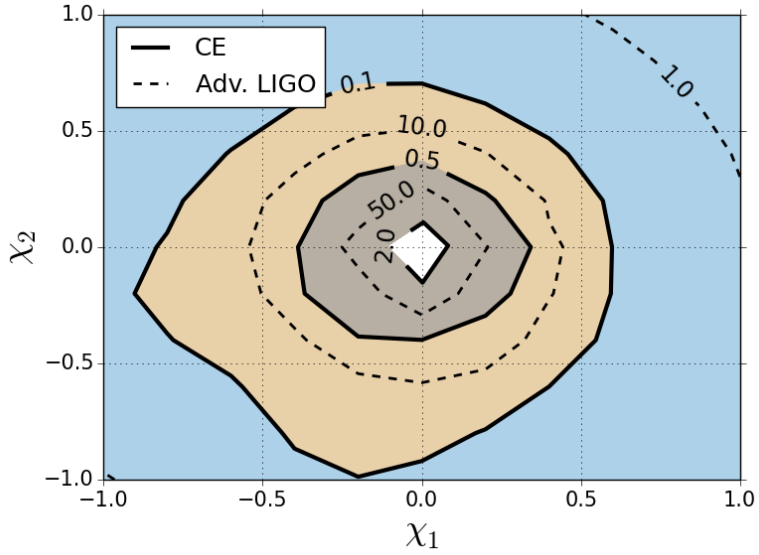


Figure 14: Errors on the spin induced quadrupole moment ($\kappa_s = (\kappa_1 + \kappa_2)/2$) of a binary system with a total mass of $(10+9)M_\odot$ in the dimensionless spin parameters plane ($\chi_1 - \chi_2$), assuming the binary components are BHs, i.e. $\kappa_s = 1$. Here κ_i are the spin induced quadrupole moment parameters of the binary constituents, i.e. $M_2^{(i)} = -\kappa_i \chi_i^2 m_i^3$. The binary is assumed to be optimally oriented at a luminosity distance of 100 Mpc; (extended from [356, 357]).

value for a generic class of ECO models (whose exterior is perturbatively close to Kerr) is given by the first term in Eq. (16). This yields $\kappa = 1 + a_2/\log\epsilon$, where $a_2 \sim \mathcal{O}(1)$ is a model-dependent parameter. Therefore, based on a constraint on $\Delta\kappa \equiv |\kappa - 1|$, we can derive the upper bound

$$\epsilon \lesssim e^{-\frac{|a_2|}{\Delta\kappa}} , \tag{102}$$

which (assuming $a_2 \sim \mathcal{O}(1)$) gives $\epsilon \lesssim 1$ with Advanced LIGO and a factor 3 more stringent with 3G and LISA. For a gravastar, $a_2 = -8/45$ [103] and we obtain approximately $\epsilon \lesssim 1$ with all detectors. These constraints require highly-spinning binaries and the analysis of Ref. [356–358] assumes that the quadrupole moment is purely quadratic in the spin. This property is true for Kerr BHs, but not generically; for example, the quadrupole moment of highly-spinning boson stars contains $O(\chi^4)$ and higher corrections [466], which are relevant for highly-spinning binaries.

In addition to projected bounds, observational bounds on parametrized corrections to the 2PN coefficient of the inspiral waveform from binary BH coalescences can be directly translated – using Eq. (81) – into a bound on (a symmetric combination of) the spin-induced quadrupole moments of the binary components [6]. This parametrized PN analysis

[6]Unfortunately, for the majority of binary BH events detected so far [461], either the spin of the binary

has been recently done for various BH merger events, the combined constraint on the deviation of the 2PN coefficient reads $\delta\varphi_2 \lesssim 0.3$ at 90% confidence level [468]. However, the component spins of these sources are compatible with zero so these constraints cannot be translated into an upper bound on the spin-induced quadrupole moment in Eq. (16). They might be translated into an upper bound on the non-spin induced quadrupole moment, which is however zero in all ECO models proposed so far.

5.6.2 Projected constraints with EMRIs

Extreme-mass ratio inspirals (EMRIs) detectable by the future space mission LISA will probe the spacetime around the central supermassive object with exquisite precision [47, 97, 99]. These binaries perform $\sim m_1/m_2$ orbits before the plunge, the majority of which are very close to the ISCO. The emitted signal can be used to constrain the multipole moments of the central object. In particular, preliminary analysis (using kludge waveforms and a simplified parameter estimation) have placed the projected constrain $\delta\mathcal{M}_2/M^3 < 10^{-4}$ [470,471]. Based on this result and assuming $\delta\mathcal{M}_2$ is spin induced, from Eq. (16) we can derive the following bound on ϵ

$$\epsilon \lesssim \exp\left(-\frac{10^4}{\zeta}\right), \tag{103}$$

where we defined $\zeta \equiv \frac{\delta\mathcal{M}_2/M^3}{10^{-4}}$ and assumed saturation of Eq. (16) with an order-unity coefficient. Notice how stringent the second bound is, easily excluding even Planckian corrections at the horizon scale [75]. For this reason, it is important to extend current analysis with more accurate waveforms (kludge waveforms are based on a PN expansion of the field equations [471] but the PN series converges very slowly in the extreme mass ratio limit [472], so results based on these waveforms are only indicative when $m_1/m_2 > 10^3$).

Model dependent studies on the ability of EMRIs to constrain quadrupolar deviations from Kerr have been presented in Refs. [466, 473, 474].

5.7 Tidal heating

Horizons absorb incoming high frequency radiation, and serve as sinks or amplifiers for low-frequency radiation able to tunnel in, see Sec. 4.5.2. UCOs and ClePhOs, on the other hand, are not expected to absorb any significant amount of GWs. Thus, a "null-hypothesis" test consists on using the phase of GWs to measure absorption or amplification at the surface of the objects [135].

Because horizon absorption is related to superradiance and the BH area theorem [89], testing this effect is an indirect proof of the second law of BH thermodynamics. While this effect is too small to be detectable from a single event with second-generation detectors,

component is compatible to zero, or the event had a low signal-to-noise ratio (SNR) in the early inspiral, where the PN approximation is valid. The most promising candidate for this test would be GW170729, for which the measured effective binary spin parameter is $\chi_{\rm eff} \approx 0.36^{+0.21}_{-0.25}$ [461,467]. However, for such event no parametrized-inspiral test has been performed so far [468]. If confirmed, the recent claimed detection [469] of a highly-spinning BH binary would be ideal to perform tests of the spin-induced quadrupole moment.

a large number ($\approx 10^4$) of LIGO-Virgo detections might support Hawking's area theorem at 90% confidence level [19].

On the other hand, highly-spinning supermassive binaries detectable with a LISA-type GW interferometer will have a large SNR and will place stringent constraints on this effect, potentially reaching Planck scales near the horizon [135]. This is shown in the left panel of Fig. 15, which presents the bounds on parameter γ defined by adding the tidal-heating term in the PN phase as $\gamma\psi^{\rm BH}_{\rm TH}$ (see Eq. (83)). For a BH $\gamma = 1$, whereas $\gamma = 0$ for a perfectly reflecting ECO. Notice that the effect is linear in the spin and it would be suppressed by two further PN orders in the nonspinning case.

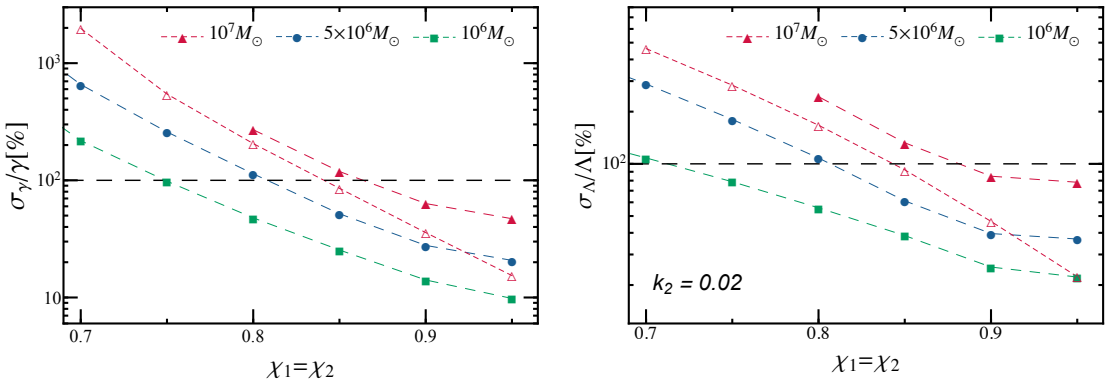


Figure 15: Percentage relative projected errors on the tidal-heating parameter γ (left panel) and on the average tidal deformability Λ (right panel) as a function of the spin parameter $\chi_1 = \chi_2$, for different values of the central mass $m_1 = (10^6, 5\times10^6, 10^7)M_\odot$ assuming a future detection with LISA. In the left and right panel we considered negligible tidal deformability ($\Lambda = 0$) and negligible tidal heating ($\gamma = 0$), respectively. Full (empty) markers refer to mass ratio $m_1/m_2 = 1.1$ ($m_1/m_2 = 2$). Points below the horizontal line correspond to detections that can distinguish between a BH and an ECO at better than 1σ level. We assume binaries at luminosity distance 2 Gpc; σ_a scales with the inverse luminosity distance, and σ_Λ scales with $1/\Lambda$ when $k \ll 1$. Taken from Ref. [135].

Absence of tidal heating leaves also a detectable imprint in EMRIs [475, 476]. In that case the point-particle motion is almost geodesic, with orbital parameters evolving adiabatically because the system loses energy and angular momentum in GWs both at infinity and at the horizon. Energy loss at the horizon is subleading but its putative absence impact the phase of the orbits (and hence the GW signal) in a detectable way, especially if the central object is highly spinning [475]. In Fig. 16 we show a comparison between the inspiral trajectories with and without the tidal-heating term.

The effect is clearly important, but the known multiple systematics involved (e.g., due to waveform modeling and to parameter estimation in a signal-driven detector like LISA) still need to be quantified. Finally, the ability of tidal heating in constraining the closeness parameter ϵ (or the blueshift of photons in Table 3 below) for EMRIs is yet to be understood, both because of the above systematics and also because the absence of tidal heating might be directly mapped into a bound on ϵ, since it depends mostly on the

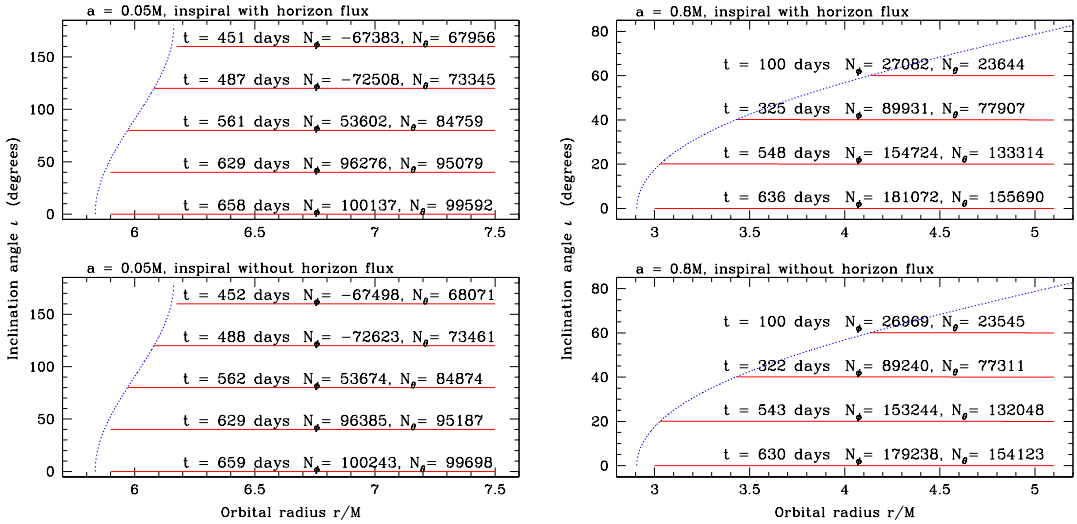


Figure 16: Inspiral trajectories in the strong field of a Kerr BH with $\chi = 0.05$ (left) and $\chi = 0.8$ (right) in the inclination-orbital radius plane for circular orbits. The top (bottom) panel includes (exclude) the effect of tidal heating, i.e. energy absorption at the horizon. Notice that tidal heating depends strongly on the spin and on the orbit. Adapted from Ref. [475], courtesy of Scott Hughes.

object interior rather than on the location of the surface (see, however, discussion at the end of Sec. 4.5.2).

5.8 Tidal deformability

As discussed in Sec. 4.5.3, the TLNs of a BH are identically zero, whereas those of an ECO are not. Although this correction enters at 5PN order in the waveform, the tidal deformability of an object with radius r_0 is proportional to $(r_0/M)^5$, so its effect in the GW phase is magnified for less compact objects. This effect has been recently explored for boson-star binaries, by investigating the distinguishability of binary boson stars from both binary BHs [133, 134, 373, 477] and binary neutron stars [134]. Second-generation GW detectors at design sensitivity should be able to distinguish boson-stars models with no self-potential and with a quartic self-potential (cf. Table 2) from BHs, whereas 3G (resp., LISA) is necessary to distinguish the most compact solitonic boson stars from stellar-mass (resp., supermassive) BHs [133]. As a rule of thumb, the stronger the boson self-interaction the more compact are stable boson-star equilibrium configurations, and hence the smaller the tidal deformability and the chances of detectability. Fits for the TLNs of various boson-star models are provided in Ref. [134]; codes to compute these quantities are publicly available [292].

For ECOs inspired by Planckian corrections at the horizon scale, the TLNs scale as $k \sim 1/|\log \epsilon|$ for a variety of models (see Sec. 4.5.3 and Table I in Ref. [133]). Due to this

scaling, in these models the TLNs are only roughly 4 orders of magnitude smaller than for an ordinary neutron star. Nonetheless, measuring such small TLN is probably out of reach even with 3G and would require LISA golden binaries [135] (see right panel of Fig. 15). Due to the logarithmic scaling, in these models the statistical errors on ϵ would depend exponentially on the TLNs and reaching a Planckian requires a very accurate measurement of k [380]. Nonetheless, this does not prevent to perform ECO model selection (see Fig. 12).

Finally, in the extreme mass-ratio limit the GW phase (93) *grows linearly* with the mass ratio $q = m_1/m_2 \gg 1$ and is proportional to the TLN of the central object, $\psi_{\rm TD}(f) \approx -0.004 k_1 q$ [478]. In this case the relative measurements errors on k_1 scale as $1/\sqrt{q}$ at large SNR. Provided one can overcome the systematics on EMRI modeling, this effect might allow to measure TLNs as small as $k_1 \approx 10^{-4}$ for EMRI with $q = 10^6$ detectable by LISA [478]. Assuming models for which $k_1 \sim 1/\log\epsilon$ (see Eq. (94)), we can derive the impressive bound

$$\epsilon \lesssim \exp\left(-\frac{10^4}{\zeta}\right), \tag{104}$$

where now we defined $\zeta \equiv \frac{k_1}{10^{-4}}$. Note that the above bound is roughly as stringent as that in Eq. (103) for $k_1 \approx \delta\mathcal{M}_2/M^3$. In both cases the dependence on the departures from the BH case is exponential, so the final bound is particularly sensitive also to the prefactors in Eqs. (94) and (16).

5.9 Resonance excitation

The contribution of the multipolar structure, tidal heating, and tidal deformability on the gravitational waveform is perturbative and produces small corrections relative to the idealized point-particle waveform. However, there are nonperturbative effects that can be triggered during inspiral, namely the excitation of the vibration modes of the inspiralling objects. In particular, if the QNMs are of sufficiently low frequency, they can be excited during inspiral [83,131,143,383,479]. This case is realized for certain models of ECOs (e.g. ultracompact gravastars and boson stars) and generically for Kerr-like ECOs in the $\epsilon \to 0$, see Eq. (71). In addition to spacetime modes, also model-dependent fluid modes might also be excited [409]. Due to redshift effects, these will presumably play a subdominant role in the GW signal.

5.10 QNM tests

One of the simplest and most elegant tools to test the BH nature of central objects, and GR itself, is to use the uniqueness properties of the Kerr family of BHs: vacuum BHs in GR are fully specified by mass and angular momentum, and so are their vibration frequencies [283, 480]. Thus, detection of one mode (i.e., ringing frequency and damping time) allows for an estimate of the mass and angular momentum of the object (assumed to be a GR BH). The detection of two or more modes allows to test GR and/or the BH nature of the object [480–484].

Current detectors can only extract one mode for massive BH mergers, and hence one can estimate the mass and spin of the final object, assumed to be a BH [5]. Future detectors will be able to detect more than one mode and perform "ECO spectroscopy" [480–484].

To exclude ECO models, one needs calculations of their vibration spectra. These are available for a wide class of objects, including boson stars [83, 131, 482], gravastars [142, 144, 250], wormholes [485, 486], or other quantum-corrected objects [163, 167]. A major challenge in these tests is how to model spin effects properly, since few spinning ECO models are available and the study of their perturbations is much more involved than for Kerr BHs. In general, the post-merger signal from a distorted ECO might be qualitatively similar to that of a neutron-star merger, with several long-lived modes excited [106] and a waveform that is more involved than a simple superposition of damped sinusoids as in the case of BH QNMs.

As discussed previously in Sec. 4.2 and in Sec. 5.12 below, all these extra features are expected to become negligible in the $\epsilon \to 0$ limit: the *prompt ringdown* of an ultracompact ECOs should become indistinguishable from that of a BH in this limit, jeopardizing standard QNM tests.

5.11 Inspiral-merger-ringdown consistency

The full nonlinear structure of GR is encoded in the complete waveform from the inspiral and merger of compact objects. Thus, while isolated tests on separate dynamical stages are important, the ultimate test is that of consistency with the full GR prediction: is the full inspiral-merger-ringdown waveform compatible with that of a binary BH coalescence? Even when the SNR of a given detection is low, such tests can be performed, with some accuracy. Unfortunately, predictions for the coalescence in theories other than GR and for objects other that BHs are practically unknown. The exceptions concern evolutions of neutron stars, boson stars, and composite fluid systems [51, 132, 388, 390], and recent progress in BH mergers in modified gravity [487–490].

A model-independent constraint comes from the high merger frequency of GW150914 [5], which was measured to be $\nu_{\rm GW} \approx 150\,{\rm Hz}$. The total mass of this system is roughly $m_1 + m_2 \approx 66.2\,M_\odot$. By assuming that the merger frequency corresponds to the Keplerian frequency at contact, when the binary is at orbital distance $r = 2m(1+\epsilon)$, we obtain the upper bound

$$\epsilon < 0.74\,. \tag{105}$$

Agreement between the mass and spin of the final object as predicted from the inspiral stage and from a ringdown analysis has been used as a consistency check of GR [5]. Although the measurement errors on the mass and spin of the final remnant are currently large, the consistency of the ringdown waveform with the full inspiral-merger-ringdown template suggests that the remnant should at least be a ClePhO, i.e. places the bound $\epsilon \lesssim \mathcal{O}(0.01)$, the exact number requires a detailed, model-dependent analysis.

5.12 Tests with GW echoes

For binaries composed of ClePhOs, the GW signal generated during inspiral and merger is expected to be very similar to that by a BH binary with the same mass and spin. Indeed,

the multipole moments of very compact objects approach those of Kerr when $\epsilon \to 0$, and so do the TLNs, etc. Constraining ϵ (or quantifying up to which point the vacuum Kerr is a description of the spacetime) is then a question of having sensitive detectors that can probe minute changes in waveforms. This would also require having sufficiently accurate waveform models to avoid systematics. However, there is a clear distinctive feature of horizonless objects: the appearance of late-time echoes in the waveforms (see Section 4.2). There has been some progress in modeling the echo waveform and data analysis strategies are in place to look for such late-time features; some strategies have been also implemented using real data [304, 311, 319, 491–494].

The ability to detect such signals depends on how much energy is converted from the main burst into echoes (i.e., on the relative amplitude between the first echo and the prompt ringdown signal in Fig. 9). Depending on the reflectivity of the ECO, the energy contained in the echoes can exceed that of the standard ringdown alone [297, 315], see left panel of Fig. 17. This suggests that it is possible to detect or constrain echoes even when the ringdown is marginally detectable or below threshold, as in the case of EMRIs or for comparable-mass coalescences at small SNR.

Searches for echo signals in the detectors based on reliable templates can be used to find new physics, or to set very stringent constraints on several models using real data. Different groups with independent search techniques *have found* structure in many of the GW events, compatible with postmerger echoes [304, 311, 491, 492, 495]. However, the statistical significance of such events has been put into question [492, 496]. For GW150914, Refs. [304, 311, 495]– using independent search techniques – report evidence for the existence of postmerger echoes in the data. However, Ref. [493] finds a lower significance and a Bayes factor indicating preference for noise over the echo hypothesis. For other GW events, there is agreement between different groups on the existence of postmerger features in the signal, found using echo waveforms. The interpretation of these features is under debate.

Any realistic search is controlled by η (cf. Eq. (59)) *and* the time delay between main burst and echoes [304, 311, 319, 491–494]. Since the SNR of the postmerger signal is controlled by η on a integration timescale controlled by τ, even negative searches can be used to place strong constraints on ϵ [492, 493].

Constraints on ϵ are currently limited by the low SNR. These constraints will greatly improve with next-generation GW detectors. A preliminary analysis in this direction [315] (based on the template (61) valid only for nonspinning objects) suggests that perfectly-reflecting ECO models can be detected or ruled out at 5σ confidence level with SNR in the ringdown of $\rho_{\rm ringdown} \approx 10$. Excluding/detecting echoes for models with smaller values of the reflectivity will require SNRs in the post-merger phase of $\mathcal{O}(100)$. This will be achievable only with ground-based 3G detectors and the planned space mission LISA [465], see right panel of Fig. 17. Simple-minded ringdown searches (using as template an exponentially damped sinusoid [497]) can be used to look for echoes, separately from the main burst. For example, if the first echo carries 20% of the energy of the main ringdown stage, then it is detectable with a simple ringdown template. LISA will see at least one ringdown event per year, even for the most pessimistic population synthesis models used to estimate the rates [484]. The proposed Einstein telescope [463] or Voyager-like [498]

3G Earth-based detectors will also be able to distinguish ClePhOs from BHs with such simple-minded searches.

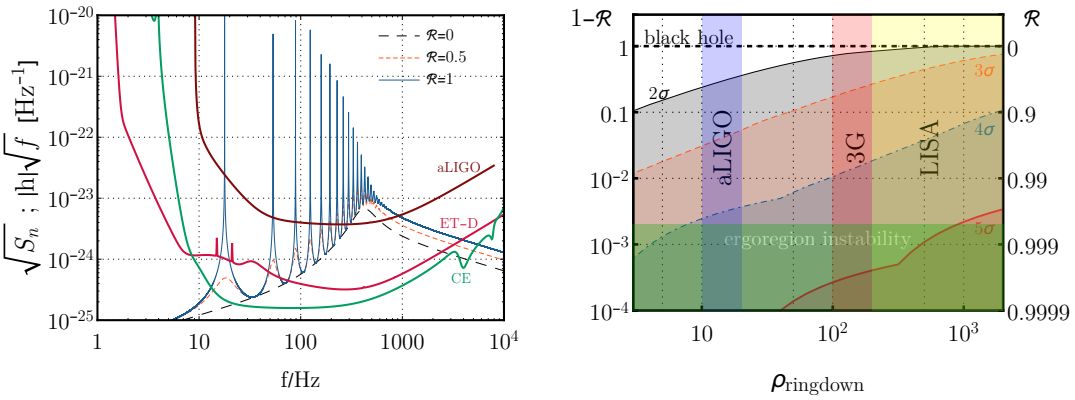


Figure 17: *Left:* Representative example of ringdown+echo template (Eq. (61)) compared to the power spectral densities of various ground-based interferometers [499–502] as functions of the GW frequency f. We considered an object with $M = 30M_\odot$, at a distance of 400 Mpc, with closeness parameter $\epsilon = 10^{-11}$, and various values of the reflectivity coefficient $\mathcal{R}$ at the surface ($\mathcal{R} = 0$ corresponds to the pure BH ringdown template). *Right:* Projected exclusion plot for the ECO reflectivity $\mathcal{R}$ as a function of the SNR in the ringdown phase and at different σ confidence levels, assuming the ringdown template (61) based on the transfer-function representation and assuming a source near the ECO surface. Shaded areas represent regions that can be excluded at a given confidence level. Vertical bands are typical SNR achievable by aLIGO/Virgo, 3G, and LISA in the ringdown phase, whereas the horizontal band is the region excluded by the ergoregion instability, see Sec. 4.4.1. Adapted from Ref. [315].

Overall, in a large region of the parameter space the signal is large enough to produce effects within reach of near-future GW detectors, even if the corrections occur at the "Planck scale" (by which we mean $\epsilon \sim 10^{-40}$). This is a truly remarkable prospect. As the sensitivity of GW detectors increases, the absence of echoes might be used to rule out many quantum-gravity models completely, and to push tests of gravity closer and closer to the horizon scale, as now routinely done for other cornerstones of GR, e.g. in tests of the equivalence principle [44, 99].

5.13 Stochastic background

Above in Section 5.5, we discussed possible features in the spin distribution of massive compact objects. If a large number of massive and dark objects are indeed horizonless and very compact, they will be subjected to the ergoregion instability (discussed in Section 4.4.1) which drains their rotational energy and transfers it to GWs. Thus, the entire universe would be radiating GWs, producing a (potentially) significant amount of stochastic GWs [344, 503, 504]. Note that such background does *not* require binaries, isolated

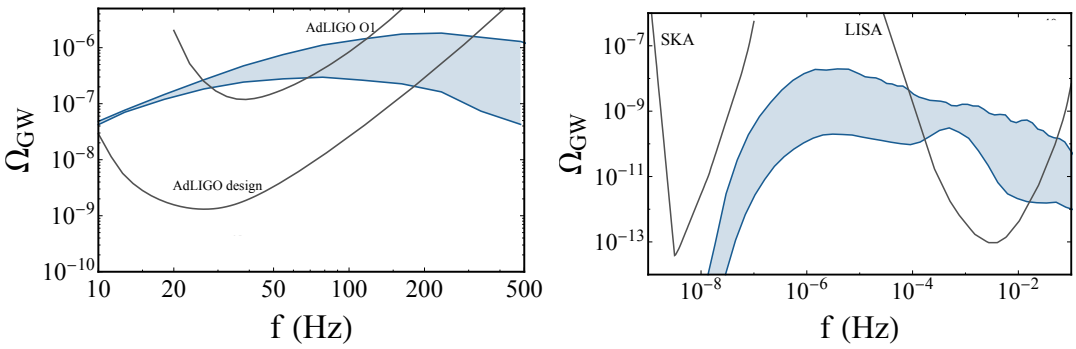


Figure 18: Extragalactic stochastic background of GWs in the LIGO/Virgo (left panel), LISA and PTA bands (right panel) assuming all BH candidates to be horizonless, described by a Kerr exterior and Dirichlet conditions at the surface $r = r_+(1+\epsilon)$, with $\epsilon = 10^{-40}$. The bands brackets different population models. The black lines are the power-law integrated curves computed using noise power spectral densities for: LISA with one year of observation time [465], LIGO's first observing runs (O1), LIGO at design sensitivity, and an SKA-based pulsar timing array. Taken from Ref. [344].

ECOs suffice (isolated compact objects are expected to be ~ 100 times more numerous than merging binaries [505]).

The background can be characterized by its (dimensionless) energy spectrum

$$\Omega_{\rm GW} = \frac{1}{\rho_c}\frac{d\rho_{\rm gw}}{d\ln f_o}\,, \tag{106}$$

$\rho_{\rm gw}$ being the background's energy density, f_o the frequency measured at the detector and ρ_c the critical density of the Universe at the present time. Results for a simple ECO, modelled with Kerr exterior and Dirichlet conditions at its surface are shown in Fig. 18. The derived constraints assume all BH candidates are horizonless, the bound scales linearly with the fraction of ECOs in the population.

5.14 Motion within ECOs

In certain models, the ECO interior might be weakly interacting and a further discriminator would be the motion of test particles *within* the object. Among other effect, this can produce non-standard signals in EMRIs. As discussed in Secs. 4.5.4 and 4.5.5, this motion is driven by the self-gravity of the central object, accretion, and dynamical friction. The study of geodesic motion inside a solitonic boson stars was analyzed in [129]. The effects of accretion and drag were included in Refs. [83,131,170,506]. These effects cannot be directly translated into bounds on ϵ, but would be a smoking-gun signature for the existence of structures in supermassive ultracompact objects.

6 Discussion and observational bounds

The purpose of physics is to describe natural phenomena in the most accurate possible way. The most outrageous prediction of GR – that BHs should exist and be always described by the Kerr geometry – remains poorly quantified. It is a foundational issue, touching on questions such as singularity formation, quantum effects in gravity, the behavior of matter at extreme densities, and even DM physics. The quest to quantify the evidence for BHs can – in more than one way – be compared with the quest to quantify the equivalence principle, and needs to be complemented with tests of the Kerr nature of ultracompact dark objects. Table 3 summarizes the observation evidence for BHs.

These bounds can be read in two different ways. On the one hand, they tell us how appropriate the Kerr metric is in describing some of the massive and dark objects in our universe. In other words, observations tell us that the Kerr description is compatible with observations at least down to $r = r_+(1+\epsilon)$. Alternatively, one can view these numbers as constraints on exotic alternatives to BHs. In both cases, the constraint on ϵ can be translated into the ratio of frequencies (or redshift, as measured by locally non-rotating observers [507]) of a photon as it travels from infinity down to the farthest point down to which observations are compatible with vacuum.

Most of the constraints shown in Table 3 are associated with large systematics or modelling uncertainties. From a proper understanding of astrophysical environments and their interaction with ultracompact objects, the development of a solid theoretical framework, to a proper modeling of the coalescence of such objects and data analysis to see such events, the challenges are immense. The pay-off for facing these oustanding issues is to be able to quantify the statement that BHs exist in nature.

	Constraints		Source	Reference
	$\epsilon(\lesssim)$	$\frac{\nu}{\nu_\infty}(\gtrsim)$		
1a.	$\mathcal{O}(1)$	$\mathcal{O}(1)$	Sgr A* & M87	[6, 10, 422, 426, 436]
1b.	0.74	1.5	GW150914	[4]
2.	$\mathcal{O}(0.01)$	$\mathcal{O}(10)$	GW150914	[4]
3.	$10^{-4.4}$	158	All with $M > 10^{7.5} M_\odot$	[405]
4.	10^{-14}	10^{7}	Sgr A*	[405]
5.	10^{-40}	10^{20}	All with $M < 100 M_\odot$	[344]
6.	10^{-47}	10^{23}	GW150914	[493]
7*.	$e^{-10^4/\zeta}$	$e^{5000/\zeta}$	EMRIs	[470, 471, 478]

	Effect and caveats
1a.	Uses detected orbiting hotspot around Sgr A* and "shadow" of Sgr A* and M87. Spin effects are poorly understood; systematic uncertainties not quantified.
1b.	Merger frequency of GW150914 and measurements of the masses. Assumes merger frequency equal to Keplerian frequency at contact.
2.	Consistency of ringdown with BH signal. Large measurement errors on the QNM frequencies. Precise bounds are model dependent. Bounds will improve significantly with detailed searches for post-merger echoes.
3.	Lack of optical/UV transients from tidal disruption events. Assumes: all objects are horizonless, have a hard surface, spherical symmetry, and isotropy.
4.	Uses absence of relative low luminosity from Sgr A*, compared to disk. Spin effects and matter-radiation interaction matter poorly understood; assumes spherical symmetry.
5.	Uses absence of GW stochastic background (from ergoregion instability). Assumes: hard surface (perfect reflection); exterior Kerr; all objects are horizonless.
6.	Uses absence of GW echoes from post-merger object. 90% confidence level for $\eta > 0.9$, deteriorates for smaller η. Simplified echo template, limited range of priors.
7*.	Projected EMRI constraints on the spin-induced quadrupole ($\zeta = (\delta\mathcal{M}_2/M^3)/10^{-4}$) and TLNs ($\zeta = k_1/10^{-4}$). Assumes saturation of Eq. (16) (for $\delta\mathcal{M}_2$) and Eq. (94) (for k_1) and order-unity coefficients in those equations. Uses PN kludge waveforms, phenomenological deviation for $\mathcal{M}_2$, and simplified parameter estimation.

Table 3: *How well does the BH geometry describe the dark compact objects in our universe?* This table quantifies the answer to this question, for selected objects, by *excluding* the presence of surfaces in the spacetime close to the gravitational radius of the object. The deviation from the vacuum Kerr geometry, of mass M and angular momentum $J = \chi M^2$, is measured with a dimensionless quantity ϵ, such that the structure is localized at a Boyer-Lindquist radius $r_+(1+\epsilon)$, where $r_+ = M(1+\sqrt{1-\chi^2})$. For $\epsilon = 0$ the spacetime is described by vacuum GR all the way to the horizon. We also express the constraint as measured by the blueshift of a radial-directed photon ν/ν_∞ (on the equatorial plane, measured by locally non-rotating observers) as it travels from large distances to the last point down to which observations are compatible with vacuum. The constraints come from a variety of observations and tests provided in the references in the last column and interpreted as discussed in Sec. 5. Alternative quantities that can parametrize the deviation from the vacuum Kerr geometry are the light travel time from the light ring to the surface (Eq. (73)) or the proper distance between the light ring and the surface. Both quantities depend on ϵ and on the spin χ of the object, and scale as $\log\epsilon$ as $\epsilon \to 0$. Entries with an asterix refer to projected constraints.

Acknowledgments. We are indebted to Niayesh Afshordi, K. G. Arun, Cosimo Bambi, Carlos Barceló, Ofek Birnholtz, Silke Britzen, Ramy Brustein, Collin Capano, Raúl Carballo-Rubio, Ana Carvalho, Miguel Correia, Jan de Boer, Kyriakos Destounis, Valeria Ferrari, Valentino Foit, Luis Garay, Steve Giddings, Eric Gourgoulhon, Tomohiro Harada, Carlos Herdeiro, Bob Holdom, Scott Hughes, Bala Iyer, Marios Karouzos, Gaurav Khanna, Joe Keir, Matthew Kleban, Kostas Kokkotas, Pawan Kumar, Claus Laemmerzahl, José Lemos, Avi Loeb, Caio Macedo, Andrea Maselli, Samir Mathur, Emil Mottola, Ken-ichi Nakao, Richard Price, Sergey Solodukhin, Chris Van den Broeck, Bert Vercnocke, Frederic Vincent, Sebastian Voelkel, Kent Yagi, and Aaron Zimmerman for providing detailed feedback, useful references, for discussions, or for suggesting corrections to an earlier version of the manuscript. V.C. acknowledges financial support provided under the European Union's H2020 ERC Consolidator Grant "Matter and strong-field gravity: New frontiers in Einstein's theory" grant agreement no. MaGRaTh–646597. PP acknowledges financial support provided under the European Union's H2020 ERC, Starting Grant agreement no. DarkGRA–757480 and support from the Amaldi Research Center funded by the MIUR program "Dipartimento di Eccellenza" (CUP: B81I18001170001). This article is based upon work from COST Action CA16104 "GWverse" supported by COST (European Cooperation in Science and Technology). This work was partially supported by the H2020-MSCA-RISE-2015 Grant No. StronGrHEP-690904.

References

[1] Quoting Subrahmanyan Chandrasekhar, "In my entire scientific life, extending over forty-five years, the most shattering experience has been the realization that an exact solution of Einstein's equations of general relativity provides the absolutely exact representation of untold numbers of black holes that populate the universe." S. Chandrasekhar, The Nora and Edward Ryerson lecture, Chicago April 22 1975.

[2] K. Schwarzschild, "On the gravitational field of a mass point according to Einstein's theory," *Sitzungsber. Preuss. Akad. Wiss. Berlin (Math. Phys.)* **1916** (1916) 189–196, `arXiv:physics/9905030 [physics]`.

[3] J. Droste, "The field of a single centre in Einstein's theory of gravitation, and the motion of a particle in that field," *Proceedings of the Royal Netherlands Academy of Arts and Science* **19** (1917) 197–215.

[4] **The LIGO/Virgo Scientific Collaboration** Collaboration, B. P. Abbott *et al.*, "Observation of Gravitational Waves from a Binary Black Hole Merger," *Phys. Rev. Lett.* **116** no. 6, (2016) 061102, `arXiv:1602.03837 [gr-qc]`.

[5] **LIGO Scientific, Virgo** Collaboration, B. P. Abbott *et al.*, "Tests of general relativity with GW150914," *Phys. Rev. Lett.* **116** no. 22, (2016) 221101, `arXiv:1602.03841 [gr-qc]`. [Erratum: Phys. Rev. Lett.121,no.12,129902(2018)].

[6] S. Doeleman *et al.*, "Event-horizon-scale structure in the supermassive black hole candidate at the Galactic Centre," *Nature* **455** (2008) 78, arXiv:0809.2442 [astro-ph].

[7] J. Antoniadis *et al.*, "A Massive Pulsar in a Compact Relativistic Binary," *Science* **340** (2013) 6131, arXiv:1304.6875 [astro-ph.HE].

[8] R. Genzel, F. Eisenhauer, and S. Gillessen, "The Galactic Center Massive Black Hole and Nuclear Star Cluster," *Rev. Mod. Phys.* **82** (2010) 3121–3195, arXiv:1006.0064 [astro-ph.GA].

[9] H. Falcke and S. B. Markoff, "Toward the event horizon – the supermassive black hole in the Galactic Center," *Class. Quant. Grav.* **30** (2013) 244003, arXiv:1311.1841 [astro-ph.HE].

[10] T. Johannsen, A. E. Broderick, P. M. Plewa, S. Chatzopoulos, S. S. Doeleman, F. Eisenhauer, V. L. Fish, R. Genzel, O. Gerhard, and M. D. Johnson, "Testing General Relativity with the Shadow Size of Sgr A*," *Phys. Rev. Lett.* **116** no. 3, (2016) 031101, arXiv:1512.02640 [astro-ph.GA].

[11] **GRAVITY** Collaboration, R. Abuter *et al.*, "Detection of the gravitational redshift in the orbit of the star S2 near the Galactic centre massive black hole," *Astron. Astrophys.* **615** (2018) L15, arXiv:1807.09409 [astro-ph.GA].

[12] R. Penrose, "Gravitational collapse: The role of general relativity," *Riv. Nuovo Cim.* **1** (1969) 252–276. [Gen. Rel. Grav.34,1141(2002)].

[13] R. M. Wald, "Gravitational collapse and cosmic censorship," in *Black Holes, Gravitational Radiation and the Universe: Essays in Honor of C.V. Vishveshwara*, pp. 69–85. 1997. arXiv:gr-qc/9710068 [gr-qc].

[14] R. Penrose, "Singularities of Spacetime (in Theoretical Principles in Astrophysics and Relativity)," in *Chicago University Press, Chicago, 1978 217 P.* 1978.

[15] H. Reall, "Viewpoint: A Possible Failure of Determinism in General Relativity," *Physics* **11** (2018) 6.

[16] M. Dafermos, "The Interior of charged black holes and the problem of uniqueness in general relativity," *Commun. Pure Appl. Math.* **58** (2005) 0445–0504, arXiv:gr-qc/0307013 [gr-qc].

[17] V. Cardoso, J. L. Costa, K. Destounis, P. Hintz, and A. Jansen, "Quasinormal modes and Strong Cosmic Censorship," *Phys. Rev. Lett.* **120** no. 3, (2018) 031103, arXiv:1711.10502 [gr-qc].

[18] S. W. Hawking, "Gravitational radiation from colliding black holes," *Phys. Rev. Lett.* **26** (1971) 1344–1346.

[19] K.-H. Lai and T. G. F. Li, "Constraining black-hole horizon effects by LIGO-Virgo detections of inspiralling binary black holes," *Phys. Rev.* **D98** no. 8, (2018) 084059, arXiv:1807.01840 [gr-qc].

[20] R. Brustein, A. J. M. Medved, and K. Yagi, "Lower limit on the entropy of black holes as inferred from gravitational wave observations," arXiv:1811.12283 [gr-qc].

[21] S. B. Giddings, "Black holes and massive remnants," *Phys. Rev.* **D46** (1992) 1347–1352, arXiv:hep-th/9203059 [hep-th].

[22] P. O. Mazur and E. Mottola, "Gravitational vacuum condensate stars," *Proc. Nat. Acad. Sci.* **101** (2004) 9545–9550, arXiv:gr-qc/0407075 [gr-qc].

[23] S. D. Mathur, "The Fuzzball proposal for black holes: An Elementary review," *Fortsch. Phys.* **53** (2005) 793–827, arXiv:hep-th/0502050 [hep-th].

[24] S. D. Mathur, "Fuzzballs and the information paradox: A Summary and conjectures," arXiv:0810.4525 [hep-th].

[25] S. B. Giddings, "Nonlocality versus complementarity: A Conservative approach to the information problem," *Class. Quant. Grav.* **28** (2011) 025002, arXiv:0911.3395 [hep-th].

[26] S. D. Mathur, "The Information paradox: A Pedagogical introduction," *Class. Quant. Grav.* **26** (2009) 224001, arXiv:0909.1038 [hep-th].

[27] S. B. Giddings, "Black holes, quantum information, and unitary evolution," *Phys. Rev.* **D85** (2012) 124063, arXiv:1201.1037 [hep-th].

[28] C. Barceló, R. Carballo-Rubio, and L. J. Garay, "Where does the physics of extreme gravitational collapse reside?," *Universe* **2** no. 2, (2016) 7, arXiv:1510.04957 [gr-qc].

[29] S. B. Giddings, "Gravitational wave tests of quantum modifications to black hole structure – with post-GW150914 update," *Class. Quant. Grav.* **33** no. 23, (2016) 235010, arXiv:1602.03622 [gr-qc].

[30] S. B. Giddings, "Nonviolent unitarization: basic postulates to soft quantum structure of black holes," *JHEP* **12** (2017) 047, arXiv:1701.08765 [hep-th].

[31] A. Almheiri, D. Marolf, J. Polchinski, and J. Sully, "Black Holes: Complementarity or Firewalls?," *JHEP* **1302** (2013) 062, arXiv:1207.3123 [hep-th].

[32] W. G. Unruh and R. M. Wald, "Information Loss," *Rept. Prog. Phys.* **80** no. 9, (2017) 092002, arXiv:1703.02140 [hep-th].

[33] S. B. Giddings, "Astronomical tests for quantum black hole structure," arXiv:1703.03387 [gr-qc].

[34] E. Bianchi, M. Christodoulou, F. D'Ambrosio, H. M. Haggard, and C. Rovelli, "White Holes as Remnants: A Surprising Scenario for the End of a Black Hole," *Class. Quant. Grav.* **35** no. 22, (2018) 225003, arXiv:1802.04264 [gr-qc].

[35] S. B. Giddings, S. Koren, and G. Treviño, "Exploring strong-field deviations from general relativity via gravitational waves," arXiv:1904.04258 [gr-qc].

[36] N. Arkani-Hamed, S. Dimopoulos, and G. R. Dvali, "The Hierarchy problem and new dimensions at a millimeter," *Phys. Lett.* **B429** (1998) 263–272, arXiv:hep-ph/9803315 [hep-ph].

[37] L. Randall and R. Sundrum, "An Alternative to compactification," *Phys. Rev. Lett.* **83** (1999) 4690–4693, arXiv:hep-th/9906064 [hep-th].

[38] V. Cardoso and P. Pani, "Tests for the existence of black holes through gravitational wave echoes," *Nat. Astron.* **1** no. 9, (2017) 586–591, arXiv:1709.01525 [gr-qc].

[39] J. D. Bekenstein and V. F. Mukhanov, "Spectroscopy of the quantum black hole," *Phys. Lett.* **B360** (1995) 7–12, arXiv:gr-qc/9505012 [gr-qc].

[40] M. Saravani, N. Afshordi, and R. B. Mann, "Empty black holes, firewalls, and the origin of Bekenstein-Hawking entropy," *Int. J. Mod. Phys.* **D23** no. 13, (2015) 1443007, arXiv:1212.4176 [hep-th].

[41] V. F. Foit and M. Kleban, "Testing Quantum Black Holes with Gravitational Waves," *Class. Quant. Grav.* **36** (2019) 035006, arXiv:1611.07009 [hep-th].

[42] V. Cardoso, V. F. Foit, and M. Kleban, "Gravitational wave echoes from black hole area quantization," arXiv:1902.10164 [hep-th].

[43] S. Chakraborty and K. Lochan, "Decoding infrared imprints of quantum origins of black holes," *Phys. Lett.* **B789** (2019) 276–286, arXiv:1711.10660 [gr-qc].

[44] C. M. Will, "The Confrontation between General Relativity and Experiment," *Living Rev. Rel.* **17** (2014) 4, arXiv:1403.7377 [gr-qc].

[45] J. Bergé, P. Brax, G. Métris, M. Pernot-Borràs, P. Touboul, and J.-P. Uzan, "MICROSCOPE Mission: First Constraints on the Violation of the Weak Equivalence Principle by a Light Scalar Dilaton," *Phys. Rev. Lett.* **120** no. 14, (2018) 141101, arXiv:1712.00483 [gr-qc].

[46] G. Bertone and M. P. Tait, Tim, "A new era in the search for dark matter," *Nature* **562** no. 7725, (2018) 51–56, arXiv:1810.01668 [astro-ph.CO].

[47] L. Barack *et al.*, "Black holes, gravitational waves and fundamental physics: a roadmap," arXiv:1806.05195 [gr-qc].

[48] D. J. E. Marsh, "Axion Cosmology," *Phys. Rept.* **643** (2016) 1–79, arXiv:1510.07633 [astro-ph.CO].

[49] T. Clifton, P. G. Ferreira, A. Padilla, and C. Skordis, "Modified Gravity and Cosmology," *Phys. Rept.* **513** (2012) 1–189, arXiv:1106.2476 [astro-ph.CO].

[50] E. Seidel and W.-M. Suen, "Formation of solitonic stars through gravitational cooling," *Phys. Rev. Lett.* **72** (1994) 2516–2519, arXiv:gr-qc/9309015 [gr-qc].

[51] S. L. Liebling and C. Palenzuela, "Dynamical Boson Stars," *Living Rev. Rel.* **15** (2012) 6, arXiv:1202.5809 [gr-qc].

[52] R. Brito, V. Cardoso, and H. Okawa, "Accretion of dark matter by stars," *Phys. Rev. Lett.* **115** no. 11, (2015) 111301, arXiv:1508.04773 [gr-qc].

[53] F. Di Giovanni, N. Sanchis-Gual, C. A. R. Herdeiro, and J. A. Font, "Dynamical formation of Proca stars and quasistationary solitonic objects," *Phys. Rev.* **D98** no. 6, (2018) 064044, arXiv:1803.04802 [gr-qc].

[54] G. Narain, J. Schaffner-Bielich, and I. N. Mishustin, "Compact stars made of fermionic dark matter," *Phys. Rev.* **D74** (2006) 063003, arXiv:astro-ph/0605724 [astro-ph].

[55] M. Raidal, S. Solodukhin, V. Vaskonen, and H. Veermäe, "Light Primordial Exotic Compact Objects as All Dark Matter," *Phys. Rev.* **D97** no. 12, (2018) 123520, arXiv:1802.07728 [astro-ph.CO].

[56] M. Deliyergiyev, A. Del Popolo, L. Tolos, M. Le Delliou, X. Lee, and F. Burgio, "Dark compact objects: an extensive overview," arXiv:1903.01183 [gr-qc].

[57] R. Emparan, D. Grumiller, and K. Tanabe, "Large-D gravity and low-D strings," *Phys. Rev. Lett.* **110** no. 25, (2013) 251102, arXiv:1303.1995 [hep-th].

[58] G. 't Hooft, "A Planar Diagram Theory for Strong Interactions," *Nucl. Phys.* **B72** (1974) 461. [,337(1973)].

[59] K. Popper, "The problem of induction," in *Popper Selections*, D. Miller, ed., pp. 101–117. Princeton, 1985.

[60] C. A. R. Herdeiro and J. P. S. Lemos, "The black hole fifty years after: Genesis of the name," arXiv:1811.06587 [physics.hist-ph].

[61] S. W. Hawking and G. F. R. Ellis, *The Large Scale Structure of Space-Time*. Cambridge Monographs on Mathematical Physics. Cambridge University Press, 2011.

[62] E. Curiel, "The many definitions of a black hole," *Nat. Astron.* **3** no. 1, (2019) 27–34, arXiv:1808.01507 [physics.hist-ph].

[63] J. Thornburg, "Event and apparent horizon finders for 3+1 numerical relativity," *Living Rev. Rel.* **10** (2007) 3, arXiv:gr-qc/0512169 [gr-qc].

[64] R. M. Wald and V. Iyer, "Trapped surfaces in the Schwarzschild geometry and cosmic censorship," *Phys. Rev.* **D44** (1991) R3719–R3722.

[65] J. M. Bardeen, "Black Holes Do Evaporate Thermally," *Phys. Rev. Lett.* **46** (1981) 382–385.

[66] J. W. York, Jr., "Dynamical Origin of Black Hole Radiance," *Phys. Rev.* **D28** (1983) 2929.

[67] M. Arzano and G. Calcagni, "What gravity waves are telling about quantum spacetime," *Phys. Rev.* **D93** no. 12, (2016) 124065, arXiv:1604.00541 [gr-qc]. [Addendum: Phys. Rev.D94,no.4,049907(2016)].

[68] M. A. Abramowicz, W. Kluzniak, and J.-P. Lasota, "No observational proof of the black hole event-horizon," *Astron. Astrophys.* **396** (2002) L31–L34, arXiv:astro-ph/0207270 [astro-ph].

[69] K.-i. Nakao, C.-M. Yoo, and T. Harada, "Gravastar formation: What can be the evidence of a black hole?," *Phys. Rev.* **D99** no. 4, (2019) 044027, arXiv:1809.00124 [gr-qc].

[70] S. B. Giddings, "Possible observational windows for quantum effects from black holes," *Phys. Rev.* **D90** no. 12, (2014) 124033, arXiv:1406.7001 [hep-th].

[71] R. Brustein and A. J. M. Medved, "Quantum hair of black holes out of equilibrium," *Phys. Rev.* **D97** no. 4, (2018) 044035, arXiv:1709.03566 [hep-th].

[72] R. Brustein, A. J. M. Medved, and K. Yagi, "Discovering the interior of black holes," *Phys. Rev.* **D96** no. 12, (2017) 124021, arXiv:1701.07444 [gr-qc].

[73] Y.-T. Wang, Z.-P. Li, J. Zhang, S.-Y. Zhou, and Y.-S. Piao, "Are gravitational wave ringdown echoes always equal-interval?," *Eur. Phys. J.* **C78** no. 6, (2018) 482, arXiv:1802.02003 [gr-qc].

[74] Y.-T. Wang, J. Zhang, S.-Y. Zhou, and Y.-S. Piao, "On echo intervals in gravitational wave echo analysis," arXiv:1904.00212 [gr-qc].

[75] G. Raposo, P. Pani, and R. Emparan, "Exotic compact objects with soft hair," arXiv:1812.07615 [gr-qc].

[76] S. Chandrasekhar, *The Mathematical Theory of Black Holes*. Oxford University Press, New York, 1983.

[77] I. D. Novikov and K. S. Thorne, "Astrophysics and black holes," in *Proceedings, Ecole d'Eté de Physique Théorique: Les Astres Occlus*, pp. 343–550. 1973.

[78] A. E. Broderick and A. Loeb, "Imaging bright-spots in the accretion flow near the black hole horizon of Sgr A*," MNRAS **363** (Oct., 2005) 353–362, astro-ph/0506433.

[79] A. E. Broderick and A. Loeb, "Imaging optically-thin hot spots near the black hole horizon of sgr a* at radio and near-infrared wavelengths," *Mon. Not. Roy. Astron. Soc.* **367** (2006) 905–916, arXiv:astro-ph/0509237 [astro-ph].

[80] V. Ferrari and B. Mashhoon, "New approach to the quasinormal modes of a black hole," *Phys. Rev.* **D30** (1984) 295–304.

[81] V. Cardoso, A. S. Miranda, E. Berti, H. Witek, and V. T. Zanchin, "Geodesic stability, Lyapunov exponents and quasinormal modes," *Phys. Rev.* **D79** (2009) 064016, arXiv:0812.1806 [hep-th].

[82] V. Cardoso, L. C. B. Crispino, C. F. B. Macedo, H. Okawa, and P. Pani, "Light rings as observational evidence for event horizons: long-lived modes, ergoregions and nonlinear instabilities of ultracompact objects," *Phys. Rev.* **D90** no. 4, (2014) 044069, arXiv:1406.5510 [gr-qc].

[83] C. F. B. Macedo, P. Pani, V. Cardoso, and L. C. B. Crispino, "Astrophysical signatures of boson stars: quasinormal modes and inspiral resonances," *Phys. Rev.* **D88** no. 6, (2013) 064046, arXiv:1307.4812 [gr-qc].

[84] P. V. P. Cunha, E. Berti, and C. A. R. Herdeiro, "Light-Ring Stability for Ultracompact Objects," *Phys. Rev. Lett.* **119** no. 25, (2017) 251102, arXiv:1708.04211 [gr-qc].

[85] B. R. Iyer, C. V. Vishveshwara, and S. V. Dhurandhar, "Ultracompact (R less than 3 M) objects in general relativity," *Classical and Quantum Gravity* **2** (Mar., 1985) 219–228.

[86] A. A. Shoom, "Metamorphoses of a photon sphere," *Phys. Rev.* **D96** no. 8, (2017) 084056, arXiv:1708.00019 [gr-qc].

[87] S. L. Shapiro and S. A. Teukolsky, *Black holes, white dwarfs, and neutron stars: The physics of compact objects*. Wiley, New York, 1983.

[88] F. H. Vincent, Z. Meliani, P. Grandclement, E. Gourgoulhon, and O. Straub, "Imaging a boson star at the Galactic center," *Class. Quant. Grav.* **33** no. 10, (2016) 105015, arXiv:1510.04170 [gr-qc].

[89] R. Brito, V. Cardoso, and P. Pani, "Superradiance," *Lect. Notes Phys.* **906** (2015) pp.1–237, arXiv:1501.06570 [gr-qc].

[90] B. Carter, "Axisymmetric black hole has only two degrees of freedom," *Phys. Rev. Lett.* **26** (Feb, 1971) 331–333. http://link.aps.org/doi/10.1103/PhysRevLett.26.331.

[91] M. Heusler, "Stationary black holes: Uniqueness and beyond," *Living Rev. Relativity* **1** no. 6, (1998) . http://www.livingreviews.org/lrr-1998-6.

[92] P. T. Chrusciel, J. L. Costa, and M. Heusler, "Stationary Black Holes: Uniqueness and Beyond," *Living Rev.Rel.* **15** (2012) 7, arXiv:1205.6112 [gr-qc].

[93] D. Robinson, *Four decades of black holes uniqueness theorems*. Cambridge University Press, 2009.

[94] R. Hansen, "Multipole moments of stationary space-times," *J.Math.Phys.* **15** (1974) 46–52.

[95] R. P. Geroch, "Multipole moments. II. Curved space," *J.Math.Phys.* **11** (1970) 2580–2588.

[96] D. Psaltis, "Probes and Tests of Strong-Field Gravity with Observations in the Electromagnetic Spectrum," *Living Rev. Rel.* **11** (2008) 9, arXiv:0806.1531 [astro-ph].

[97] J. R. Gair, M. Vallisneri, S. L. Larson, and J. G. Baker, "Testing General Relativity with Low-Frequency, Space-Based Gravitational-Wave Detectors," *Living Rev.Rel.* **16** (2013) 7, arXiv:1212.5575 [gr-qc].

[98] N. Yunes and X. Siemens, "Gravitational-Wave Tests of General Relativity with Ground-Based Detectors and Pulsar Timing-Arrays," *Living Rev. Rel.* **16** (2013) 9, arXiv:1304.3473 [gr-qc].

[99] E. Berti *et al.*, "Testing General Relativity with Present and Future Astrophysical Observations," *Class. Quant. Grav.* **32** (2015) 243001, arXiv:1501.07274 [gr-qc].

[100] V. Cardoso and L. Gualtieri, "Testing the black hole no-hair hypothesis," *Class. Quant. Grav.* **33** no. 17, (2016) 174001, arXiv:1607.03133 [gr-qc].

[101] B. S. Sathyaprakash *et al.*, "Extreme Gravity and Fundamental Physics," arXiv:1903.09221 [astro-ph.HE].

[102] C. Barceló, R. Carballo-Rubio, and S. Liberati, "Generalized no-hair theorems without horizons," arXiv:1901.06388 [gr-qc].

[103] P. Pani, "I-Love-Q relations for gravastars and the approach to the black-hole limit," *Phys. Rev.* **D92** no. 12, (2015) 124030, arXiv:1506.06050 [gr-qc].

[104] K. Glampedakis and G. Pappas, "How well can ultracompact bodies imitate black hole ringdowns?," *Phys. Rev.* **D97** no. 4, (2018) 041502, arXiv:1710.02136 [gr-qc].

[105] R. Carballo-Rubio, F. Di Filippo, S. Liberati, and M. Visser, "Phenomenological aspects of black holes beyond general relativity," *Phys. Rev.* **D98** no. 12, (2018) 124009, arXiv:1809.08238 [gr-qc].

[106] K. D. Kokkotas and B. G. Schmidt, "Quasinormal modes of stars and black holes," *Living Rev. Rel.* **2** (1999) 2, arXiv:gr-qc/9909058 [gr-qc].

[107] H. Saida, A. Fujisawa, C.-M. Yoo, and Y. Nambu, "Spherical polytropic balls cannot mimic black holes," *PTEP* **2016** no. 4, (2016) 043E02, arXiv:1503.01840 [gr-qc].

[108] Z. Stuchlík, J. Schee, B. Toshmatov, J. Hladík, and J. Novotný, "Gravitational instability of polytropic spheres containing region of trapped null geodesics: a possible explanation of central supermassive black holes in galactic halos," *JCAP* **1706** no. 06, (2017) 056, arXiv:1704.07713 [gr-qc].

[109] S. H. Völkel and K. D. Kokkotas, "A Semi-analytic Study of Axial Perturbations of Ultra Compact Stars," *Class. Quant. Grav.* **34** no. 12, (2017) 125006, arXiv:1703.08156 [gr-qc].

[110] S. H. Völkel and K. D. Kokkotas, "Ultra Compact Stars: Reconstructing the Perturbation Potential," *Class. Quant. Grav.* **34** no. 17, (2017) 175015, arXiv:1704.07517 [gr-qc].

[111] V. Ferrari and K. D. Kokkotas, "Scattering of particles by neutron stars: Time evolutions for axial perturbations," *Phys. Rev.* **D62** (2000) 107504, arXiv:gr-qc/0008057 [gr-qc].

[112] G. Raposo, P. Pani, M. Bezares, C. Palenzuela, and V. Cardoso, "Anisotropic stars as ultracompact objects in General Relativity," arXiv:1811.07917 [gr-qc].

[113] K. Dev and M. Gleiser, "Anisotropic stars. 2. Stability," *Gen. Rel. Grav.* **35** (2003) 1435–1457, arXiv:gr-qc/0303077 [gr-qc].

[114] D. D. Doneva and S. S. Yazadjiev, "Gravitational wave spectrum of anisotropic neutron stars in Cowling approximation," *Phys. Rev.* **D85** (2012) 124023, arXiv:1203.3963 [gr-qc].

[115] H. O. Silva, C. F. B. Macedo, E. Berti, and L. C. B. Crispino, "Slowly rotating anisotropic neutron stars in general relativity and scalar-tensor theory," *Class. Quant. Grav.* **32** (2015) 145008, arXiv:1411.6286 [gr-qc].

[116] K. Yagi and N. Yunes, "Relating follicly-challenged compact stars to bald black holes: A link between two no-hair properties," *Phys. Rev.* **D91** no. 10, (2015) 103003, arXiv:1502.04131 [gr-qc].

[117] K. Yagi and N. Yunes, "I-Love-Q anisotropically: Universal relations for compact stars with scalar pressure anisotropy," *Phys.Rev.* **D91** no. 12, (2015) 123008.

[118] E. Seidel and W. Suen, "Oscillating soliton stars," *Phys.Rev.Lett.* **66** (1991) 1659–1662.

[119] H. Okawa, V. Cardoso, and P. Pani, "Collapse of self-interacting fields in asymptotically flat spacetimes: do self-interactions render Minkowski spacetime unstable?," *Phys. Rev.* **D89** no. 4, (2014) 041502, arXiv:1311.1235 [gr-qc].

[120] R. Brito, V. Cardoso, C. F. B. Macedo, H. Okawa, and C. Palenzuela, "Interaction between bosonic dark matter and stars," *Phys. Rev.* **D93** no. 4, (2016) 044045, arXiv:1512.00466 [astro-ph.SR].

[121] M. Gleiser and R. Watkins, "Gravitational Stability of Scalar Matter," *Nucl. Phys.* **B319** (1989) 733.

[122] T. D. Lee and Y. Pang, "Stability of Mini - Boson Stars," *Nucl. Phys.* **B315** (1989) 477.

[123] E. P. Honda and M. W. Choptuik, "Fine structure of oscillons in the spherically symmetric phi**4 Klein-Gordon model," *Phys. Rev.* **D65** (2002) 084037, arXiv:hep-ph/0110065 [hep-ph].

[124] V. Cardoso, P. Pani, M. Cadoni, and M. Cavaglia, "Ergoregion instability of ultracompact astrophysical objects," *Phys. Rev.* **D77** (2008) 124044, arXiv:0709.0532 [gr-qc].

[125] R. Brito, V. Cardoso, C. A. R. Herdeiro, and E. Radu, "Proca stars: Gravitating Bose-Einstein condensates of massive spin 1 particles," *Phys. Lett.* **B752** (2016) 291–295, arXiv:1508.05395 [gr-qc].

[126] Z. Cao, A. Cardenas-Avendano, M. Zhou, C. Bambi, C. A. R. Herdeiro, and E. Radu, "Iron Kα line of boson stars," *JCAP* **1610** no. 10, (2016) 003, arXiv:1609.00901 [gr-qc].

[127] T. Shen, M. Zhou, C. Bambi, C. A. R. Herdeiro, and E. Radu, "Iron Kα line of Proca stars," *JCAP* **1708** (2017) 014, arXiv:1701.00192 [gr-qc].

[128] C. Palenzuela, L. Lehner, and S. L. Liebling, "Orbital Dynamics of Binary Boson Star Systems," *Phys. Rev.* **D77** (2008) 044036, arXiv:0706.2435 [gr-qc].

[129] M. Kesden, J. Gair, and M. Kamionkowski, "Gravitational-wave signature of an inspiral into a supermassive horizonless object," *Phys. Rev.* **D71** (2005) 044015, arXiv:astro-ph/0411478 [astro-ph].

[130] M. W. Choptuik and F. Pretorius, "Ultra Relativistic Particle Collisions," *Phys. Rev. Lett.* **104** (2010) 111101, arXiv:0908.1780 [gr-qc].

[131] C. F. B. Macedo, P. Pani, V. Cardoso, and L. C. B. Crispino, "Into the lair: gravitational-wave signatures of dark matter," *Astrophys. J.* **774** (2013) 48, arXiv:1302.2646 [gr-qc].

[132] V. Cardoso, S. Hopper, C. F. B. Macedo, C. Palenzuela, and P. Pani, "Gravitational-wave signatures of exotic compact objects and of quantum corrections at the horizon scale," *Phys. Rev.* **D94** no. 8, (2016) 084031, arXiv:1608.08637 [gr-qc].

[133] V. Cardoso, E. Franzin, A. Maselli, P. Pani, and G. Raposo, "Testing strong-field gravity with tidal Love numbers," *Phys. Rev.* **D95** no. 8, (2017) 084014, arXiv:1701.01116 [gr-qc].

[134] N. Sennett, T. Hinderer, J. Steinhoff, A. Buonanno, and S. Ossokine, "Distinguishing Boson Stars from Black Holes and Neutron Stars from Tidal Interactions in Inspiraling Binary Systems," *Phys. Rev.* **D96** no. 2, (2017) 024002, arXiv:1704.08651 [gr-qc].

[135] A. Maselli, P. Pani, V. Cardoso, T. Abdelsalhin, L. Gualtieri, and V. Ferrari, "Probing Planckian corrections at the horizon scale with LISA binaries," *Phys. Rev. Lett.* **120** no. 8, (2018) 081101, arXiv:1703.10612 [gr-qc].

[136] M. Visser and D. L. Wiltshire, "Stable gravastars: An Alternative to black holes?," *Class. Quant. Grav.* **21** (2004) 1135–1152, arXiv:gr-qc/0310107 [gr-qc].

[137] N. Sakai, H. Saida, and T. Tamaki, "Gravastar Shadows," *Phys. Rev.* **D90** no. 10, (2014) 104013, arXiv:1408.6929 [gr-qc].

[138] N. Uchikata and S. Yoshida, "Slowly rotating thin shell gravastars," *Class. Quant. Grav.* **33** no. 2, (2016) 025005, arXiv:1506.06485 [gr-qc].

[139] N. Uchikata, S. Yoshida, and P. Pani, "Tidal deformability and I-Love-Q relations for gravastars with polytropic thin shells," *Phys. Rev.* **D94** no. 6, (2016) 064015, arXiv:1607.03593 [gr-qc].

[140] C. B. M. H. Chirenti and L. Rezzolla, "How to tell a gravastar from a black hole," *Class. Quant. Grav.* **24** (2007) 4191–4206, arXiv:0706.1513 [gr-qc].

[141] P. Pani, E. Berti, V. Cardoso, Y. Chen, and R. Norte, "Gravitational-wave signature of a thin-shell gravastar," *J. Phys. Conf. Ser.* **222** (2010) 012032.

[142] P. Pani, E. Berti, V. Cardoso, Y. Chen, and R. Norte, "Gravitational wave signatures of the absence of an event horizon. I. Nonradial oscillations of a thin-shell gravastar," *Phys. Rev.* **D80** (2009) 124047, arXiv:0909.0287 [gr-qc].

[143] P. Pani, E. Berti, V. Cardoso, Y. Chen, and R. Norte, "Gravitational-wave signatures of the absence of an event horizon. II. Extreme mass ratio inspirals in the spacetime of a thin-shell gravastar," *Phys. Rev.* **D81** (2010) 084011, arXiv:1001.3031 [gr-qc].

[144] C. Chirenti and L. Rezzolla, "Did GW150914 produce a rotating gravastar?," *Phys. Rev.* **D94** no. 8, (2016) 084016, arXiv:1602.08759 [gr-qc].

[145] V. Cardoso, E. Franzin, and P. Pani, "Is the gravitational-wave ringdown a probe of the event horizon?," *Phys. Rev. Lett.* **116** no. 17, (2016) 171101, arXiv:1602.07309 [gr-qc].

[146] U. H. Danielsson, G. Dibitetto, and S. Giri, "Black holes as bubbles of AdS," *JHEP* **10** (2017) 171, arXiv:1705.10172 [hep-th].

[147] J. A. Gonzalez, F. S. Guzman, and O. Sarbach, "Instability of wormholes supported by a ghost scalar field. I. Linear stability analysis," *Class. Quant. Grav.* **26** (2009) 015010, arXiv:0806.0608 [gr-qc].

[148] J. A. Gonzalez, F. S. Guzman, and O. Sarbach, "Instability of wormholes supported by a ghost scalar field. II. Nonlinear evolution," *Class. Quant. Grav.* **26** (2009) 015011, arXiv:0806.1370 [gr-qc].

[149] P. G. Nedkova, V. K. Tinchev, and S. S. Yazadjiev, "Shadow of a rotating traversable wormhole," *Phys. Rev.* **D88** no. 12, (2013) 124019, arXiv:1307.7647 [gr-qc].

[150] T. Ohgami and N. Sakai, "Wormhole shadows," *Phys. Rev.* **D91** no. 12, (2015) 124020, arXiv:1704.07065 [gr-qc].

[151] A. Abdujabbarov, B. Juraev, B. Ahmedov, and Z. Stuchlík, "Shadow of rotating wormhole in plasma environment," *Astrophys. Space Sci.* **361** no. 7, (2016) 226.

[152] M. Zhou, A. Cardenas-Avendano, C. Bambi, B. Kleihaus, and J. Kunz, "Search for astrophysical rotating Ellis wormholes with X-ray reflection spectroscopy," *Phys. Rev.* **D94** no. 2, (2016) 024036, arXiv:1603.07448 [gr-qc].

[153] V. Cardoso, O. J. C. Dias, J. L. Hovdebo, and R. C. Myers, "Instability of non-supersymmetric smooth geometries," *Phys. Rev.* **D73** (2006) 064031, arXiv:hep-th/0512277 [hep-th].

[154] B. D. Chowdhury and S. D. Mathur, "Radiation from the non-extremal fuzzball," *Class. Quant. Grav.* **25** (2008) 135005, arXiv:0711.4817 [hep-th].

[155] F. C. Eperon, H. S. Reall, and J. E. Santos, "Instability of supersymmetric microstate geometries," *JHEP* **10** (2016) 031, arXiv:1607.06828 [hep-th].

[156] F. C. Eperon, "Geodesics in supersymmetric microstate geometries," *Class. Quant. Grav.* **34** no. 16, (2017) 165003, arXiv:1702.03975 [gr-qc].

[157] T. Hertog and J. Hartle, "Observational Implications of Fuzzball Formation," arXiv:1704.02123 [hep-th].

[158] V. Cardoso, P. Pani, M. Cadoni, and M. Cavaglia, "Instability of hyper-compact Kerr-like objects," *Class. Quant. Grav.* **25** (2008) 195010, arXiv:0808.1615 [gr-qc].

[159] P. Pani, E. Barausse, E. Berti, and V. Cardoso, "Gravitational instabilities of superspinars," *Phys. Rev.* **D82** (2010) 044009, arXiv:1006.1863 [gr-qc].

[160] M. Patil, T. Harada, K.-i. Nakao, P. S. Joshi, and M. Kimura, "Infinite efficiency of the collisional Penrose process: Can a overspinning Kerr geometry be the source of ultrahigh-energy cosmic rays and neutrinos?," *Phys. Rev.* **D93** no. 10, (2016) 104015, arXiv:1510.08205 [gr-qc].

[161] B. Holdom and J. Ren, "Not quite a black hole," *Phys. Rev.* **D95** no. 8, (2017) 084034, arXiv:1612.04889 [gr-qc].

[162] R. Brustein and A. J. M. Medved, "Black holes as collapsed polymers," *Fortsch. Phys.* **65** (2017) 0114, arXiv:1602.07706 [hep-th].

[163] R. Brustein, A. J. M. Medved, and K. Yagi, "When black holes collide: Probing the interior composition by the spectrum of ringdown modes and emitted gravitational waves," *Phys. Rev.* **D96** no. 6, (2017) 064033, arXiv:1704.05789 [gr-qc].

[164] R. Brustein and A. J. M. Medved, "Resisting collapse: How matter inside a black hole can withstand gravity," *Phys. Rev.* **D99** no. 6, (2019) 064019, arXiv:1805.11667 [hep-th].

[165] C. Bambi, D. Malafarina, and L. Modesto, "Non-singular quantum-inspired gravitational collapse," *Phys. Rev.* **D88** (2013) 044009, arXiv:1305.4790 [gr-qc].

[166] C. Barcelo, S. Liberati, S. Sonego, and M. Visser, "Fate of gravitational collapse in semiclassical gravity," *Phys. Rev.* **D77** (2008) 044032, arXiv:0712.1130 [gr-qc].

[167] C. Barceló, R. Carballo-Rubio, and L. J. Garay, "Gravitational wave echoes from macroscopic quantum gravity effects," *JHEP* **05** (2017) 054, arXiv:1701.09156 [gr-qc].

[168] G. Dvali and C. Gomez, "Black Hole's Quantum N-Portrait," *Fortsch. Phys.* **61** (2013) 742–767, arXiv:1112.3359 [hep-th].

[169] G. Dvali and C. Gomez, "Black Hole's 1/N Hair," *Phys. Lett.* **B719** (2013) 419–423, arXiv:1203.6575 [hep-th].

[170] E. Barausse, V. Cardoso, and P. Pani, "Can environmental effects spoil precision gravitational-wave astrophysics?," *Phys. Rev.* **D89** no. 10, (2014) 104059, arXiv:1404.7149 [gr-qc].

[171] H. A. Buchdahl, "General Relativistic Fluid Spheres," *Phys. Rev.* **116** (1959) 1027.

[172] A. Urbano and H. Veermäe, "On gravitational echoes from ultracompact exotic stars," arXiv:1810.07137 [gr-qc].

[173] D. J. Kaup, "Klein-Gordon Geon," *Phys. Rev.* **172** (1968) 1331–1342.

[174] R. Ruffini and S. Bonazzola, "Systems of selfgravitating particles in general relativity and the concept of an equation of state," *Phys. Rev.* **187** (1969) 1767–1783.

[175] M. Khlopov, B. A. Malomed, and I. B. Zeldovich, "Gravitational instability of scalar fields and formation of primordial black holes," *Mon. Not. Roy. Astron. Soc.* **215** (1985) 575–589.

[176] A. H. Guth, M. P. Hertzberg, and C. Prescod-Weinstein, "Do Dark Matter Axions Form a Condensate with Long-Range Correlation?," *Phys. Rev.* **D92** no. 10, (2015) 103513, arXiv:1412.5930 [astro-ph.CO].

[177] M. Minamitsuji, "Vector boson star solutions with a quartic order self-interaction," *Phys. Rev.* **D97** no. 10, (2018) 104023, arXiv:1805.09867 [gr-qc].

[178] P. Jetzer, "Boson stars," *Phys. Rept.* **220** (1992) 163–227.

[179] F. Schunck and E. Mielke, "General relativistic boson stars," *Class. Quant. Grav.* **20** (2003) R301–R356, arXiv:0801.0307 [astro-ph].

[180] M. Choptuik, R. Masachs, and B. Way, "Multi-oscillating Boson Stars," arXiv:1904.02168 [gr-qc].

[181] D. Garfinkle, R. B. Mann, and C. Vuille, "Critical collapse of a massive vector field," *Phys. Rev.* **D68** (2003) 064015, arXiv:gr-qc/0305014 [gr-qc].

[182] M. Colpi, S. L. Shapiro, and I. Wasserman, "Boson Stars: Gravitational Equilibria of Selfinteracting Scalar Fields," *Phys. Rev. Lett.* **57** (1986) 2485–2488.

[183] R. Friedberg, T. D. Lee, and Y. Pang, "Scalar Soliton Stars and Black Holes," *Phys. Rev.* **D35** (1987) 3658. [,73(1986)].

[184] P. Grandclément, "Light rings and light points of boson stars," *Phys. Rev.* **D95** no. 8, (2017) 084011, arXiv:1612.07507 [gr-qc].

[185] L. Hui, J. P. Ostriker, S. Tremaine, and E. Witten, "Ultralight scalars as cosmological dark matter," *Phys. Rev.* **D95** no. 4, (2017) 043541, arXiv:1610.08297 [astro-ph.CO].

[186] J. M. Lattimer and M. Prakash, "Neutron Star Observations: Prognosis for Equation of State Constraints," *Phys. Rept.* **442** (2007) 109–165, arXiv:astro-ph/0612440 [astro-ph].

[187] F. Özel and P. Freire, "Masses, Radii, and the Equation of State of Neutron Stars," *Ann. Rev. Astron. Astrophys.* **54** (2016) 401–440, arXiv:1603.02698 [astro-ph.HE].

[188] http://xtreme.as.arizona.edu/NeutronStars/.

[189] P. Pani and V. Ferrari, "On gravitational-wave echoes from neutron-star binary coalescences," *Class. Quant. Grav.* **35** no. 15, (2018) 15LT01, arXiv:1804.01444 [gr-qc].

[190] W. H. Press and D. N. Spergel, "Capture by the sun of a galactic population of weakly interacting massive particles," *Astrophys.J.* **296** (1985) 679–684.

[191] A. Gould, B. T. Draine, R. W. Romani, and S. Nussinov, "Neutron Stars: Graveyard of Charged Dark Matter," *Phys.Lett.* **B238** (1990) 337.

[192] I. Goldman and S. Nussinov, "Weakly Interacting Massive Particles and Neutron Stars," *Phys. Rev.* **D40** (1989) 3221–3230.

[193] G. Bertone and M. Fairbairn, "Compact Stars as Dark Matter Probes," *Phys. Rev.* **D77** (2008) 043515, arXiv:0709.1485 [astro-ph].

[194] A. Henriques, A. R. Liddle, and R. Moorhouse, "COMBINED BOSON - FERMION STARS," *Phys.Lett.* **B233** (1989) 99.

[195] A. Henriques, A. R. Liddle, and R. Moorhouse, "Combined Boson - Fermion Stars: Configurations and Stability," *Nucl.Phys.* **B337** (1990) 737.

[196] L. Lopes and A. Henriques, "Boson - fermion stars: Going to larger boson masses," *Phys.Lett.* **B285** (1992) 80–84.

[197] A. B. Henriques and L. E. Mendes, "Boson - fermion stars: Exploring different configurations," *Astrophys.Space Sci.* **300** (2005) 367–379, arXiv:astro-ph/0301015 [astro-ph].

[198] K. Sakamoto and K. Shiraishi, "Exact solutions for boson fermion stars in (2+1)-dimensions," *Phys.Rev.* **D58** (1998) 124017, arXiv:gr-qc/9806040 [gr-qc].

[199] F. Pisano and J. Tomazelli, "Stars of WIMPs," *Mod.Phys.Lett.* **A11** (1996) 647–652, arXiv:gr-qc/9509022 [gr-qc].

[200] S. C. Leung, M. C. Chu, and L. M. Lin, "Dark-matter admixed neutron stars," *Phys. Rev.* **D84** (2011) 107301, arXiv:1111.1787 [astro-ph.CO].

[201] S.-C. Leung, M.-C. Chu, L.-M. Lin, and K.-W. Wong, "Dark-matter admixed white dwarfs," *Phys.Rev.* **D87** no. 12, (2013) 123506, arXiv:1305.6142 [astro-ph.CO].

[202] L. Tolos and J. Schaffner-Bielich, "Dark Compact Planets," *Phys. Rev.* **D92** (2015) 123002, arXiv:1507.08197 [astro-ph.HE].

[203] H. Andreasson, "Sharp bounds on 2m/r of general spherically symmetric static objects," *J. Diff. Eq.* **245** (2008) 2243–2266, arXiv:gr-qc/0702137 [gr-qc].

[204] R. Kippenhahn, A. Weigert, and A. Weiss, *Stellar Structure and Evolution*. Springer, 2012.

[205] M. Ruderman, "Pulsars: structure and dynamics," *Ann. Rev. Astron. Astrophys.* **10** (1972) 427–476.

[206] V. Canuto and S. M. Chitre, "Crystallization of dense neutron matter," *Phys. Rev.* **D9** (1974) 1587–1613.

[207] R. F. Sawyer and D. J. Scalapino, "Pion condensation in superdense nuclear matter," *Phys. Rev.* **D7** (1973) 953–964.

[208] B. Carter and D. Langlois, "Relativistic models for superconducting superfluid mixtures," *Nucl. Phys.* **B531** (1998) 478–504, arXiv:gr-qc/9806024 [gr-qc].

[209] J. Guven and N. O'Murchadha, "Bounds on 2m / R for static spherical objects," *Phys. Rev.* **D60** (1999) 084020, arXiv:gr-qc/9903067 [gr-qc].

[210] R. L. Bowers and E. P. T. Liang, "Anisotropic Spheres in General Relativity," *Astrophys. J.* **188** (Mar., 1974) 657.

[211] P. S. Letelier, "Anisotropic fluids with two-perfect-fluid components," *Phys. Rev.* **D22** no. 4, (1980) 807.

[212] S. S. Bayin, "Anisotropic Fluid Spheres in General Relativity," *Phys. Rev.* **D26** (1982) 1262.

[213] K. Dev and M. Gleiser, "Anisotropic stars: Exact solutions," *Gen. Rel. Grav.* **34** (2002) 1793–1818, arXiv:astro-ph/0012265 [astro-ph].

[214] M. K. Mak and T. Harko, "Anisotropic stars in general relativity," *Proc. Roy. Soc. Lond.* **A459** (2003) 393–408, arXiv:gr-qc/0110103 [gr-qc].

[215] L. Herrera, A. Di Prisco, J. Martin, J. Ospino, N. O. Santos, and O. Troconis, "Spherically symmetric dissipative anisotropic fluids: A General study," *Phys. Rev.* **D69** (2004) 084026, arXiv:gr-qc/0403006 [gr-qc].

[216] W. Hillebrandt and K. O. Steinmetz, "Anisotropic neutron star models - Stability against radial and nonradial pulsations," A&A **53** (Dec., 1976) 283–287.

[217] K. Yagi and N. Yunes, "I-Love-Q anisotropically: Universal relations for compact stars with scalar pressure anisotropy," *Phys. Rev.* **D91** no. 12, (2015) 123008, arXiv:1503.02726 [gr-qc].

[218] K. Yagi and N. Yunes, "I-Love-Q Relations: From Compact Stars to Black Holes," *Class. Quant. Grav.* **33** no. 9, (2016) 095005, arXiv:1601.02171 [gr-qc].

[219] S. Carloni and D. Vernieri, "Covariant Tolman-Oppenheimer-Volkoff equations. II. The anisotropic case," *Phys. Rev.* **D97** no. 12, (2018) 124057, arXiv:1709.03996 [gr-qc].

[220] A. A. Isayev, "Comment on "Covariant Tolman-Oppenheimer-Volkoff equations. II. The anisotropic case"," *Phys. Rev.* **D98** no. 8, (2018) 088503, arXiv:1808.05699 [gr-qc].

[221] M. S. Morris and K. S. Thorne, "Wormholes in space-time and their use for interstellar travel: A tool for teaching general relativity," *Am. J. Phys.* **56** (1988) 395–412.

[222] M. Visser, *Lorentzian wormholes: From Einstein to Hawking*. 1995.

[223] J. P. S. Lemos, F. S. N. Lobo, and S. Quinet de Oliveira, "Morris-Thorne wormholes with a cosmological constant," *Phys. Rev.* **D68** (2003) 064004, arXiv:gr-qc/0302049 [gr-qc].

[224] J. Maldacena, A. Milekhin, and F. Popov, "Traversable wormholes in four dimensions," arXiv:1807.04726 [hep-th].

[225] T. Damour and S. N. Solodukhin, "Wormholes as black hole foils," *Phys. Rev.* **D76** (2007) 024016, arXiv:0704.2667 [gr-qc].

[226] M. Visser, *Lorentzian wormholes: From Einstein to Hawking*. AIP, Woodbury, USA, 1996.

[227] R. Shaikh and S. Kar, "Wormholes, the weak energy condition, and scalar-tensor gravity," *Phys. Rev.* **D94** no. 2, (2016) 024011, arXiv:1604.02857 [gr-qc].

[228] M. Chianese, E. Di Grezia, M. Manfredonia, and G. Miele, "Characterising exotic matter driving wormholes," *Eur. Phys. J. Plus* **132** no. 4, (2017) 164, arXiv:1701.08770 [gr-qc].

[229] M. Hohmann, C. Pfeifer, M. Raidal, and H. Veermäe, "Wormholes in conformal gravity," *JCAP* **1810** no. 10, (2018) 003, arXiv:1802.02184 [gr-qc].

[230] R. Shaikh, "Wormholes with nonexotic matter in Born-Infeld gravity," *Phys. Rev.* **D98** no. 6, (2018) 064033, arXiv:1807.07941 [gr-qc].

[231] A. Khaybullina and G. Tuleganova, "Stability of Schwarzschild-$f(R)$ gravity thin-shell wormholes," *Mod. Phys. Lett.* **A34** no. 01, (2019) 1950006, arXiv:1810.09222 [gr-qc].

[232] P. Kanti, B. Kleihaus, and J. Kunz, "Wormholes in Dilatonic Einstein-Gauss-Bonnet Theory," *Phys. Rev. Lett.* **107** (2011) 271101, arXiv:1108.3003 [gr-qc].

[233] N. D. Birrell and P. C. W. Davies, *Quantum Fields in Curved Space*. Cambridge Monographs on Mathematical Physics. Cambridge Univ. Press, Cambridge, UK, 1984. http://www.cambridge.org/mw/academic/subjects/physics/theoretical-physics-and-mathematical-physics/quantum-fields-curved-space?format=PB.

[234] M. Visser, C. Barcelo, S. Liberati, and S. Sonego, "Small, dark, and heavy: But is it a black hole?," arXiv:0902.0346 [gr-qc]. [PoSBHGRS,010(2008)].

[235] D.-f. Zeng, "Resolving the Schwarzschild singularity in both classic and quantum gravity," *Nucl. Phys.* **B917** (2017) 178–192, arXiv:1606.06178 [hep-th].

[236] P. Chen, W. G. Unruh, C.-H. Wu, and D.-H. Yeom, "Pre-Hawking radiation cannot prevent the formation of apparent horizon," *Phys. Rev.* **D97** no. 6, (2018) 064045, arXiv:1710.01533 [gr-qc].

[237] C. Berthiere, D. Sarkar, and S. N. Solodukhin, "The fate of black hole horizons in semiclassical gravity," *Phys. Lett.* **B786** (2018) 21–27, arXiv:1712.09914 [hep-th].

[238] L. Buoninfante and A. Mazumdar, "Nonlocal star as a blackhole mimicker," arXiv:1903.01542 [gr-qc].

[239] D. Terno, "Self-consistent description of a spherically-symmetric gravitational collapse," arXiv:1903.04744 [gr-qc].

[240] D. Malafarina, "Classical collapse to black holes and quantum bounces: A review," *Universe* **3** no. 2, (2017) 48, arXiv:1703.04138 [gr-qc].

[241] C. Barceló, S. Liberati, S. Sonego, and M. Visser, "Black Stars, Not Holes," *Sci. Am.* **301** no. 4, (2009) 38–45.

[242] H. Kawai, Y. Matsuo, and Y. Yokokura, "A Self-consistent Model of the Black Hole Evaporation," *Int. J. Mod. Phys.* **A28** (2013) 1350050, arXiv:1302.4733 [hep-th].

[243] V. Baccetti, R. B. Mann, and D. R. Terno, "Role of evaporation in gravitational collapse," *Class. Quant. Grav.* **35** no. 18, (2018) 185005, arXiv:1610.07839 [gr-qc].

[244] V. Baccetti, R. B. Mann, and D. R. Terno, "Do event horizons exist?," *Int. J. Mod. Phys.* **D26** no. 12, (2017) 1743008, arXiv:1706.01180 [gr-qc].

[245] R. Carballo-Rubio, "Stellar equilibrium in semiclassical gravity," *Phys. Rev. Lett.* **120** no. 6, (2018) 061102, arXiv:1706.05379 [gr-qc].

[246] V. Baccetti, S. Murk, and D. R. Terno, "Thin shell collapse in semiclassical gravity," arXiv:1812.07727 [gr-qc].

[247] P. O. Mazur and E. Mottola, "Gravitational condensate stars: An alternative to black holes," arXiv:gr-qc/0109035 [gr-qc].

[248] E. Mottola and R. Vaulin, "Macroscopic Effects of the Quantum Trace Anomaly," *Phys. Rev.* **D74** (2006) 064004, arXiv:gr-qc/0604051 [gr-qc].

[249] C. Cattoen, T. Faber, and M. Visser, "Gravastars must have anisotropic pressures," *Class. Quant. Grav.* **22** (2005) 4189–4202, arXiv:gr-qc/0505137 [gr-qc].

[250] P. O. Mazur and E. Mottola, "Surface tension and negative pressure interior of a non-singular "black hole"," *Class. Quant. Grav.* **32** no. 21, (2015) 215024, arXiv:1501.03806 [gr-qc].

[251] U. Danielsson and S. Giri, "Observational signatures from horizonless black shells imitating rotating black holes," *JHEP* **07** (2018) 070, arXiv:1712.00511 [hep-th].

[252] C. Posada and C. Chirenti, "On the radial stability of ultra compact Schwarzschild stars beyond the Buchdahl limit," *Class. Quant. Grav.* **36** (2019) 065004, arXiv:1811.09589 [gr-qc].

[253] Y.-T. Wang, J. Zhang, and Y.-S. Piao, "Primordial gravastar from inflation," arXiv:1810.04885 [gr-qc].

[254] A. Strominger and C. Vafa, "Microscopic origin of the Bekenstein-Hawking entropy," *Phys. Lett.* **B379** (1996) 99–104, arXiv:hep-th/9601029 [hep-th].

[255] A. W. Peet, "The Bekenstein formula and string theory (N-brane theory)," *Class. Quant. Grav.* **15** (1998) 3291–3338, arXiv:hep-th/9712253 [hep-th].

[256] S. R. Das and S. D. Mathur, "The quantum physics of black holes: Results from string theory," *Ann. Rev. Nucl. Part. Sci.* **50** (2000) 153–206, arXiv:gr-qc/0105063 [gr-qc].

[257] J. R. David, G. Mandal, and S. R. Wadia, "Microscopic formulation of black holes in string theory," *Phys. Rept.* **369** (2002) 549–686, arXiv:hep-th/0203048 [hep-th].

[258] I. Bena and N. P. Warner, "Black holes, black rings and their microstates," *Lect. Notes Phys.* **755** (2008) 1–92, arXiv:hep-th/0701216 [hep-th].

[259] R. C. Myers, "Pure states don't wear black," *Gen. Rel. Grav.* **29** (1997) 1217–1222, arXiv:gr-qc/9705065 [gr-qc].

[260] V. Balasubramanian, J. de Boer, S. El-Showk, and I. Messamah, "Black Holes as Effective Geometries," *Class. Quant. Grav.* **25** (2008) 214004, arXiv:0811.0263 [hep-th].

[261] I. Bena and N. P. Warner, "Resolving the Structure of Black Holes: Philosophizing with a Hammer," arXiv:1311.4538 [hep-th].

[262] O. Lunin and S. D. Mathur, "Statistical interpretation of Bekenstein entropy for systems with a stretched horizon," *Phys. Rev. Lett.* **88** (2002) 211303, arXiv:hep-th/0202072 [hep-th].

[263] O. Lunin and S. D. Mathur, "AdS / CFT duality and the black hole information paradox," *Nucl. Phys.* **B623** (2002) 342–394, arXiv:hep-th/0109154 [hep-th].

[264] E. G. Gimon and P. Horava, "Astrophysical violations of the Kerr bound as a possible signature of string theory," *Phys. Lett.* **B672** (2009) 299–302, arXiv:0706.2873 [hep-th].

[265] T. Harada, H. Iguchi, and K.-i. Nakao, "Naked singularity explosion," *Phys. Rev.* **D61** (2000) 101502, arXiv:gr-qc/0003036 [gr-qc].

[266] K. S. Stelle, "Renormalization of Higher Derivative Quantum Gravity," *Phys. Rev.* **D16** (1977) 953–969.

[267] B. L. Voronov and I. V. Tyutin, "ON RENORMALIZATION OF R**2 GRAVITATION. (IN RUSSIAN)," *Yad. Fiz.* **39** (1984) 998–1010.

[268] B. Holdom and J. Ren, "QCD analogy for quantum gravity," *Phys. Rev.* **D93** no. 12, (2016) 124030, arXiv:1512.05305 [hep-th].

[269] J. Beltran Jimenez, L. Heisenberg, G. J. Olmo, and D. Rubiera-Garcia, "Born Infeld inspired modifications of gravity," *Phys. Rept.* **727** (2018) 1–129, arXiv:1704.03351 [gr-qc].

[270] V. I. Afonso, G. J. Olmo, and D. Rubiera-Garcia, "Scalar geons in Born Infeld gravity," *JCAP* **1708** no. 08, (2017) 031, arXiv:1705.01065 [gr-qc].

[271] V. Afonso, G. J. Olmo, and D. Rubiera-Garcia, "Mapping Ricci-based theories of gravity into general relativity," *Phys. Rev.* **D97** no. 2, (2018) 021503, arXiv:1801.10406 [gr-qc].

[272] E. Franzin, M. Cadoni, and M. Tuveri, "Sine-Gordon solitonic scalar stars and black holes," *Phys. Rev.* **D97** no. 12, (2018) 124018, arXiv:1805.08976 [gr-qc].

[273] L. Sebastiani, L. Vanzo, and S. Zerbini, "On a WKB formula for echoes," arXiv:1808.06939 [gr-qc].

[274] A. S. Koshelev and A. Mazumdar, "Do massive compact objects without event horizon exist in infinite derivative gravity?," *Phys. Rev.* **D96** no. 8, (2017) 084069, arXiv:1707.00273 [gr-qc].

[275] L. Buoninfante, A. S. Koshelev, G. Lambiase, J. Marto, and A. Mazumdar, "Conformally-flat, non-singular static metric in infinite derivative gravity," *JCAP* **1806** no. 06, (2018) 014, arXiv:1804.08195 [gr-qc].

[276] S. B. Giddings, "Nonviolent information transfer from black holes: A field theory parametrization," *Phys. Rev.* **D88** no. 2, (2013) 024018, arXiv:1302.2613 [hep-th].

[277] D. E. Kaplan and S. Rajendran, "Firewalls in General Relativity," *Phys. Rev.* **D99** no. 4, (2019) 044033, arXiv:1812.00536 [hep-th].

[278] J. Zhang and S.-Y. Zhou, "Can the graviton have a large mass near black holes?," *Phys. Rev.* **D97** no. 8, (2018) 081501, arXiv:1709.07503 [gr-qc].

[279] N. Oshita and N. Afshordi, "Probing microstructure of black hole spacetimes with gravitational wave echoes," *Phys. Rev.* **D99** no. 4, (2019) 044002, arXiv:1807.10287 [gr-qc].

[280] A. Buonanno, G. B. Cook, and F. Pretorius, "Inspiral, merger and ring-down of equal-mass black-hole binaries," *Phys. Rev.* **D75** (2007) 124018, arXiv:gr-qc/0610122 [gr-qc].

[281] E. Berti, V. Cardoso, J. A. Gonzalez, U. Sperhake, M. Hannam, S. Husa, and B. Bruegmann, "Inspiral, merger and ringdown of unequal mass black hole binaries: A Multipolar analysis," *Phys. Rev.* **D76** (2007) 064034, arXiv:gr-qc/0703053 [GR-QC].

[282] U. Sperhake, E. Berti, and V. Cardoso, "Numerical simulations of black-hole binaries and gravitational wave emission," *Comptes Rendus Physique* **14** (2013) 306–317, arXiv:1107.2819 [gr-qc].

[283] E. Berti, V. Cardoso, and A. O. Starinets, "Quasinormal modes of black holes and black branes," *Class. Quantum Grav.* **26** (2009) 163001, arXiv:0905.2975 [gr-qc].

[284] L. Blanchet, "Gravitational Radiation from Post-Newtonian Sources and Inspiralling Compact Binaries," *Living Rev. Rel.* **17** (2014) 2, arXiv:1310.1528 [gr-qc].

[285] F. Zerilli, "Gravitational field of a particle falling in a schwarzschild geometry analyzed in tensor harmonics," *Phys. Rev.* **D2** (1970) 2141–2160.

[286] S. Chandrasekhar and S. L. Detweiler, "The quasi-normal modes of the Schwarzschild black hole," *Proc. Roy. Soc. Lond.* **A344** (1975) 441–452.

[287] J. L. Blázquez-Salcedo, C. F. B. Macedo, V. Cardoso, V. Ferrari, L. Gualtieri, F. S. Khoo, J. Kunz, and P. Pani, "Perturbed black holes in Einstein-dilaton-Gauss-Bonnet gravity: Stability, ringdown, and gravitational-wave emission," *Phys. Rev.* **D94** no. 10, (2016) 104024, arXiv:1609.01286 [gr-qc].

[288] V. Cardoso and L. Gualtieri, "Perturbations of Schwarzschild black holes in Dynamical Chern-Simons modified gravity," *Phys. Rev.* **D80** (2009) 064008, arXiv:0907.5008 [gr-qc]. [Erratum: Phys. Rev.D81,089903(2010)].

[289] O. J. Tattersall, P. G. Ferreira, and M. Lagos, "General theories of linear gravitational perturbations to a Schwarzschild Black Hole," *Phys. Rev.* **D97** no. 4, (2018) 044021, arXiv:1711.01992 [gr-qc].

[290] V. Cardoso, M. Kimura, A. Maselli, and L. Senatore, "Black Holes in an Effective Field Theory Extension of General Relativity," *Phys. Rev. Lett.* **121** no. 25, (2018) 251105, arXiv:1808.08962 [gr-qc].

[291] C. Molina, P. Pani, V. Cardoso, and L. Gualtieri, "Gravitational signature of Schwarzschild black holes in dynamical Chern-Simons gravity," *Phys. Rev.* **D81** (2010) 124021, arXiv:1004.4007 [gr-qc].

[292] Webpage with Mathematica notebooks and numerical quasinormal mode Tables: http://centra.tecnico.ulisboa.pt/network/grit/files/ http://www.darkgra.org .

[293] A. Vilenkin, "Exponential Amplification of Waves in the Gravitational Field of Ultrarelativistic Rotating Body," *Phys. Lett.* **B78** (1978) 301–303.

[294] E. Maggio, P. Pani, and V. Ferrari, "Exotic Compact Objects and How to Quench their Ergoregion Instability," *Phys. Rev.* **D96** no. 10, (2017) 104047, arXiv:1703.03696 [gr-qc].

[295] E. Maggio, V. Cardoso, S. R. Dolan, and P. Pani, "Ergoregion instability of exotic compact objects: electromagnetic and gravitational perturbations and the role of absorption," *Phys. Rev.* **D99** no. 6, (2019) 064007, arXiv:1807.08840 [gr-qc].

[296] A. A. Starobinskij and S. M. Churilov, "Amplification of electromagnetic and gravitational waves scattered by a rotating black hole.," *Zhurnal Eksperimentalnoi i Teoreticheskoi Fiziki* **65** (1973) 3–11.

[297] Z. Mark, A. Zimmerman, S. M. Du, and Y. Chen, "A recipe for echoes from exotic compact objects," *Phys. Rev.* **D96** no. 8, (2017) 084002, arXiv:1706.06155 [gr-qc].

[298] S. H. Völkel and K. D. Kokkotas, "Wormhole Potentials and Throats from Quasi-Normal Modes," *Class. Quant. Grav.* **35** no. 10, (2018) 105018, arXiv:1802.08525 [gr-qc].

[299] S. H. Völkel, "Inverse spectrum problem for quasi-stationary states," *J. Phys. Commun.* **2** (2018) 025029, arXiv:1802.08684 [quant-ph].

[300] S. D. Mathur and D. Turton, "Comments on black holes I: The possibility of complementarity," *JHEP* **01** (2014) 034, arXiv:1208.2005 [hep-th].

[301] R. A. Konoplya and Z. Stuchlík, "Are eikonal quasinormal modes linked to the unstable circular null geodesics?," *Phys. Lett.* **B771** (2017) 597–602, arXiv:1705.05928 [gr-qc].

[302] R. H. Price and G. Khanna, "Gravitational wave sources: reflections and echoes," *Class. Quant. Grav.* **34** no. 22, (2017) 225005, arXiv:1702.04833 [gr-qc].

[303] J. T. G. Ghersi, A. V. Frolov, and D. A. Dobre, "Echoes from the scattering of wavepackets on wormholes," arXiv:1901.06625 [gr-qc].

[304] J. Abedi, H. Dykaar, and N. Afshordi, "Echoes from the Abyss: Tentative evidence for Planck-scale structure at black hole horizons," *Phys. Rev.* **D96** no. 8, (2017) 082004, arXiv:1612.00266 [gr-qc].

[305] O. Ramos and E. Barausse, "Constraints on Horava gravity from binary black hole observations," *Phys. Rev.* **D99** no. 2, (2019) 024034, arXiv:1811.07786 [gr-qc].

[306] R. A. Konoplya, Z. Stuchlík, and A. Zhidenko, "Echoes of compact objects: new physics near the surface and matter at a distance," *Phys. Rev.* **D99** no. 2, (2019) 024007, arXiv:1810.01295 [gr-qc].

[307] K. Lin, W.-L. Qian, X. Fan, and H. Zhang, "Tail wavelets in the merger of binary compact objects," arXiv:1903.09039 [gr-qc].

[308] M. Mannarelli and F. Tonelli, "Gravitational wave echoes from strange stars," *Phys. Rev.* **D97** no. 12, (2018) 123010, arXiv:1805.02278 [gr-qc].

[309] C. M. Bender and S. A. Orszag, *Advanced mathematical methods for scientists and engineers*. Springer-Verlag, New York, 1999.

[310] H. Nakano, N. Sago, H. Tagoshi, and T. Tanaka, "Black hole ringdown echoes and howls," *PTEP* **2017** no. 7, (2017) 071E01, arXiv:1704.07175 [gr-qc].

[311] R. S. Conklin, B. Holdom, and J. Ren, "Gravitational wave echoes through new windows," *Phys. Rev.* **D98** no. 4, (2018) 044021, arXiv:1712.06517 [gr-qc].

[312] C. P. Burgess, R. Plestid, and M. Rummel, "Effective Field Theory of Black Hole Echoes," *JHEP* **09** (2018) 113, arXiv:1808.00847 [gr-qc].

[313] G. Khanna and R. H. Price, "Black Hole Ringing, Quasinormal Modes, and Light Rings," *Phys. Rev.* **D95** no. 8, (2017) 081501, arXiv:1609.00083 [gr-qc].

[314] M. R. Correia and V. Cardoso, "Characterization of echoes: A Dyson-series representation of individual pulses," *Phys. Rev.* **D97** no. 8, (2018) 084030, arXiv:1802.07735 [gr-qc].

[315] A. Testa and P. Pani, "Analytical template for gravitational-wave echoes: signal characterization and prospects of detection with current and future interferometers," *Phys. Rev.* **D98** no. 4, (2018) 044018, arXiv:1806.04253 [gr-qc].

[316] Q. Wang and N. Afshordi, "Black hole echology: The observer's manual," *Phys. Rev.* **D97** no. 12, (2018) 124044, arXiv:1803.02845 [gr-qc].

[317] A. Maselli, S. H. Völkel, and K. D. Kokkotas, "Parameter estimation of gravitational wave echoes from exotic compact objects," *Phys. Rev.* **D96** no. 6, (2017) 064045, arXiv:1708.02217 [gr-qc].

[318] G. Poschl and E. Teller, "Bemerkungen zur Quantenmechanik des anharmonischen Oszillators," *Z. Phys.* **83** (1933) 143–151.

[319] K. W. Tsang, M. Rollier, A. Ghosh, A. Samajdar, M. Agathos, K. Chatziioannou, V. Cardoso, G. Khanna, and C. Van Den Broeck, "A morphology-independent data analysis method for detecting and characterizing gravitational wave echoes," *Phys. Rev.* **D98** no. 2, (2018) 024023, arXiv:1804.04877 [gr-qc].

[320] S. Chandrasekhar and V. Ferrari, "On the Non-Radial Oscillations of a Star III. A Reconsideration of the Axial Modes," *Proceedings of the Royal Society of London A: Mathematical, Physical and Engineering Sciences* **434** no. 1891, (1991) 449–457.

[321] S. Giusto, S. D. Mathur, and A. Saxena, "3-charge geometries and their CFT duals," *Nucl. Phys.* **B710** (2005) 425–463, arXiv:hep-th/0406103 [hep-th].

[322] S. A. Teukolsky, "Rotating black holes - separable wave equations for gravitational and electromagnetic perturbations," *Phys. Rev. Lett.* **29** (1972) 1114–1118.

[323] S. A. Teukolsky, "Perturbations of a rotating black hole. 1. Fundamental equations for gravitational electromagnetic and neutrino field perturbations," *Astrophys. J.* **185** (1973) 635–647.

[324] S. Detweiler, "On resonant oscillations of a rapidly rotating black hole," *Proceedings of the Royal Society of London Series A* **352** (July, 1977) 381–395.

[325] H. Yang, D. A. Nichols, F. Zhang, A. Zimmerman, Z. Zhang, and Y. Chen, "Quasinormal-mode spectrum of Kerr black holes and its geometric interpretation," *Phys. Rev.* **D86** (2012) 104006, arXiv:1207.4253 [gr-qc].

[326] C. Posada, "Slowly rotating supercompact Schwarzschild stars," *Mon. Not. Roy. Astron. Soc.* **468** no. 2, (2017) 2128–2139, arXiv:1612.05290 [gr-qc].

[327] G. O. Papadopoulos and K. D. Kokkotas, "Preserving Kerr symmetries in deformed spacetimes," *Class. Quant. Grav.* **35** no. 18, (2018) 185014, arXiv:1807.08594 [gr-qc].

[328] G. Pappas and K. Glampedakis, "On the connection of spacetime separability and spherical photon orbits," arXiv:1806.04091 [gr-qc].

[329] K. Glampedakis and G. Pappas, "The absence of spherical photon orbits as a diagnostic of non-Kerr spacetimes," arXiv:1806.09333 [gr-qc].

[330] S. A. Teukolsky and W. H. Press, "Perturbations of a rotating black hole. III - Interaction of the hole with gravitational and electromagnet ic radiation," *Astrophys. J.* **193** (1974) 443–461.

[331] E. Berti, V. Cardoso, and M. Casals, "Eigenvalues and eigenfunctions of spin-weighted spheroidal harmonics in four and higher dimensions," *Phys.Rev.* **D73** (2006) 024013, arXiv:gr-qc/0511111 [gr-qc].

[332] R. Vicente, V. Cardoso, and J. C. Lopes, "Penrose process, superradiance, and ergoregion instabilities," *Phys. Rev.* **D97** no. 8, (2018) 084032, arXiv:1803.08060 [gr-qc].

[333] J. L. Friedman, "Generic instability of rotating relativistic stars," *Commun. Math. Phys.* **62** no. 3, (1978) 247–278.

[334] G. Moschidis, "A Proof of Friedman's Ergosphere Instability for Scalar Waves," *Commun. Math. Phys.* **358** no. 2, (2018) 437–520, arXiv:1608.02035 [math.AP].

[335] S. Hod, "Onset of superradiant instabilities in rotating spacetimes of exotic compact objects," *JHEP* **06** (2017) 132, arXiv:1704.05856 [hep-th].

[336] P. Bueno, P. A. Cano, F. Goelen, T. Hertog, and B. Vercnocke, "Echoes of Kerr-like wormholes," *Phys. Rev.* **D97** no. 2, (2018) 024040, arXiv:1711.00391 [gr-qc].

[337] A. Testa, E. Maggio, S. Bhagwat, and P. Pani, "Analytical template for gravitational-wave echoes from spinning remnants (in preparation),".

[338] M. Dafermos and I. Rodnianski, "Lectures on black holes and linear waves," *Clay Math. Proc.* **17** (2013) 97–205, arXiv:0811.0354 [gr-qc].

[339] L. A. Oliveira, V. Cardoso, and L. C. B. Crispino, "Ergoregion instability: The hydrodynamic vortex," *Phys. Rev.* **D89** no. 12, (2014) 124008, arXiv:1405.4038 [gr-qc].

[340] J. L. Friedman, "Ergosphere instability," *Communications in Mathematical Physics* **63** no. 3, (1978) 243–255. http://projecteuclid.org/euclid.cmp/1103904565.

[341] N. Comins and B. F. Schutz, "On the ergoregion instability," *Proceedings of the Royal Society of London. Series A, Mathematical and Physical Sciences* **364** no. 1717, (1978) pp. 211–226. http://www.jstor.org/stable/79759.

[342] S. Yoshida and Y. Eriguchi, "Ergoregion instability revisited - a new and general method for numerical analysis of stability," *Mon.Not.Roy.Astron.Soc.* **282** (Sept., 1996) 580–586.

[343] C. B. M. H. Chirenti and L. Rezzolla, "On the ergoregion instability in rotating gravastars," *Phys. Rev.* **D78** (2008) 084011, arXiv:0808.4080 [gr-qc].

[344] E. Barausse, R. Brito, V. Cardoso, I. Dvorkin, and P. Pani, "The stochastic gravitational-wave background in the absence of horizons," *Class. Quant. Grav.* **35** no. 20, (2018) 20LT01, arXiv:1805.08229 [gr-qc].

[345] B. Guo, S. Hampton, and S. D. Mathur, "Can we observe fuzzballs or firewalls?," *JHEP* **07** (2018) 162, arXiv:1711.01617 [hep-th].

[346] J. Keir, "Slowly decaying waves on spherically symmetric spacetimes and ultracompact neutron stars," *Class. Quant. Grav.* **33** no. 13, (2016) 135009, arXiv:1404.7036 [gr-qc].

[347] T. Shiromizu, Y. Tomikawa, K. Izumi, and H. Yoshino, "Area bound for a surface in a strong gravity region," *PTEP* **2017** no. 3, (2017) 033E01, arXiv:1701.00564 [gr-qc].

[348] H. Yoshino, K. Izumi, T. Shiromizu, and Y. Tomikawa, "Extension of photon surfaces and their area: Static and stationary spacetimes," *PTEP* **2017** no. 6, (2017) 063E01, arXiv:1704.04637 [gr-qc].

[349] F. John, "Blow-up for quasi-linear wave equations in three space dimensions," *Communications on Pure and Applied Mathematics* **34** (1981) 29–51.

[350] R. Carballo-Rubio, P. Kumar, and W. Lu, "Seeking observational evidence for the formation of trapping horizons in astrophysical black holes," *Phys. Rev.* **D97** no. 12, (2018) 123012, arXiv:1804.00663 [gr-qc].

[351] B. Chen, Y. Chen, Y. Ma, K.-L. R. Lo, and L. Sun, "Instability of exotic compact objects and its implications for gravitational-wave echoes," arXiv:1902.08180 [gr-qc].

[352] K. Thorne, "Nonspherical gravitational collapse: A short review," in *Magic Without Magic: John Archibald Wheeler. A Collection of Essays in Honor of his Sixtieth Birthday*, J. Klauder, ed., pp. 231–258. W.H. Freeman, San Francisco, 1972.

[353] D. M. Eardley and S. B. Giddings, "Classical black hole production in high-energy collisions," *Phys. Rev.* **D66** (2002) 044011, arXiv:gr-qc/0201034 [gr-qc].

[354] U. Sperhake, E. Berti, V. Cardoso, and F. Pretorius, "Universality, maximum radiation and absorption in high-energy collisions of black holes with spin," *Phys. Rev. Lett.* **111** no. 4, (2013) 041101, arXiv:1211.6114 [gr-qc].

[355] L. Blanchet, "Gravitational radiation from post-Newtonian sources and inspiralling compact binaries," *Living Rev. Rel.* **9** (2006) 4.

[356] N. V. Krishnendu, K. G. Arun, and C. K. Mishra, "Testing the binary black hole nature of a compact binary coalescence," *Phys. Rev. Lett.* **119** no. 9, (2017) 091101, arXiv:1701.06318 [gr-qc].

[357] N. V. Krishnendu, C. K. Mishra, and K. G. Arun, "Spin-induced deformations and tests of binary black hole nature using third-generation detectors," *Phys. Rev.* **D99** no. 6, (2019) 064008, arXiv:1811.00317 [gr-qc].

[358] S. Kastha, A. Gupta, K. G. Arun, B. S. Sathyaprakash, and C. Van Den Broeck, "Testing the multipole structure of compact binaries using gravitational wave observations," *Phys. Rev.* **D98** no. 12, (2018) 124033, arXiv:1809.10465 [gr-qc].

[359] E. Poisson and C. Will, *Gravity: Newtonian, Post-Newtonian, Relativistic.* Cambridge University Press, Cambridge, UK, 1953.

[360] J. B. Hartle, "Tidal Friction in Slowly Rotating Black Holes," *Phys. Rev.* **D8** (1973) 1010–1024.

[361] S. A. Hughes, "Evolution of circular, nonequatorial orbits of kerr black holes due to gravitational-wave emission. ii. inspiral trajectories and gravitational waveforms," *Phys. Rev. D* **64** (Aug, 2001) 064004. https://link.aps.org/doi/10.1103/PhysRevD.64.064004.

[362] E. Poisson, "Tidal interaction of black holes and Newtonian viscous bodies," *Phys. Rev.* **D80** (2009) 064029, arXiv:0907.0874 [gr-qc].

[363] V. Cardoso and P. Pani, "Tidal acceleration of black holes and superradiance," *Class. Quant. Grav.* **30** (2013) 045011, arXiv:1205.3184 [gr-qc].

[364] K. Alvi, "Energy and angular momentum flow into a black hole in a binary," *Phys. Rev.* **D64** (2001) 104020, arXiv:gr-qc/0107080 [gr-qc].

[365] E. Poisson, "Absorption of mass and angular momentum by a black hole: Time-domain formalisms for gravitational perturbations, and the small-hole / slow-motion approximation," *Phys. Rev.* **D70** (2004) 084044, arXiv:gr-qc/0407050 [gr-qc].

[366] T. Binnington and E. Poisson, "Relativistic theory of tidal Love numbers," *Phys. Rev.* **D80** (2009) 084018, arXiv:0906.1366 [gr-qc].

[367] T. Damour and A. Nagar, "Relativistic tidal properties of neutron stars," *Phys. Rev.* **D80** (2009) 084035, arXiv:0906.0096 [gr-qc].

[368] N. Gürlebeck, "No-hair theorem for Black Holes in Astrophysical Environments," *Phys. Rev. Lett.* **114** no. 15, (2015) 151102, arXiv:1503.03240 [gr-qc].

[369] E. Poisson, "Tidal deformation of a slowly rotating black hole," *Phys. Rev.* **D91** no. 4, (2015) 044004, arXiv:1411.4711 [gr-qc].

[370] P. Pani, L. Gualtieri, A. Maselli, and V. Ferrari, "Tidal deformations of a spinning compact object," *Phys. Rev.* **D92** no. 2, (2015) 024010, arXiv:1503.07365 [gr-qc].

[371] P. Landry and E. Poisson, "Tidal deformation of a slowly rotating material body. External metric," *Phys. Rev.* **D91** (2015) 104018, arXiv:1503.07366 [gr-qc].

[372] R. A. Porto, "The Tune of Love and the Nature(ness) of Spacetime," *Fortsch. Phys.* **64** (2016) 723–729, arXiv:1606.08895 [gr-qc].

[373] M. Wade, J. D. E. Creighton, E. Ochsner, and A. B. Nielsen, "Advanced LIGO's ability to detect apparent violations of the cosmic censorship conjecture and the no-hair theorem through compact binary coalescence detections," *Phys. Rev.* **D88** no. 8, (2013) 083002, arXiv:1306.3901 [gr-qc].

[374] J. Vines, E. E. Flanagan, and T. Hinderer, "Post-1-Newtonian tidal effects in the gravitational waveform from binary inspirals," *Phys. Rev.* **D83** (2011) 084051, arXiv:1101.1673 [gr-qc].

[375] P. Pani, L. Gualtieri, and V. Ferrari, "Tidal Love numbers of a slowly spinning neutron star," *Phys. Rev.* **D92** (2015) 124003, arXiv:1509.02171 [gr-qc].

[376] T. Abdelsalhin, L. Gualtieri, and P. Pani, "Post-Newtonian spin-tidal couplings for compact binaries," *Phys. Rev.* **D98** no. 10, (2018) 104046, arXiv:1805.01487 [gr-qc].

[377] X. Jiménez Forteza, T. Abdelsalhin, P. Pani, and L. Gualtieri, "Impact of high-order tidal terms on binary neutron-star waveforms," *Phys. Rev.* **D98** no. 12, (2018) 124014, arXiv:1807.08016 [gr-qc].

[378] A. Maselli, P. Pani, V. Cardoso, T. Abdelsalhin, L. Gualtieri, and V. Ferrari, "From micro to macro and back: probing near-horizon quantum structures with gravitational waves," arXiv:1811.03689 [gr-qc].

[379] **LIGO Scientific, Virgo** Collaboration, B. P. Abbott *et al.*, "GW170817: Measurements of neutron star radii and equation of state," *Phys. Rev. Lett.* **121** no. 16, (2018) 161101, arXiv:1805.11581 [gr-qc].

[380] A. Addazi, A. Marciano, and N. Yunes, "Can we probe Planckian corrections at the horizon scale with gravitational waves?," *Phys. Rev. Lett.* **122** no. 8, (2019) 081301, arXiv:1810.10417 [gr-qc].

[381] T. Hinderer, B. D. Lackey, R. N. Lang, and J. S. Read, "Tidal deformability of neutron stars with realistic equations of state and their gravitational wave signatures in binary inspiral," *Physical Review D* **81** no. 12, (June, 2010) 101–12.

[382] A. Maselli, L. Gualtieri, and V. Ferrari, "Constraining the equation of state of nuclear matter with gravitational wave observations: Tidal deformability and tidal disruption," *Physical Review D* **88** no. 10, (Nov., 2013) 104040–12.

[383] V. Cardoso, A. del Río, and M. Kimura, "Distinguishing black holes from horizonless objects through the excitation of resonances," *in preparation* (2019) .

[384] R. F. P. Mendes and H. Yang, "Tidal deformability of boson stars and dark matter clumps," *Class. Quant. Grav.* **34** no. 18, (2017) 185001, arXiv:1606.03035 [astro-ph.CO].

[385] K. Eda, Y. Itoh, S. Kuroyanagi, and J. Silk, "Gravitational waves as a probe of dark matter minispikes," *Phys. Rev.* **D91** no. 4, (2015) 044045, arXiv:1408.3534 [gr-qc].

[386] X.-J. Yue and W.-B. Han, "Gravitational waves with dark matter minispikes: the combined effect," *Phys. Rev.* **D97** no. 6, (2018) 064003, arXiv:1711.09706 [gr-qc].

[387] O. A. Hannuksela, K. W. K. Wong, R. Brito, E. Berti, and T. G. F. Li, "Probing the existence of ultralight bosons with a single gravitational-wave measurement," *Nature Astron.* (2019) , arXiv:1804.09659 [astro-ph.HE].

[388] M. Bezares, C. Palenzuela, and C. Bona, "Final fate of compact boson star mergers," *Phys. Rev.* **D95** no. 12, (2017) 124005, arXiv:1705.01071 [gr-qc].

[389] C. Palenzuela, P. Pani, M. Bezares, V. Cardoso, L. Lehner, and S. Liebling, "Gravitational Wave Signatures of Highly Compact Boson Star Binaries," *Phys. Rev.* **D96** no. 10, (2017) 104058, arXiv:1710.09432 [gr-qc].

[390] M. Bezares and C. Palenzuela, "Gravitational Waves from Dark Boson Star binary mergers," *Class. Quant. Grav.* **35** no. 23, (2018) 234002, arXiv:1808.10732 [gr-qc].

[391] T. Helfer, E. A. Lim, M. A. G. Garcia, and M. A. Amin, "Gravitational Wave Emission from Collisions of Compact Scalar Solitons," *Phys. Rev.* **D99** no. 4, (2019) 044046, arXiv:1802.06733 [gr-qc].

[392] T. Dietrich, S. Ossokine, and K. Clough, "Full 3D numerical relativity simulations of neutron star boson star collisions with BAM," *Class. Quant. Grav.* **36** no. 2, (2019) 025002, arXiv:1807.06959 [gr-qc].

[393] K. Clough, T. Dietrich, and J. C. Niemeyer, "Axion star collisions with black holes and neutron stars in full 3D numerical relativity," *Phys. Rev.* **D98** no. 8, (2018) 083020, arXiv:1808.04668 [gr-qc].

[394] A. Maselli, P. Pnigouras, N. G. Nielsen, C. Kouvaris, and K. D. Kokkotas, "Dark stars: gravitational and electromagnetic observables," *Phys. Rev.* **D96** no. 2, (2017) 023005, arXiv:1704.07286 [astro-ph.HE].

[395] C. J. Horowitz and S. Reddy, "Gravitational Waves from Compact Dark Objects in Neutron Stars," arXiv:1902.04597 [astro-ph.HE].

[396] J. Ellis, A. Hektor, G. Hütsi, K. Kannike, L. Marzola, M. Raidal, and V. Vaskonen, "Search for Dark Matter Effects on Gravitational Signals from Neutron Star Mergers," *Phys. Lett.* **B781** (2018) 607–610, arXiv:1710.05540 [astro-ph.CO].

[397] G. F. Giudice, M. McCullough, and A. Urbano, "Hunting for Dark Particles with Gravitational Waves," *JCAP* **1610** no. 10, (2016) 001, arXiv:1605.01209 [hep-ph].

[398] J. Y. Widdicombe, T. Helfer, D. J. E. Marsh, and E. A. Lim, "Formation of Relativistic Axion Stars," *JCAP* **1810** no. 10, (2018) 005, arXiv:1806.09367 [astro-ph.CO].

[399] P. Beltracchi and P. Gondolo, "Formation of dark energy stars," *Phys. Rev.* **D99** no. 4, (2019) 044037, arXiv:1810.12400 [gr-qc].

[400] R. Narayan, M. R. Garcia, and J. E. McClintock, "Advection dominated accretion and black hole event horizons," *Astrophys. J.* **478** (1997) L79–L82, arXiv:astro-ph/9701139 [astro-ph].

[401] R. Narayan and J. S. Heyl, "On the lack of type I x-ray bursts in black hole x-ray binaries: Evidence for the event horizon?," *Astrophys. J.* **574** (2002) L139–L142, arXiv:astro-ph/0203089 [astro-ph].

[402] J. E. McClintock, R. Narayan, and G. B. Rybicki, "On the lack of thermal emission from the quiescent black hole XTE J1118+480: Evidence for the event horizon," *Astrophys. J.* **615** (2004) 402–415, arXiv:astro-ph/0403251 [astro-ph].

[403] R. Narayan and J. E. McClintock, "Advection-Dominated Accretion and the Black Hole Event Horizon," *New Astron. Rev.* **51** (2008) 733–751, arXiv:0803.0322 [astro-ph].

[404] A. E. Broderick, A. Loeb, and R. Narayan, "The Event Horizon of Sagittarius A*," *Astrophys. J.* **701** (2009) 1357–1366, arXiv:0903.1105 [astro-ph.HE].

[405] W. Lu, P. Kumar, and R. Narayan, "Stellar disruption events support the existence of the black hole event horizon," *Mon. Not. Roy. Astron. Soc.* **468** no. 1, (2017) 910–919, arXiv:1703.00023 [astro-ph.HE].

[406] A. Paranjape and T. Padmanabhan, "Radiation from collapsing shells, semiclassical backreaction and black hole formation," *Phys. Rev.* **D80** (2009) 044011, arXiv:0906.1768 [gr-qc].

[407] C. Barcelo, S. Liberati, S. Sonego, and M. Visser, "Hawking-like radiation from evolving black holes and compact horizonless objects," *JHEP* **02** (2011) 003, arXiv:1011.5911 [gr-qc].

[408] T. Harada, V. Cardoso, and D. Miyata, "Particle creation in gravitational collapse to a horizonless compact object," *Phys. Rev.* **D99** no. 4, (2019) 044039, arXiv:1811.05179 [gr-qc].

[409] N. Yunes, K. Yagi, and F. Pretorius, "Theoretical Physics Implications of the Binary Black-Hole Mergers GW150914 and GW151226," *Phys. Rev.* **D94** no. 8, (2016) 084002, arXiv:1603.08955 [gr-qc].

[410] T. Alexander, "Stellar processes near the massive black hole in the Galactic Center," *Phys. Rept.* **419** (2005) 65–142, arXiv:astro-ph/0508106 [astro-ph].

[411] J. Binney and S. Tremaine, *Galactic Dynamics: (Second Edition)*. Princeton Series in Astrophysics. Princeton University Press, 2011. https://books.google.ch/books?id=6mF4CKxlbLsC.

[412] M. A. Abramowicz, T. Bulik, G. F. R. Ellis, K. A. Meissner, and M. Wielgus, "The electromagnetic afterglows of gravitational waves as a test for Quantum Gravity," arXiv:1603.07830 [gr-qc].

[413] D. Malafarina and P. S. Joshi, "Electromagnetic Counterparts to Gravitational Waves from Black Hole Mergers and Naked Singularities," arXiv:1603.02848 [gr-qc].

[414] S.-N. Zhang, Y. Liu, S. Yi, Z. Dai, and C. Huang, "Do we expect to detect electromagnetic radiation from merging stellar mass black binaries like GW150914? No," arXiv:1604.02537 [gr-qc].

[415] C. A. Benavides-Gallego, A. Abdujabbarov, D. Malafarina, B. Ahmedov, and C. Bambi, "Charged particle motion and electromagnetic field in γ spacetime," *Phys. Rev.* **D99** no. 4, (2019) 044012, arXiv:1812.04846 [gr-qc].

[416] K. C. Chambers *et al.*, "The Pan-STARRS1 Surveys," arXiv:1612.05560 [astro-ph.IM].

[417] T. Johannsen, "Sgr A* and General Relativity," *Class. Quant. Grav.* **33** no. 11, (2016) 113001, arXiv:1512.03818 [astro-ph.GA].

[418] A. Eckart, A. Huttemann, C. Kiefer, S. Britzen, M. Zajacek, C. Lammerzahl, M. Stockler, M. Valencia S, V. Karas, and M. Garcia Marin, "The Milky Way's Supermassive Black Hole: How Good a Case Is It?," *Found. Phys.* **47** no. 5, (2017) 553–624, arXiv:1703.09118 [astro-ph.HE].

[419] V. Cardoso and P. Pani, "The observational evidence for horizons: from echoes to precision gravitational-wave physics," arXiv:1707.03021 [gr-qc].

[420] M. Banados, J. Silk, and S. M. West, "Kerr Black Holes as Particle Accelerators to Arbitrarily High Energy," *Phys. Rev. Lett.* **103** (2009) 111102, arXiv:0909.0169 [hep-ph].

[421] S. R. Kelner, F. A. Aharonian, and V. V. Bugayov, "Energy spectra of gamma-rays, electrons and neutrinos produced at proton-proton interactions in the very high energy regime," *Phys. Rev.* **D74** (2006) 034018, arXiv:astro-ph/0606058 [astro-ph]. [Erratum: Phys. Rev.D79,039901(2009)].

[422] S. S. Doeleman *et al.*, "Jet Launching Structure Resolved Near the Supermassive Black Hole in M87," *Science* **338** (2012) 355, arXiv:1210.6132 [astro-ph.HE].

[423] A. E. Broderick, T. Johannsen, A. Loeb, and D. Psaltis, "Testing the No-Hair Theorem with Event Horizon Telescope Observations of Sagittarius A*," *Astrophys. J.* **784** (2014) 7, arXiv:1311.5564 [astro-ph.HE].

[424] C. Goddi *et al.*, "BlackHoleCam: fundamental physics of the Galactic center," *Int. J. Mod. Phys.* **D26** no. 02, (2016) 1730001, arXiv:1606.08879 [astro-ph.HE].

[425] **GRAVITY** Collaboration, A. Amorim *et al.*, "Test of Einstein equivalence principle near the Galactic center supermassive black hole," *Submitted to: Phys. Rev. Lett.* (2019) , arXiv:1902.04193 [astro-ph.GA].

[426] The Event Horizon Telescope Collaboration et al., "First M87 Event Horizon Telescope Results. I. The Shadow of the Supermassive Black Hole," *ApJL* **877** (2019) 1.

[427] P. V. P. Cunha, C. A. R. Herdeiro, E. Radu, and H. F. Runarsson, "Shadows of Kerr black holes with scalar hair," *Phys. Rev. Lett.* **115** no. 21, (2015) 211102, arXiv:1509.00021 [gr-qc].

[428] P. V. P. Cunha, J. A. Font, C. Herdeiro, E. Radu, N. Sanchis-Gual, and M. Zilhão, "Lensing and dynamics of ultracompact bosonic stars," *Phys. Rev.* **D96** no. 10, (2017) 104040, arXiv:1709.06118 [gr-qc].

[429] P. V. P. Cunha and C. A. R. Herdeiro, "Shadows and strong gravitational lensing: a brief review," *Gen. Rel. Grav.* **50** no. 4, (2018) 42, arXiv:1801.00860 [gr-qc].

[430] P. V. P. Cunha, C. A. R. Herdeiro, and M. J. Rodriguez, "Does the black hole shadow probe the event horizon geometry?," *Phys. Rev.* **D97** no. 8, (2018) 084020, arXiv:1802.02675 [gr-qc].

[431] A. Cardenas-Avendano, J. Godfrey, N. Yunes, and A. Lohfink, "Experimental Relativity with Accretion Disk Observations," arXiv:1903.04356 [gr-qc].

[432] K. K. Nandi, R. N. Izmailov, E. R. Zhdanov, and A. Bhattacharya, "Strong field lensing by Damour-Solodukhin wormhole," *JCAP* **1807** no. 07, (2018) 027, arXiv:1805.04679 [gr-qc].

[433] R. Shaikh, P. Banerjee, S. Paul, and T. Sarkar, "An analytical approach to strong gravitational lensing from ultra-compact objects," arXiv:1903.08211 [gr-qc].

[434] C. Sabín, "Quantum detection of wormholes," *Sci. Rep.* **7** no. 1, (2017) 716, arXiv:1702.01720 [quant-ph].

[435] M. Gracia-Linares and F. S. Guzman, "Accretion of Supersonic Winds on Boson Stars," *Phys. Rev.* **D94** no. 6, (2016) 064077, arXiv:1609.06398 [gr-qc].

[436] Gravity Collaboration, R. Abuter, A. Amorim, M. Bauböck, J. P. Berger, H. Bonnet, W. Brandner, Y. Clénet, V. Coudé Du Foresto, P. T. de Zeeuw, C. Deen, J. Dexter, G. Duvert, A. Eckart, F. Eisenhauer, N. M. Förster Schreiber, P. Garcia, F. Gao, E. Gendron, R. Genzel, S. Gillessen, P. Guajardo, M. Habibi, X. Haubois, T. Henning, S. Hippler, M. Horrobin, A. Huber, A. Jiménez-Rosales, L. Jocou, P. Kervella, S. Lacour, V. Lapeyrère, B. Lazareff, J.-B. Le Bouquin, P. Léna, M. Lippa, T. Ott, J. Panduro, T. Paumard, K. Perraut, G. Perrin, O. Pfuhl, P. M. Plewa, S. Rabien, G. Rodríguez-Coira, G. Rousset, A. Sternberg, O. Straub, C. Straubmeier, E. Sturm, L. J. Tacconi, F. Vincent, S. von Fellenberg, I. Waisberg, F. Widmann, E. Wieprecht, E. Wiezorrek, J. Woillez, and S. Yazici, "Detection of orbital motions near the last stable circular orbit of the massive black hole SgrA*," *Astronomy and Astrophysics* **618** (Oct., 2018) L10, arXiv:1810.12641.

[437] D. N. Page and K. S. Thorne, "Disk-accretion onto a black hole. time-averaged structure of accretion disk," *The Astrophysical Journal* **191** (1974) 499–506.

[438] C. Bambi, "Testing black hole candidates with electromagnetic radiation," *Rev. Mod. Phys.* **89** no. 2, (2017) 025001, arXiv:1509.03884 [gr-qc].

[439] A. Fabian, M. Rees, L. Stella, and N. E. White, "X-ray fluorescence from the inner disc in cygnus x-1," *Monthly Notices of the Royal Astronomical Society* **238** no. 3, (1989) 729–736.

[440] C. S. Reynolds, "Measuring Black Hole Spin using X-ray Reflection Spectroscopy," *Space Sci. Rev.* **183** no. 1-4, (2014) 277–294, arXiv:1302.3260 [astro-ph.HE].

[441] T. Johannsen and D. Psaltis, "Testing the No-Hair Theorem with Observations in the Electromagnetic Spectrum: I. Properties of a Quasi-Kerr Spacetime," *Astrophys. J.* **716** (2010) 187–197, arXiv:1003.3415 [astro-ph.HE].

[442] T. Johannsen and D. Psaltis, "Testing the No-Hair Theorem with Observations in the Electromagnetic Spectrum. IV. Relativistically Broadened Iron Lines," *Astrophys. J.* **773** (2013) 57, arXiv:1202.6069 [astro-ph.HE].

[443] C. Bambi, "Testing the space-time geometry around black hole candidates with the analysis of the broad Kα iron line," *Phys. Rev.* **D87** (2013) 023007, arXiv:1211.2513 [gr-qc].

[444] J. Jiang, C. Bambi, and J. F. Steiner, "Using iron line reverberation and spectroscopy to distinguish Kerr and non-Kerr black holes," *JCAP* **1505** no. 05, (2015) 025, arXiv:1406.5677 [gr-qc].

[445] T. Johannsen, "X-ray Probes of Black Hole Accretion Disks for Testing the No-Hair Theorem," *Phys. Rev.* **D90** no. 6, (2014) 064002, arXiv:1501.02815 [astro-ph.HE].

[446] C. J. Moore and J. R. Gair, "Testing the no-hair property of black holes with x-ray observations of accretion disks," *Phys. Rev.* **D92** no. 2, (2015) 024039, arXiv:1507.02998 [gr-qc].

[447] J. K. Hoormann, B. Beheshtipour, and H. Krawczynski, "Testing general relativity's no-hair theorem with x-ray observations of black holes," *Phys. Rev.* **D93** no. 4, (2016) 044020, arXiv:1601.02055 [astro-ph.HE].

[448] L.-X. Li, E. R. Zimmerman, R. Narayan, and J. E. McClintock, "Multi-temperature blackbody spectrum of a thin accretion disk around a Kerr black hole: Model computations and comparison with observations," *Astrophys. J. Suppl.* **157** (2005) 335–370, arXiv:astro-ph/0411583 [astro-ph].

[449] J. E. McClintock, R. Narayan, and J. F. Steiner, "Black Hole Spin via Continuum Fitting and the Role of Spin in Powering Transient Jets," *Space Sci. Rev.* **183** (2014) 295–322, arXiv:1303.1583 [astro-ph.HE].

[450] C. Bambi and E. Barausse, "Constraining the quadrupole moment of stellar-mass black-hole candidates with the continuum fitting method," *Astrophys. J.* **731** (2011) 121, arXiv:1012.2007 [gr-qc].

[451] C. Bambi, "A code to compute the emission of thin accretion disks in non-Kerr space-times and test the nature of black hole candidates," *Astrophys. J.* **761** (2012) 174, arXiv:1210.5679 [gr-qc].

[452] L. Kong, Z. Li, and C. Bambi, "Constraints on the spacetime geometry around 10 stellar-mass black hole candidates from the disk's thermal spectrum," *Astrophys. J.* **797** no. 2, (2014) 78, arXiv:1405.1508 [gr-qc].

[453] C. Bambi, "Note on the Cardoso-Pani-Rico parametrization to test the Kerr black hole hypothesis," *Phys. Rev.* **D90** (2014) 047503, arXiv:1408.0690 [gr-qc].

[454] T. Johannsen, "Testing the No-Hair Theorem with Observations of Black Holes in the Electromagnetic Spectrum," *Class. Quant. Grav.* **33** no. 12, (2016) 124001, arXiv:1602.07694 [astro-ph.HE].

[455] L. Stella and M. Vietri, "Khz quasi periodic oscillations in low mass x-ray binaries as probes of general relativity in the strong field regime," *Phys. Rev. Lett.* **82** (1999) 17–20, arXiv:astro-ph/9812124 [astro-ph].

[456] L. Stella, M. Vietri, and S. Morsink, "Correlations in the qpo frequencies of low mass x-ray binaries and the relativistic precession model," *Astrophys. J.* **524** (1999) L63–L66, arXiv:astro-ph/9907346 [astro-ph].

[457] M. A. Abramowicz and W. Kluzniak, "A Precise determination of angular momentum in the black hole candidate GRO J1655-40," *Astron. Astrophys.* **374** (2001) L19, arXiv:astro-ph/0105077 [astro-ph].

[458] M. van der Klis, "Millisecond oscillations in x-ray binaries," *Ann. Rev. Astron. Astrophys.* **38** (2000) 717–760, arXiv:astro-ph/0001167 [astro-ph].

[459] N. Franchini, P. Pani, A. Maselli, L. Gualtieri, C. A. R. Herdeiro, E. Radu, and V. Ferrari, "Constraining black holes with light boson hair and boson stars using epicyclic frequencies and quasiperiodic oscillations," *Phys. Rev.* **D95** no. 12, (2017) 124025, arXiv:1612.00038 [astro-ph.HE].

[460] D. R. Wilkins and A. C. Fabian, "The origin of the lag spectra observed in AGN: Reverberation and the propagation of X-ray source fluctuations," *Mon. Not. Roy. Astron. Soc.* **430** (2013) 247, arXiv:1212.2213 [astro-ph.HE].

[461] **LIGO Scientific, Virgo** Collaboration, B. P. Abbott *et al.*, "GWTC-1: A Gravitational-Wave Transient Catalog of Compact Binary Mergers Observed by LIGO and Virgo during the First and Second Observing Runs," arXiv:1811.12907 [astro-ph.HE].

[462] M. Middleton, "Black hole spin: theory and observation," arXiv:1507.06153 [astro-ph.HE].

[463] M. Punturo *et al.*, "The Einstein Telescope: A third-generation gravitational wave observatory," *Class. Quant. Grav.* **27** (2010) 194002.

[464] S. Dwyer, D. Sigg, S. W. Ballmer, L. Barsotti, N. Mavalvala, and M. Evans, "Gravitational wave detector with cosmological reach," *Phys. Rev. D* **91** (Apr, 2015) 082001. https://link.aps.org/doi/10.1103/PhysRevD.91.082001.

[465] H. Audley, S. Babak, J. Baker, E. Barausse, P. Bender, E. Berti, P. Binetruy, M. Born, D. Bortoluzzi, J. Camp, C. Caprini, V. Cardoso, M. Colpi, J. Conklin, N. Cornish, C. Cutler, *et al.*, "Laser Interferometer Space Antenna," *ArXiv e-prints* (Feb., 2017) , arXiv:1702.00786 [astro-ph.IM].

[466] F. D. Ryan, "Spinning boson stars with large selfinteraction," *Phys. Rev.* **D55** (1997) 6081–6091.

[467] K. Chatziioannou *et al.*, "On the properties of the massive binary black hole merger GW170729," arXiv:1903.06742 [gr-qc].

[468] **LIGO Scientific, Virgo** Collaboration, "Tests of General Relativity with the Binary Black Hole Signals from the LIGO-Virgo Catalog GWTC-1," arXiv:1903.04467 [gr-qc].

[469] B. Zackay, T. Venumadhav, L. Dai, J. Roulet, and M. Zaldarriaga, "A Highly Spinning and Aligned Binary Black Hole Merger in the Advanced LIGO First Observing Run," arXiv:1902.10331 [astro-ph.HE].

[470] S. Babak, J. Gair, A. Sesana, E. Barausse, C. F. Sopuerta, C. P. L. Berry, E. Berti, P. Amaro-Seoane, A. Petiteau, and A. Klein, "Science with the space-based interferometer LISA. V: Extreme mass-ratio inspirals," *Phys. Rev.* **D95** no. 10, (2017) 103012, arXiv:1703.09722 [gr-qc].

[471] L. Barack and C. Cutler, "Using LISA EMRI sources to test off-Kerr deviations in the geometry of massive black holes," *Phys. Rev.* **D75** (2007) 042003, arXiv:gr-qc/0612029 [gr-qc].

[472] R. Fujita, "Gravitational radiation for extreme mass ratio inspirals to the 14th post-Newtonian order," *Prog. Theor. Phys.* **127** (2012) 583–590, arXiv:1104.5615 [gr-qc].

[473] S. J. Vigeland and S. A. Hughes, "Spacetime and orbits of bumpy black holes," *Phys. Rev.* **D81** (2010) 024030, arXiv:0911.1756 [gr-qc].

[474] C. J. Moore, A. J. K. Chua, and J. R. Gair, "Gravitational waves from extreme mass ratio inspirals around bumpy black holes," *Class. Quant. Grav.* **34** no. 19, (2017) 195009, arXiv:1707.00712 [gr-qc].

[475] S. A. Hughes, "Evolution of circular, nonequatorial orbits of Kerr black holes due to gravitational wave emission. II. Inspiral trajectories and gravitational wave forms," *Phys. Rev.* **D64** (2001) 064004, arXiv:gr-qc/0104041 [gr-qc]. [Erratum: Phys. Rev.D88,no.10,109902(2013)].

[476] S. Datta and S. Bose, "Probing the nature of central objects in extreme-mass-ratio inspirals with gravitational waves," arXiv:1902.01723 [gr-qc].

[477] N. K. Johnson-Mcdaniel, A. Mukherjee, R. Kashyap, P. Ajith, W. Del Pozzo, and S. Vitale, "Constraining black hole mimickers with gravitational wave observations," arXiv:1804.08026 [gr-qc].

[478] P. Pani and A. Maselli, "Love in Extrema Ratio (to appear),".

[479] C. F. B. Macedo, T. Stratton, S. Dolan, and L. C. B. Crispino, "Spectral lines of extreme compact objects," *Phys. Rev.* **D98** no. 10, (2018) 104034, arXiv:1807.04762 [gr-qc].

[480] E. Berti, V. Cardoso, and C. M. Will, "On gravitational-wave spectroscopy of massive black holes with the space interferometer LISA," *Phys. Rev.* **D73** (2006) 064030, arXiv:gr-qc/0512160 [gr-qc].

[481] O. Dreyer, B. J. Kelly, B. Krishnan, L. S. Finn, D. Garrison, and R. Lopez-Aleman, "Black hole spectroscopy: Testing general relativity through gravitational wave observations," *Class. Quant. Grav.* **21** (2004) 787–804, arXiv:gr-qc/0309007 [gr-qc].

[482] E. Berti and V. Cardoso, "Supermassive black holes or boson stars? Hair counting with gravitational wave detectors," *Int. J. Mod. Phys.* **D15** (2006) 2209–2216, arXiv:gr-qc/0605101 [gr-qc].

[483] J. Meidam, M. Agathos, C. Van Den Broeck, J. Veitch, and B. S. Sathyaprakash, "Testing the no-hair theorem with black hole ringdowns using TIGER," *Phys. Rev.* **D90** no. 6, (2014) 064009, arXiv:1406.3201 [gr-qc].

[484] E. Berti, A. Sesana, E. Barausse, V. Cardoso, and K. Belczynski, "Spectroscopy of Kerr black holes with Earth- and space-based interferometers," *Phys. Rev. Lett.* **117** no. 10, (2016) 101102, arXiv:1605.09286 [gr-qc].

[485] R. A. Konoplya and A. Zhidenko, "Wormholes versus black holes: quasinormal ringing at early and late times," *JCAP* **1612** no. 12, (2016) 043, arXiv:1606.00517 [gr-qc].

[486] K. K. Nandi, R. N. Izmailov, A. A. Yanbekov, and A. A. Shayakhmetov, "Ring-down gravitational waves and lensing observables: How far can a wormhole mimic those of a black hole?," *Phys. Rev.* **D95** no. 10, (2017) 104011, arXiv:1611.03479 [gr-qc].

[487] M. Okounkova, L. C. Stein, M. A. Scheel, and D. A. Hemberger, "Numerical binary black hole mergers in dynamical Chern-Simons gravity: Scalar field," *Phys. Rev.* **D96** no. 4, (2017) 044020, arXiv:1705.07924 [gr-qc].

[488] E. W. Hirschmann, L. Lehner, S. L. Liebling, and C. Palenzuela, "Black Hole Dynamics in Einstein-Maxwell-Dilaton Theory," *Phys. Rev.* **D97** no. 6, (2018) 064032, arXiv:1706.09875 [gr-qc].

[489] H. Witek, L. Gualtieri, P. Pani, and T. P. Sotiriou, "Black holes and binary mergers in scalar Gauss-Bonnet gravity: scalar field dynamics," *Phys. Rev.* **D99** no. 6, (2019) 064035, arXiv:1810.05177 [gr-qc].

[490] M. Okounkova, M. A. Scheel, and S. A. Teukolsky, "Evolving Metric Perturbations in dynamical Chern-Simons Gravity," *Phys. Rev.* **D99** no. 4, (2019) 044019, arXiv:1811.10713 [gr-qc].

[491] J. Abedi, H. Dykaar, and N. Afshordi, "Echoes from the Abyss: The Holiday Edition!," arXiv:1701.03485 [gr-qc].

[492] J. Westerweck, A. Nielsen, O. Fischer-Birnholtz, M. Cabero, C. Capano, T. Dent, B. Krishnan, G. Meadors, and A. H. Nitz, "Low significance of evidence for black hole echoes in gravitational wave data," *Phys. Rev.* **D97** no. 12, (2018) 124037, arXiv:1712.09966 [gr-qc].

[493] A. B. Nielsen, C. D. Capano, O. Birnholtz, and J. Westerweck, "Parameter estimation for black hole echo signals and their statistical significance," arXiv:1811.04904 [gr-qc].

[494] R. K. L. Lo, T. G. F. Li, and A. J. Weinstein, "Template-based Gravitational-Wave Echoes Search Using Bayesian Model Selection," arXiv:1811.07431 [gr-qc].

[495] G. Ashton, O. Birnholtz, M. Cabero, C. Capano, T. Dent, B. Krishnan, G. D. Meadors, A. B. Nielsen, A. Nitz, and J. Westerweck, "Comments on: "Echoes from the abyss: Evidence for Planck-scale structure at black hole horizons"," arXiv:1612.05625 [gr-qc].

[496] J. Abedi, H. Dykaar, and N. Afshordi, "Comment on: "Low significance of evidence for black hole echoes in gravitational wave data"," arXiv:1803.08565 [gr-qc].

[497] **LIGO Scientific** Collaboration, B. P. Abbott *et al.*, "Search for gravitational wave ringdowns from perturbed black holes in LIGO S4 data," *Phys. Rev.* **D80** (2009) 062001, arXiv:0905.1654 [gr-qc].

[498] LIGO Instrument Science White Paper, https://dcc.ligo.org/public/0120/T1500290/002/.

[499] **LIGO** Collaboration, D. Shoemaker, "Advanced ligo anticipated sensitivity curves," Tech. Rep. T0900288-v3, 2010. https://dcc.ligo.org/LIGO-T0900288/public.

[500] **LIGO Scientific** Collaboration, B. P. Abbott *et al.*, "Exploring the Sensitivity of Next Generation Gravitational Wave Detectors," *Class. Quant. Grav.* **34** no. 4, (2017) 044001, arXiv:1607.08697 [astro-ph.IM].

[501] R. Essick, S. Vitale, and M. Evans, "Frequency-dependent responses in third generation gravitational-wave detectors," *Phys. Rev.* **D96** no. 8, (2017) 084004, arXiv:1708.06843 [gr-qc].

[502] S. Hild *et al.*, "Sensitivity Studies for Third-Generation Gravitational Wave Observatories," *Class. Quant. Grav.* **28** (2011) 094013, arXiv:1012.0908 [gr-qc].

[503] X.-L. Fan and Y.-B. Chen, "Stochastic gravitational-wave background from spin loss of black holes," *Phys. Rev.* **D98** no. 4, (2018) 044020, arXiv:1712.00784 [gr-qc].

[504] S. M. Du and Y. Chen, "Searching for near-horizon quantum structures in the binary black-hole stochastic gravitational-wave background," *Phys. Rev. Lett.* **121** no. 5, (2018) 051105, arXiv:1803.10947 [gr-qc].

[505] I. Dvorkin, E. Vangioni, J. Silk, J.-P. Uzan, and K. A. Olive, "Metallicity-constrained merger rates of binary black holes and the stochastic gravitational wave background," *Mon. Not. Roy. Astron. Soc.* **461** no. 4, (2016) 3877–3885, arXiv:1604.04288 [astro-ph.HE].

[506] E. Barausse, V. Cardoso, and P. Pani, "Environmental Effects for Gravitational-wave Astrophysics," *J. Phys. Conf. Ser.* **610** no. 1, (2015) 012044, arXiv:1404.7140 [astro-ph.CO].

[507] J. M. Bardeen, W. H. Press, and S. A. Teukolsky, "Rotating black holes: Locally nonrotating frames, energy extraction, and scalar synchrotron radiation," *Astrophys. J.* **178** (1972) 347.